

IN-05-CR

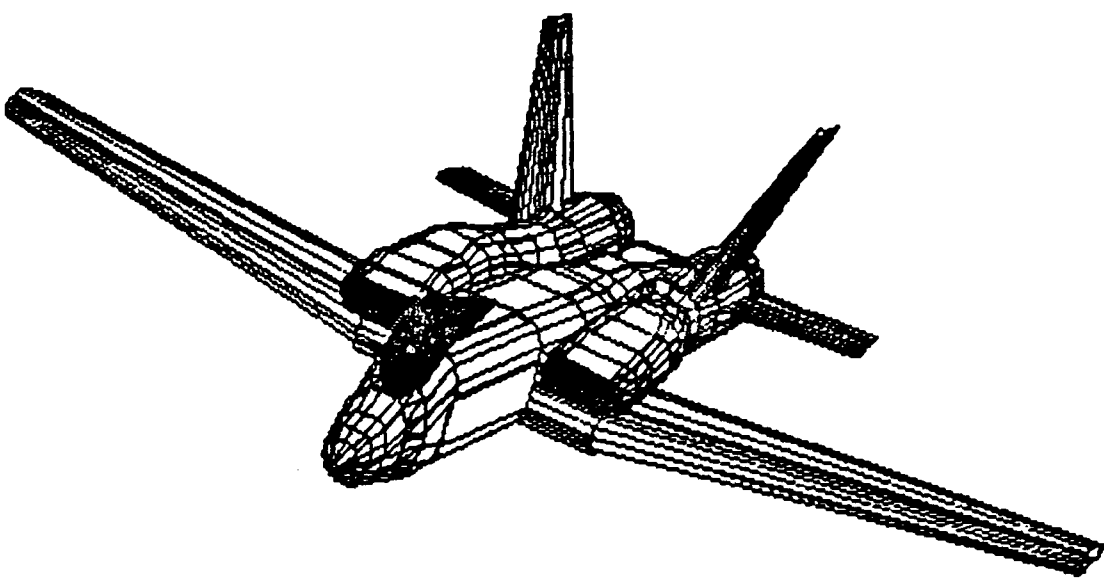
73909

NASW-4435

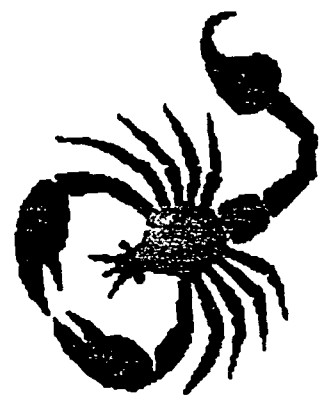


SCORPION

P. 107



PROPOSED CLOSE AIR SUPPORT AIRCRAFT



CAL POLY, SLO

(NASA-CR-189974) SCORPION: CLOSE AIR
SUPPORT (CAS) AIRCRAFT (California
Polytechnic State Univ.) 107 p CSCL 01C

N92-20664

Unclas
63/05 0073909

SCORPION

CLOSE AIR SUPPORT (CAS) AIRCRAFT

CHRIS ALLEN : Chris Allen

RENDY CHENG : Rendy Cheng

GRANT KOEHLER : Grant Koehler

SEAN LYON : Se D. Lyon

CECILIA PAGUIO : Cecilia Pagui

AERONAUTICAL ENGINEERING DEPARTMENT
CALIFORNIA POLYTECHNIC STATE UNIVERSITY
SAN LUIS OBISPO, CALIFORNIA

ABSTRACT

The objective of this report is to outline the results of the preliminary design of the Scorpion, a proposed close air support aircraft. The results obtained include complete preliminary analyses of the aircraft in the areas of 1) aerodynamics, 2) structures, 3) avionics and electronics, 4) stability and control, 5) weight and balance, 6) propulsion systems and 7) costs. A conventional wing, twin-jet, twin-tail aircraft was chosen to maximize the desirable characteristics the Scorpion will include such as low-speed maneuverability, high survivability, low cost and low maintenance. Results obtained include:

Life Cycle Cost Per Aircraft: \$17.5 million

Maximum Take-Off Weight: 52,760 lbs

Wing Loading : 90 psf

Thrust-to-Weight: 0.6 lbs/lb

This aircraft meets the mission requirements specified. However, in addition to the analyses performed and results obtained, some modifications have been suggested to further optimize the design.

TABLE OF CONTENTS

ABSTRACT	i
LIST OF TABLES	v
LIST OF FIGURES	vi
LIST OF SYMBOLS	viii
1.0 INTRODUCTION	1
2.0 DESIGN CRITERIA	
2.1 DESIGN REQUIREMENTS	2
2.2 MISSION PROFILES	3
3.0 FINAL DESIGN RESULTS	
3.1 THREE-VIEW DRAWINGS	6
3.2 SCORPION SPECIFICATIONS	8
3.3 PERFORMANCE	9
3.3.1. EXCESS POWER AND RATE OF CLIMB	10
3.3.2. RANGE-PAYLOAD CAPABILITIES	10
3.3.3. TAKE-OFF & LANDING PERFORMANCE	13
3.3.4. V-n DIAGRAM	13
4.0 SIZING ANALYSIS	
4.1. TAKE-OFF WEIGHT ESTIMATION	
4.1.1. MISSION FUEL FRACTION	15
4.2 SENSITIVITY STUDY	19
4.3 DRAG POLARS FOR PRELIMINARY SIZING	20
4.4 SIZING TO TAKE-OFF & LANDING CONFIGURATION	22

4.5 SIZING TO TAKE-OFF & LANDING DISTANCES	22
4.6 SIZING TO CRUISE AND MANEUVER	26
4.7 DESIGN POINT DETERMINATION	28
5.0 CONFIGURATION COMPARISON & JUSTIFICATION	
5.1 COMPARISON TO EXISTING CONFIGURATIONS	30
5.2 CONFIGURATION SELECTION & JUSTIFICATION	
5.2.1. HIGH-SPEED ROTORCRAFT	33
5.2.2. POWERED LIFT	34
5.2.3. FINAL RESULTS OF PRELIMINARY ANALYSIS	35
6.0 COMPONENT DESIGN	
6.1 FUSELAGE & COCKPIT LAYOUT	
6.1.1. FUSELAGE	36
6.1.2. COCKPIT DESIGN	38
6.2 WING AND LIFT AUGMENTATION	
6.2.1. WING PLANFORM PARAMETERS	42
6.2.2. LIFT AUGMENTATION	43
6.3 EMPENNAGE	44
6.4 PROPULSION INTEGRATION	45
6.4.1. INLET EFFICIENCY	45
6.4.2. POWER EXTRACTION	46
6.5 LANDING GEAR	49
7.0 STRUCTURES AND MATERIAL	
7.1. STRUCTURES	52
7.2. MATERIALS	57

8.0 CENTER OF GRAVITY & MOMENT OF INERTIA ANALYSIS	
8.1 WEIGHT AND BALANCE & C.G. EXCURSION	59
8.2 MOMENTS & PRODUCTS OF INERTIAS	62
9.0 AERODYNAMICS	64
9.1 LIFT	64
9.2 WETTED AREAS	67
9.3 DRAG POLARS	69
10.0 STABILITY	72
11.0 AVIONICS	76
12.0 SYSTEM LAYOUT	78
13.0 WEAPONS INTEGRATION	81
14.0 GROUND SUPPORT REQUIREMENTS	87
15.0 COST ANALYSIS	89
15.1 RESEARCH, DEVELOPMENT, TESTING & EVALUATION	90
15.2 PRODUCTION	91
15.3 OPERATIONS AND MAINTENANCE	93
15.4 DISPOSAL	94
15.5 TOTAL LIFE CYCLE COST	94
16.0 MANUFACTURING BREAKDOWN	95
17.0 CONCLUSION	96
REFERENCES	97

LIST OF TABLES

3.2.A. SCORPION SPECIFICATIONS	8
3.3.A. PERFORMANCE COMPARISON	9
3.3.4.A. FLIGHT SPEEDS AT SEA-LEVEL	14
4.1.1.A. MISSION FUEL FRACTION RESULTS	18
4.2.A. SENSITIVITY STUDY & GROWTH FACTORS	19
5.1.A. AIRCRAFT COMPARISON	31
6.5.A. LANDING GEAR SIZING RESULTS	50
8.1.A. WEIGHT AND BALANCE CALCULATION	61
8.2.A. MOMENTS & PRODUCTS OF INERTIAS	63
9.2.A. SUMMARY OF WETTED AREAS	67

LIST OF FIGURES

2.2.1. DESIGN MISSION PROFILE	4
2.2.2. HIGH-LOW-LOW-HIGH PROFILE	5
2.2.3. FERRY PROFILE	5
3.1.1. TOP VIEW	7
3.1.2. SIDE VIEW	7
3.1.3. FRONT VIEW	7
3.3.1.1. SPECIFIC EXCESS POWER	11
3.3.2.1. PAYLOAD-RANGE DIAGRAM	11
3.3.4.1. V-n DIAGRAM	14
4.4.1. TAKE-OFF & LANDING CONFIGURATION SIZING	23
4.5.1. SIZING TO TAKE-OFF DISTANCE	23
4.5.2. LANDING APPROACH DIAGRAM	24
4.5.3. SIZING TO LANDING DISTANCE	25
4.6.1. SIZING TO CRUISE AND MANEUVER	27
4.7.1. PRELIMINARY SIZING RESULTS	29
5.1.1. SIZING ENVELOPE COMPARISON	30
6.1.1.1. FUSELAGE LAYOUT	37
6.1.2.1. COCKPIT LINE OF SIGHT	39
6.1.2.2A,B. INSTRUMENT PANEL LAYOUT	40,41
6.2.2.1. FLAP SYSTEM	43
6.4.2.1. UNAUGMENTED THRUST VERSUS VELOCITY AT ALTITUDE	47
6.4.2.2. AUGMENTED THRUST VERSUS VELOCITY AT ALTITUDE	47

6.4.2.3. UNAUGMENTED SPECIFIC FUEL CONSUMPTION VS ALTITUDE	47
6.5.1. LANDING GEAR RETRACTION	51
7.1.1. STRUCTURE LAYOUT TOP VIEW	53
7.1.2. WING STRUCTURE	54
7.1.3. WING FUSELAGE STRUCTURE INTEGRATION	54
7.1.4. STABILATOR STRUCTURE	56
7.1.5. STRUCTURE LAYOUT SIDE VIEW	55
7.1.6. VERTICAL TAIL STRUCTURE	56
7.2.1. SCORPION MATERIAL DISTRIBUTION	57
7.2.2. TITANIUM ARMOR LOCATION	58
8.1.1. CENTER OF GRAVITY EXCURSION	60
9.1.1. SPANWISE LIFT DISTRIBUTION FOR MACH = 0.2	66
9.1.2. CL VERSUS ANGLE OF ATTACK FOR DIFFERENT FLIGHT SPEEDS	68
9.1.3. CL VS ANGLE OF ATTACK FOR DIFFERENT FLAP DEFLECTIONS	68
9.3.1. DRAG COEFFICIENT VERSUS MACH NUMBER	69
9.3.2. DRAG POLARS AT SEA-LEVEL WITH NO STORES	70
9.3.3 DRAG POLARS AT SEA-LEVEL WITH STORES	70
9.3.4. DRAG POLAR AT LANDING	71
9.3.5. AREA RULING RESULT	71
11.0.1. AVIONICS LAYOUT	77
12.0.1. SYSTEMS LAYOUT	79
12.0.2. FUEL SYSTEM LAYOUT	80
13.0.1A,B ALTERNATIVE MISSION LOADS	83,84
13.0.2A,B. WEAPON DIMENSIONS	85,86
14.1. ACCESS PANELS	88
16.0.1.1. MANUFACTURING BREAKDOWN	95

SYMBOLS

<u>SYMBOL</u>		<u>UNITS</u>
AR	aspect ratio	non-dimensional
CAvionics	avionics costs	dollars
CD	development support costs	dollars
CD	drag coefficient	non-dimensional
CD ₀	profile drag coefficient	non-dimensional
CEng	engine costs	dollars
CF	flight test costs	dollars
CGR	climb gradient	non-dimensional
CL	lift coefficient	non-dimensional
Cm	manufacturing materials costs	dollars
D	drag	lbf
E	endurance	hours
F	factor	non-dimensional
FTA	flight test aircraft	non-dimensional
HE	engineering hours	hours
HM	manufacturing hours	hours
HQ	quality control hours	hours
HT	tooling hours	hours
I	moment or product of inertia	feet ⁴
L	lift	lbf
Neng	number of engines	non-dimensional
Q	production quantity	non-dimensional
R	range	nautical miles
RC	rate of climb	feet per minute
RE	engineering wrap rate	dollars per hour
RM	manufacturing wrap rate	dollars per hour
RQ	quality control wrap rate	dollars per hour
RT	tooling wrap rate	dollars per hour
S	surface area	square feet
S _{fl}	take-off or landing field length	feet
T	thrust	lbf
U ₁	flight speed	feet per second or knots
V	velocity	feet per second
W	weight	lbf
c	specific fuel consumption	non-dimensional
e	Oswald efficiency factor	non-dimensional
f	parasite area	square feet
h	height	feet
η _i /η _c	inlet efficiency	non-dimensional
n	g-loading	non-dimensional
q	dynamic pressure	pounds per square foot
t	time	seconds or minutes

SUBSCRIPTS

AV	available	extr	extracted
E	empty	j	jet
G	ground roll	ltr	loiter
L	landing	max	maximum
REQ	required	stall	at stall
TO	take-off	wet	wetted
approach	at approach	4	prior to dash out mission leg
cl	climb	5	after dash out mission leg
cr	cruise	6	after combat leg

L.O INTRODUCTION

Technology has caused battlefield warfare to become increasingly complex. The concept of the close air support aircraft has not changed, but the close air support aircraft and its role has had to continually evolve to maintain pace with the battlefield. Early close air support (CAS) aircraft provided strafing and light bombing attacks as well as reconnaissance information to help ground forces. The CAS aircraft of the future will have a much more complicated task. Intense and lethal conflict will demand CAS aircraft be able to identify, interdict and destroy opposing forces with maximum efficiency while evading increasingly effective enemy anti-aircraft weapons. Close air support aircraft must also be able to fulfill the ground firepower shortfalls with responsive, effective and accurate ordnance delivery during day, night and all weather conditions. In addition to these requirements, the speed with which modern armed forces advance requires this aircraft to have high sortie rates for continuous operation, which will command the design of a rugged and reliable aircraft that will operate with limited maintenance from unimproved airstrips with limited facilities.

The design objectives of this program are to meet the battlefield requirements and mission constraints, outlined in the following section, with a low cost aircraft that is easily maintainable and supportable. This report contains the preliminary sizing and detailed preliminary analyses for the Scorpion close air support aircraft, designed to meet these future battlefield challenges.

2.0 DESIGN CRITERIA

2.1 DESIGN REQUIREMENTS

Several design constraints were considered for preliminary sizing. These requirements were categorized in two major divisions, specifications and design mission profiles. The first division, specifications, was further divided into three subcategories: 1) payload, 2) landing/take-off and 3) structural requirements. The most stringent requirement that affected the weight determination was the payload. The aircraft must be able to carry a total load of 13,952 lbs consisting of the following items:

One GAU-8 30mm cannon @1,840 lbs with 1,350 rounds of ammunition @ 2,106 lbs.

Two AIM-9L Sidewinder Missiles @ 235 lbs each including a 40 lb. launch rail for each missile

Twenty Mk 82 bombs @ 505 lbs each with four multiple ejection racks @ 219 lbs each

One crew member @ 225 lbs including equipment

The aircraft must also be able to land with a ground roll of less than 2,000 feet on a hard dry strip, although the Scorpion was designed to meet this requirement on a unimproved strip. The aircraft must also be able to take-off in this distance with full internal fuel and external stores. The following structural requirements were also taken into account, a maximum normal service load of 7.5 g's and a minimum normal service load of -3 g's. With a safety factor of 1.5, the ultimate g-loadings for the Scorpion become 11.25 and -4.5 respectively.

2.2 MISSION PROFILES

Three missions were specified to outline the design criteria; 1) the primary design mission, 2) high-low-low-high mission, and 3) the ferry mission. The primary design mission was the most stringent and constricting. It consists of a dash out, 250 nmi. at sea-level at a speed of 500 kts, two combat passes at a speed of military power minus 50 kts where ground weapons are dropped, and another 250 nmi. dash at sea-level back to base at 500 kts. The combat leg also included two 4.5 g, 360 degree sustained turns and a 4000 ft. energy increase. Refer to Figure 2.2.1. for the design mission profile.

The high-low-low-high mission is comprised of a climb at intermediate power to best cruise speed and altitude, cruise for 150 nmi, then descend to sea-level for a dash at 500 knots for 100 nmi. to the battle site. The aircraft must then loiter for a time determined by the payload and fuel remaining, drop its ordnance, dash out at 500 knots for 100 nmi. from the battle site, climb back to best cruise speed and altitude, and cruise back to base for the last 150 nmi. Refer to Figure 2.2.2 for a profile of the high-low-low-high mission.

The ferry mission requires the greatest range capability, but is least restrictive. It involves a climb to best cruise altitude and speed, a cruise out from base covering a total of 1,500 nmi and a descent back to sea-level. Refer to Figure 2.2.3 for a profile of the ferry mission. All missions require landing with twenty minutes of reserve fuel, and estimate a total of five minutes of fuel used for warm-up, taxi, take-off and accelerate to climb speed.

The following additional requirements are to be met by the aircraft while carrying full external stores with 50% of internal fuel: 1) accelerate from Mach 0.3 to 0.5 at sea-level in less than twenty seconds, 2) a sustained turn of 4.5 g's at combat speed and an instantaneous loading of 6.0 g's, again at combat speed, and a re-attack time between combat passes of less than twenty-five seconds.

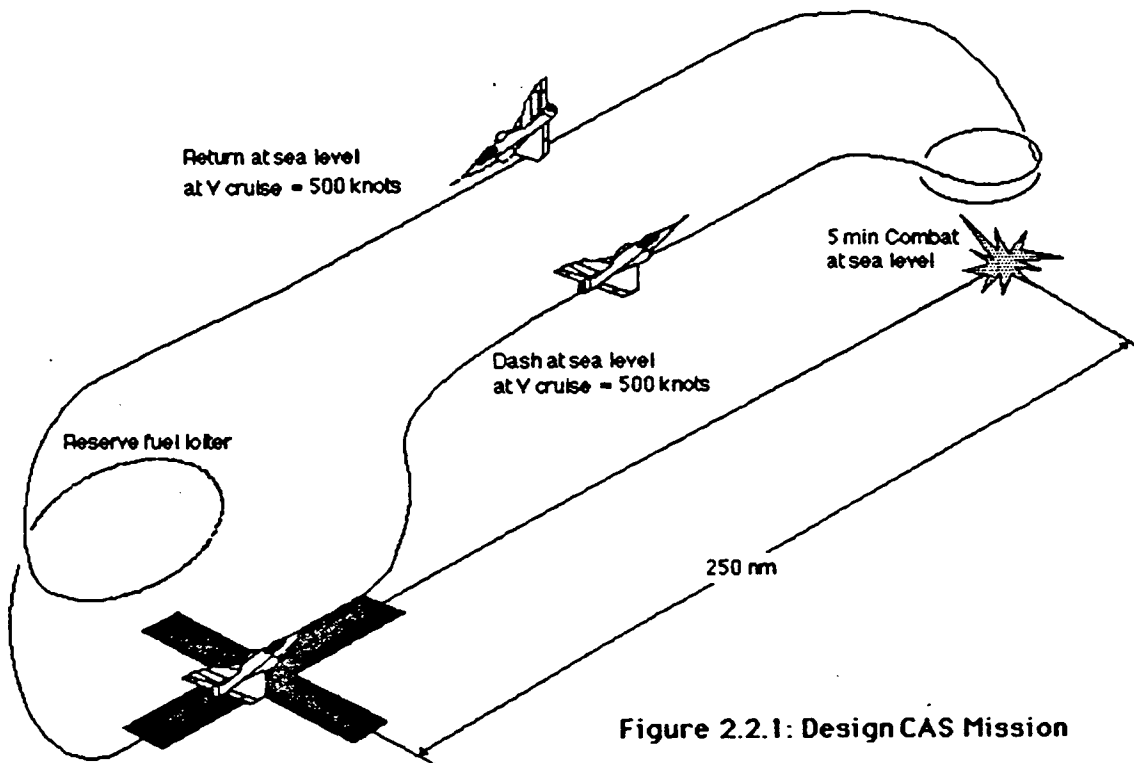


Figure 2.2.1: Design CAS Mission

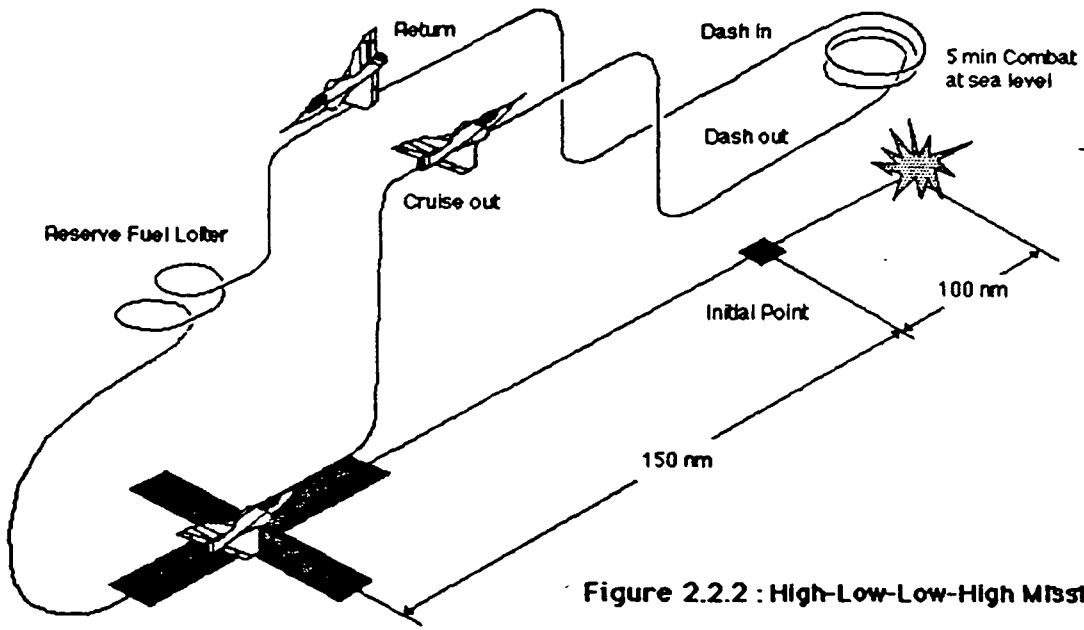


Figure 2.2.2 : High-Low-Low-High Mission

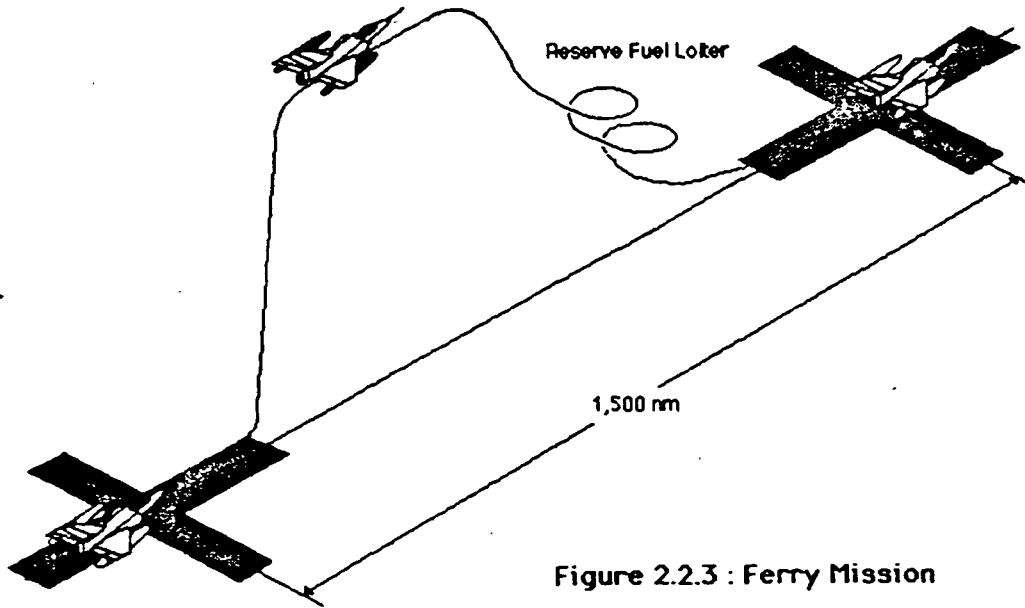


Figure 2.2.3 : Ferry Mission

3.0 FINAL DESIGN RESULTS

3.1 THREE VIEW DRAWINGS

The final configuration selected is presented in the following three view drawings, Figures 3.1.1, 3.1.2, 3.1.3; the Scorpion's specifications follow in Table 3.2.A. The Scorpion has a conventional configuration, with twin-tails, twin-engines and tricycle landing gear. Figure 3.1.1 features the wing which is a conventional planform slightly swept aft. The horizontal tail is a fully controllable stabilator arrangement with the same aft sweep angle as the wing. The spacing of the twin rear engines and inlet placement are also clearly shown in Figure 3.1.1. The engines are separated to provide better survivability and the inlets were placed high, on top of the wings extended to the leading edge, to help prevent foreign object ingestion during take off and landing ground time. Figure 3.1.2 shows the side view featuring a high canopy for better pilot visibility, landing gear locations, and the location of the vertical tails forward of the horizontal stabilators to allow for maximum deflection of the rudder and stabilators. Figure 3.1.3 shows the front view featuring the semi-circular inlets, placed to receive uniform freestream flow and eliminating the need for boundary layer splitter plates, and canted twin vertical tails for better survivability and increased controllability in high angle of attack flight conditions. The nose gear is offset to allow volume for the large GAU-8 cannon in the nose of the aircraft. Details of configuration selection and design are found in section 6.0 Component Design.

THREE - VIEW OF SCORPION

FIGURE 3.1.1: TOP VIEW

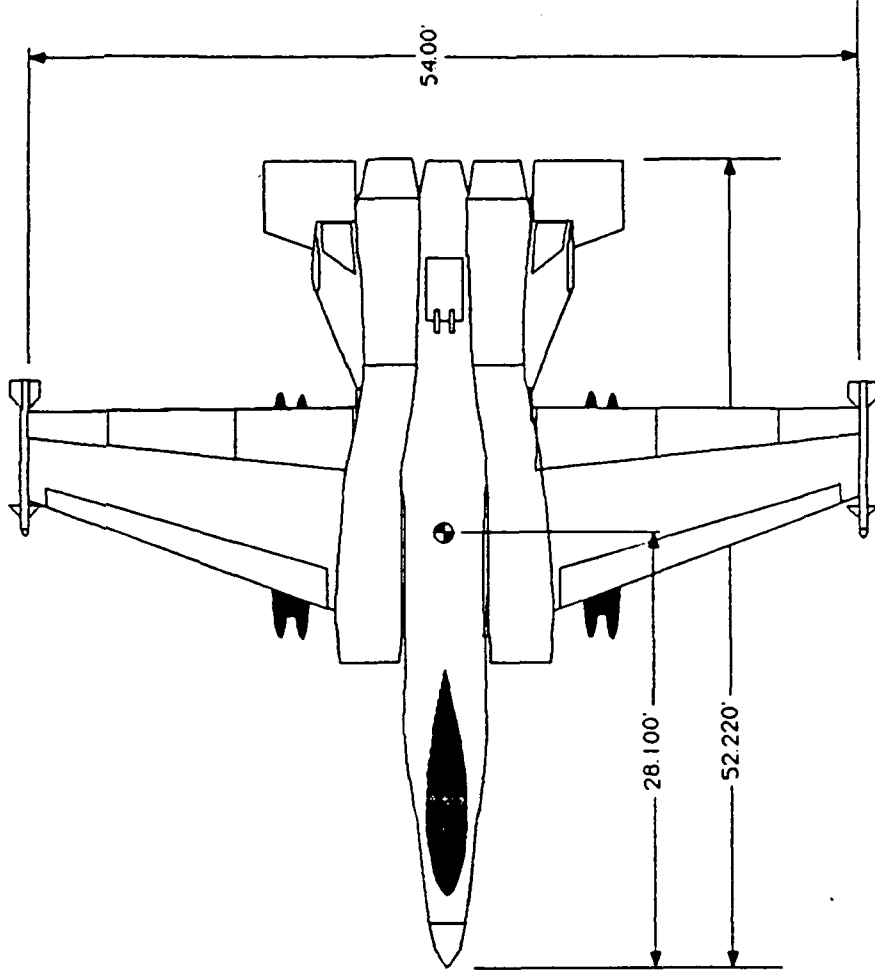


FIGURE 3.1.2: SIDE VIEW

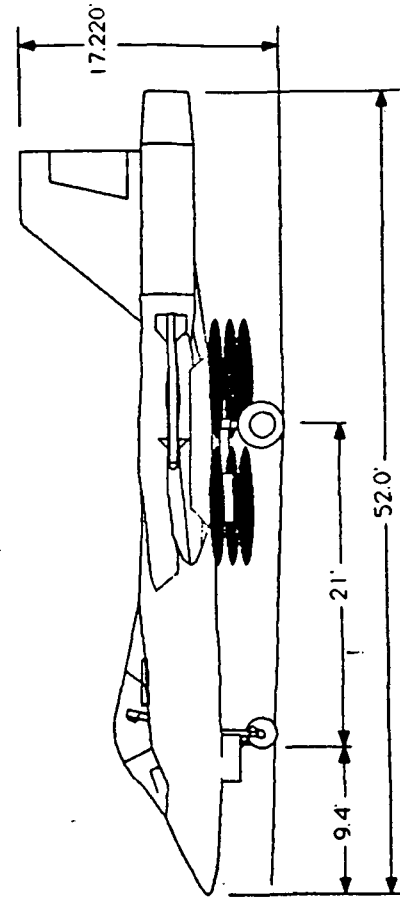


FIGURE 3.1.3: FRONT VIEW

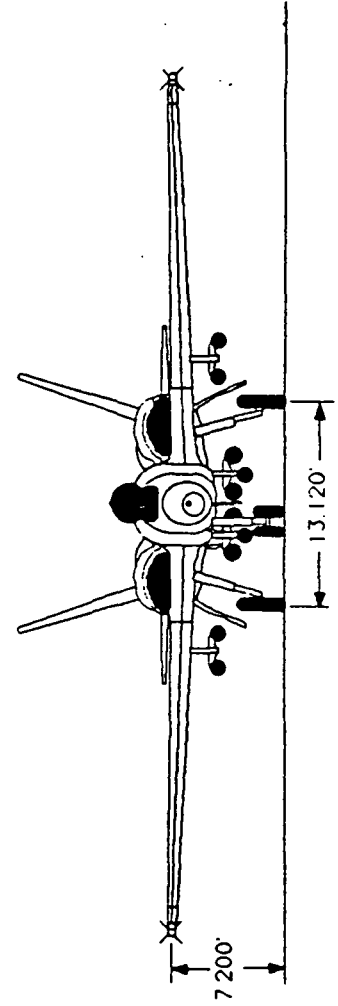


TABLE 3.2.A : SCORPION SPECIFICATIONS

WEIGHTS

LENGTHS

TAKE-OFF PAYLOAD FUEL	52760 lbs 13952 lbs 12045 lbs	OVERALL LENGTH SPAN HEIGHT	52.2 ft. 54 ft. 17.2 ft.
OPERATING EMPTY TOTAL EMPTY	26763 lbs 26278 lbs		

WING

FLAP SYSTEM

EQUIVALENT PLANFORM AREA SPAN ASPECT RATIO TAPER RATIO	90 psf 590 square feet 54 feet 4.94 0.36	LEADING EDGE SLATS: SPAN CHORD	0.4 b/2 0.20c
DIHEDRAL WASHOUT INCIDENCE SWEEP (L.E.) AIRFOIL	2 degrees 2 degrees 0 20 degrees NACA 64A410	FOWLER FLAPS: SPAN CHORD	0.4b/2 0.30c

HORIZONTAL STABILATORS

VERTICAL TAILS

SPAN ASPECT RATIO TAPER RATIO SWEEP AREA AIRFOIL	21 feet 3.64 0.47 20 degrees 60.5 ft.^2 NACA 0009	TOTAL SURFACE AREA INCIDENCE SPAN RUDDER SIZE CHORD SPAN AIRFOIL	128 square feet 20 degrees 8.6 ft. 0.30c 0.60b NACA 0009
---	--	--	---

3.3 PERFORMANCE:

The performance of the Scorpion was analyzed to determine whether or not the design requirements were met. A summary of these requirements and the Scorpion's capabilities are presented in Table 3.3.A

TABLE 3.3.A: PERFORMANCE COMPARISON

PARAMETER	REQUIRED	ACHIEVED
ACCELERATION FROM M=.3 TO M=.5 AT SEA-LEVEL	20 SEC	18.6 SEC
TURN RATES AT MILITARY POWER - 50 KTS		
4.5 G SUSTAINED	NOT SPEC.	10.65 DEG/SEC
6.0 INSTANTANEOUS	NOT SPEC.	14.36 DEG/SEC
TURN RADIUS AT MILITARY POWER-50 KTS		
4.5 G SUSTAINED	NOT SPEC.	4088 FT
6.0 G INSTANTANEOUS	NOT SPEC.	3032 FT
TURN RATES AT AERODYNAMIC LIMIT		
4.5 G SUSTAINED	NOT SPEC.	16.51 DEG/SEC
6.0 G INSTANTANEOUS	NOT SPEC.	19.80 DEG/SEC
TURN RADIUS AT AERODYNAMIC LIMIT		
4.5 G SUSTAINED	NOT SPEC.	1700 FT
6.0 G INSTANTANEOUS	NOT SPEC.	1588 FT
RE-ATTACK TIME	25 SEC	18 SEC
GROUND ROLL DISTANCES		
TAKE-OFF	2000 FT	1600 FT
LANDING	2000 FT	1589 FT
RANGE FOR FERRY MISSION	1500 N MI	4300 N MI
RANGE W/ FULL PAYLOAD AT BEST ALTITUDE	NOT SPEC	2006 N MI

3.3.1 EXCESS POWER AND RATE OF CLIMB:

Aerodynamic and propulsion analyses yielded excess thrust for various flight conditions. Using these values the specific excess power was obtained using the maximum take-off weight minus fifty percent of the internal fuel as shown in Figure 3.3.1.1. As the curve indicates, the absolute ceiling is 40,000 feet and the combat ceiling is 38,000 feet. This was then used to evaluate the performance of the Scorpion.

3.3.2 RANGE AND PAYLOAD CAPABILITIES

Figure 3.3.2.1 shows the results of the payload-range analysis for the Scorpion. Breguet's range equation for constant altitude cruise was used to determine the maximum range with weapons payload at maximum take-off weight, and maximum ferry range with external fuel tanks replacing the weapons payload. The best altitude for cruise was determined using the specific excess power plots shown in the previous section in Figure 3.3.1.1, the aerodynamic analysis from section 9.0, and from the propulsion analysis in section 6.4. The rate of climb plots were used to determine the service ceiling of 38,000 feet at maximum take-off weight, and the propulsion and aerodynamic analyses performed on the resulting envelope showed the drag and specific fuel consumption were minimized at that altitude. The following relations were then used to plot points A and B, indicating the harmonic range of 2006 nmi., in the figure shown.

$$R = (1.677/c_j) (S)^{-1/2} \{ (C_L)^{1/2}/C_D \} \{ (W_{\text{initial}})^{1/2} - (W_{\text{end}})^{1/2} \}$$

$$W_{\text{initial}} = 52,760 \text{ lb} \quad (\text{take-off wt})$$

$$W_{\text{end}} = 40,715 \text{ lb} \quad (\text{take-off wt} - \text{fuel wt})$$

The lift and drag coefficients were taken from the drag polar at cruise Mach number. The point C indicates maximum range of 4,300 nmi. if the entire weapons payload was replaced by external fuel tanks. It was determined that the volume of the bombs, when replaced by fuel, is adequate to contain the fuel externally. Hence, the parasite drag with external tanks was assumed to be equivalent to the parasite drag for the aircraft fully laden with bombs. Using Breguet's range equation from above, point C was determined with,

$$W_{\text{end}} = 26,760 \text{ lb}$$

all other values remained constant. The specific excess power curves were also used to estimate the time to climb and range for climb for the ferry mission using,

$$T_{\text{cl}} = \int (RC) dH \text{ (at 5K increments)} = (h_{\text{cl}})(RC_{\text{ave}})$$

where,

$$h_{\text{cl}} = 38,000 \text{ ft.}$$

$$RC_{\text{ave}} = 5,000 \text{ ft/min}$$

which yielded a time to climb of approximately 7.2 minutes in a climb range of 47 miles, when starting with a climb at Mach 0.4 at sea level.

PRECEDING PAGE BLANK NOT FILMED

3.3.3 LANDING AND TAKE-OFF

The Scorpion is the capable of taking off and landing on a 2000 foot hard, dry strip. The maximum landing weight of the aircraft is 51160 pounds. This at the worst case scenario, i.e. the Scorpion took off and then had to immediately land without jettisoning any fuel. With this weight an analysis was performed to determine if the Scorpion is capable of undergoing a bailed landing with one engine inoperative.

To meet the 2000 foot strip requirement, the Scorpion must approach at a minimum angle of attack of ten degrees with a fifty degree flap deflection and a fifteen degree leading edge slat deflection. This configuration incurs thirteen thousands pounds of drag that must be overcome. With one engine out, the Scorpion's powerplant is still capable of generating sixteen thousand pounds of augmented thrust. This excess thrust is sufficient to perform a bailed landing.

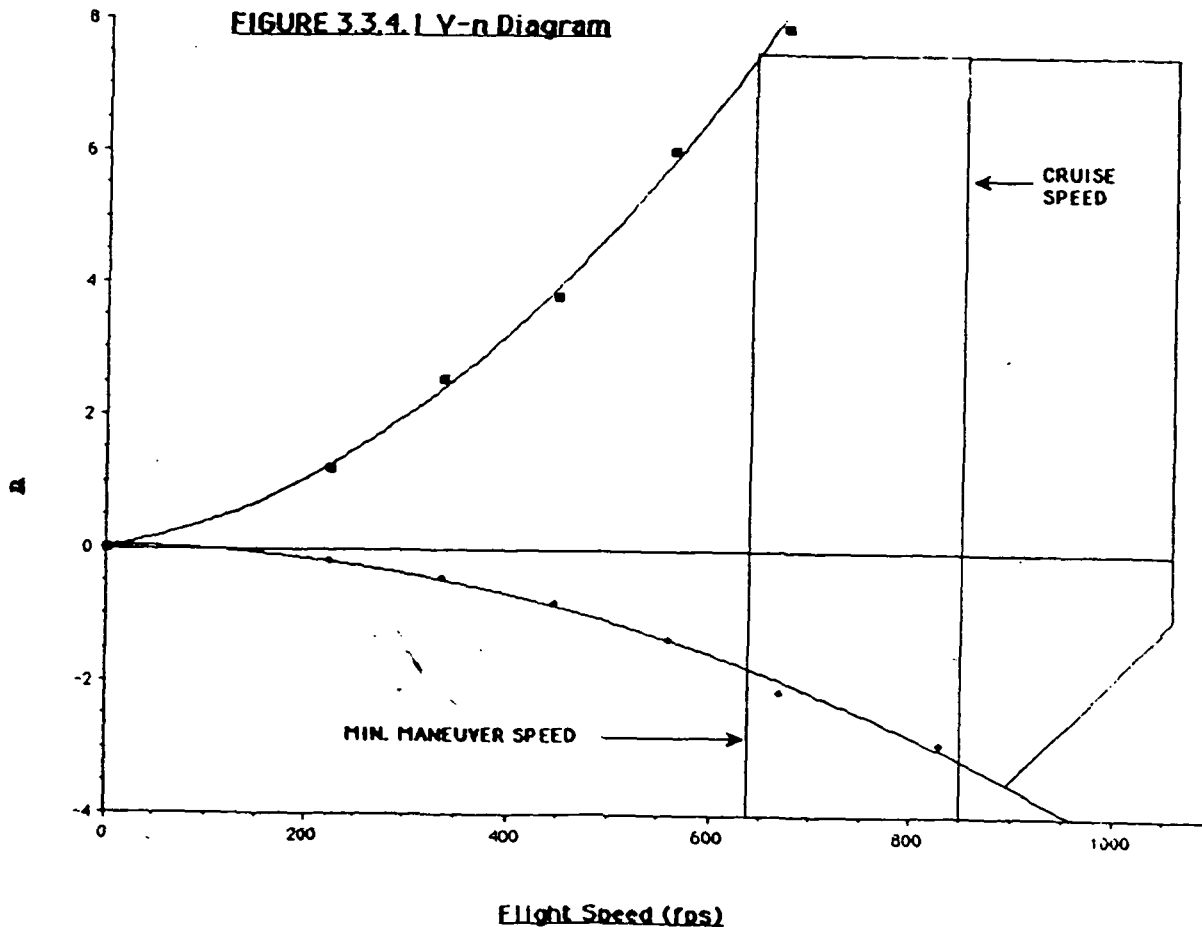
3.3.4 V-n Diagram:

From the analysis of the aerodynamic limits and the structural limits, the V-n diagram was constructed. This is presented in Figure 3.3.4.1. The diagram is based on maximum take-off weight at standard sea-level flying conditions. This was done because the primary design mission takes place at sea-level. From the diagram, the minimum dive speed and the minimum maneuver speed were determined. A summary of the Scorpion's minimum flight speeds are shown on Table 3.3.4A. Gust lines were also determined to ensure that the structural limits do not fall short of the loads that gusts create as defined by FAR 25 regulations. The Scorpion meets and exceeds the gust requirements.

**TABLE 3.3.4.A: FLIGHT SPEEDS AT SEA-
LEVEL**

Flight Condition	Speed (knts)
stall (flaps up)	126
maneuver	380
maximum	500
dive speed	625

Unfortunately, it is apparent that a very narrow maneuver envelope exists for the Scorpion. One can also deduce that low speed maneuverability is limited to low g-loadings. This is not desirable for the CAS role. The specific excess power curves show that the Scorpion has good climb performance. Therefore, the choice of engine is not the limiting factor, but the aerodynamic limits -- especially at low speeds -- have resulted in a narrow flight envelope. In order to rectify this, a supercritical airfoil is being considered to improve the aerodynamic capabilities of the Scorpion.



4.0 SIZING ANALYSIS

4.1 TAKE-OFF WEIGHT ESTIMATION

4.1.1 MISSION FUEL FRACTION

Upon prioritizing the design criteria and missions, the preliminary iterative process to estimate the minimum take-off weight was performed. An initial take-off weight was assumed and the corresponding empty weights were calculated using two different methods. The first method used a formula based on empirical data of similar type aircraft. The other method determined the empty weight by using the primary mission as the design parameter. The final minimum take-off weight was determined by repeatedly substituting different take-off weights until the two different empty weights converged.

The simpler of the two methods was to utilize the formula developed from empirical data. The following formula was used

$$(1) W_E = \text{inv. log}_{10} \{(\log_{10} W_{TO} - A) / B\}$$

where $A = .1362$ and $B = 1.00116$ for jet aircraft with a clean configuration.

The second method was used to determine the mission fuel weight. By doing this, one was able to subtract the weight of the fuel and the payload from the initial assumption for minimum take-off weight to obtain the corresponding empty weight. The fuel weight was ascertained by determining how much fuel was used for each leg of the primary design mission. The primary design mission consisted of six parts. Again, empirical data was used to determine the fraction of fuel used for,

1) start/warm-up, 2) taxi, 3) take-off, 4) landing and taxi. A summary of the total mission fuel fraction and the weight estimations can be found in Table 4.1.1.A For this particular mission, the aircraft stays at sea-level and therefore no fuel credit was accounted for climb or descent.

However, for the rest of the mission, several assumptions and interpretations had to be made. The rest of the mission legs were given either endurance credits or range credits depending on the maneuver. After take-off, the aircraft dashed out 250 nmi. to the bomb site at a speed of 500 kts, therefore Breguet's range equation

$$(2) R_{cr} = (Y/c_j)_{cr} (L/D)_{cr} \ln (W_4/W_5)$$

was used. By solving the above equation for the inverse of the ratio of initial to final weights, the fuel fraction for the dash out to target can be obtained. The range and velocity are given in the mission profile. The specific fuel consumption was assumed to be 0.85. This number was chosen from a range of empirical data supplied in Reference 1. The lower end of the range was chosen since the maneuver was a cruise using no afterburners. Also, a slightly higher number than the minimum was used because the values given were for an aircraft flying at altitude and the primary design mission required the aircraft to fly at sea-level, therefore, a conjecture was made that slightly more fuel would be used to fly at a lower altitude. The lift-to-drag ratio used was an average value, from empirical data supplied in Reference 1, for a range of L/Ds for fighters. The same method was used to determine the fuel fraction for a dash back to base.

The combat maneuver was given endurance credits. Thus Breguet's endurance equation was used.

$$(3) E_{1tr} = (1/c_j) (L/D)_{1tr} \ln (W_5/W_6)$$

By solving for the inverse of the ratio of initial to final weight, the fuel fraction used for the dropping of bombs was determined. The entire maneuver to drop the bombs in two low-altitude combat passes was estimated to take approximately five minutes to perform. A higher average specific fuel consumption of 1.2 was used during this phase since the aircraft performed rapid actions, possibly requiring the use of the afterburner, resulting in greater fuel consumptions. An average L/D for the combat passes was determined by taking the L/D of the dashes and dividing it by 3.5, an assumed average number of g's the aircraft might pull repeatedly during the combat phase.

After the combat phase, weight compensation for the weight of bombs dropped was made so that the bomb weight would not be calculated as part of the fuel used during combat. This was done by subtracting the weight of the bombs from the current weight of the aircraft after the combat phase.

For the true empty weight of the the aircraft, the weight of the reserve fuel was also calculated and subtracted from the take-off weight. Again, this phase was given endurance credit and the endurance equation was used. Since the aircraft was assumed to be loitering with no afterburners, a lower specific fuel consumption value of 0.85 and a high L/D value of 9 were assumed for an endurance time of twenty minutes (as specified in the design requirements).

After multiplying the mission fuel fractions obtained for each leg of the mission, an overall mission fuel fraction of 0.77 and a total fuel weight

of 12,045 lbs were determined. This fuel weight plus the weight of trapped fuel and oil and entire payload weight, i.e. the crew and total payload (including the external stores) were subtracted from the weight at take-off. After several iterations, the final take-off weight was estimated to be 53,050 lbs. and the empty weight was 27,228 lbs. A summary of these weights can be found in Table 4.1.1.A.

TABLE 4.1.1.A : RESULTS OF MISSION FUEL FRACTION

TAKE-OFF WEIGHT	53050 LB
EMPTY WEIGHT	27235 LB
FUEL WEIGHT	12045 LB
MISSION FUEL FRACTION	0.77

4.2 SENSITIVITY STUDY

After determining the take-off weight using the method outlined in the previous section, and tabulated in the mission fuel fraction, it was desirable to determine the take-off weight sensitivity with respect to several parameters. The parameters chosen were payload weight, empty weight, range, lift to drag ratio, and specific fuel consumption. The growth factor due to payload weight was computed to be six pounds of added weight for each pound of added payload, a typical value when compared to existing aircraft. The growth factors due to range, velocity, lift to drag ratio, and specific fuel consumption were also determined using standard relations found in Reference 1. The aircraft was most sensitive to variations in specific fuel consumption and lift-to-drag ratio since these values strongly effect the amount of fuel needed to complete the mission. A summary of the sensitivity results obtained are shown in Table 4.2.A.

TABLE 4.2.A SENSITIVITY STUDY AND GROWTH FACTORS

SENSITIVITY OF TAKE-OFF WEIGHT AND GROWTH FACTORS FOR SEVERAL PARAMETERS

PARAMETER	VALUE	MISSION LEG		
		CRUISE #1	CRUISE #2	LOITER #1
PAYLOAD WEIGHT (w_{pl})	dW_{to}/dw_{pl}	6.02 lbs/lb	6.02 lbs/lb	6.02 lbs/lb
EMPTY WEIGHT (w_e)	dW_{to}/dw_e	1.85 lbs/lb	1.85 lbs/lb	1.85 lbs/lb
RANGE (R)	dW_{to}/dR	92.8 lbs/nm	92.8 lbs/nm	N.A.
VELOCITY (V)	dW_{to}/dV	-46.4 lbs/kt	-46.4 lbs/kt	N.A.
SPECIFIC FUEL CONSUMPTION (C _f)	dW_{to}/dC_f	27,291 lbs	27,291 lbs	16,180 lbs
LIFT TO DRAG RATIO	$dW_{to}/d(L/D)$	-4640 lbs.	-4640 lbs.	-13780 lbs.

4.3 DRAG POLARS FOR PRELIMINARY SIZING

A drag polar is a graphical solution of the relationship between the total drag and total lift generated by an aircraft. The equation used to find the drag polar is

$$C_D = C_{D0} + C_L^2/\pi eAR$$

An aspect ratio of 4 was assumed. This number was chosen by comparing the empirical values of existing fighters with moderate to high aspect ratios. The zero-lift parasite drag coefficient was found using

$$C_{D0} = f/S$$

Both of these areas (f and S) are dependent on the estimated take-off weight obtained in the first part of the procedure. A range of surface areas (S) were calculated by multiplying the take-off weight by the range of wing loadings chosen. A linear relationship between the take-off and the equivalent parasite area was determined based on empirical values, supplied by Reference 1 for hundreds of aircraft.

The wetted surface area can be calculated by

$$\log_{10} S_{\text{wet}} = c + d \log_{10} W_{\text{to}}$$

where the c and d are linear regression coefficients. These values were obtained from empirical data from previous designs. However, typical values for these coefficients were supplied in Reference 1. The same equation can be used to find the wetted surface area

$$\log_{10} f = a + b \log_{10} S_{\text{wet}}$$

where a and b pertain to the linear relationship. They are dependent on the fineness ratio of the design. Representative quantities were again supplied in Reference 1.

Once these areas and the zero-lift drag coefficient were obtained, drag polars for specific configurations could be calculated. The five configurations considered were: 1) clean, 2) landing -- gear-up, 3) landing - gear-down, 4) take-off -- gear-up, and 5) take-off -- gear-down. Note that for the landing configurations, one engine was assumed to be inoperative. The zero-lift drag coefficient varied with each configuration. The deviations for Oswald efficiency factor and parasite drag coefficient were given in Reference 1. An assumed range of maximum lift coefficients were chosen for each configuration. However, CL_{max} was not used in calculating the drag polars. Remembering that the ratio CL_{max}/CL is proportional to the square of the ratio of velocity to stall velocity, the constant used to determine the actual CL used in the drag polars can be found in the climb requirements specified in Reference 1. Finally, substituting these values along with the varying C_{do} values in the drag equation, the drag polars for the desired configurations were acquired.

4.4 SIZING TO TAKE-OFF AND LANDING CONFIGURATIONS

The drag polars determined the range of lift to drag ratios for each take off and landing configuration. These values in turn were used to determine the corresponding thrust to weight ratios (T/W) for the assumed range of wing loadings. The following formula was used for both engines operating, and for one engine out.

$$(T/W) = \{(L/D)^{-1} + CGR \}$$

The climb gradient used for each configuration were standard military climb requirements, since none were given in the design criteria. A summary of these results are plotted in Figure 4.4.1.

4.5 SIZING TO TAKE-OFF AND LANDING DISTANCE REQUIREMENTS

Only one design parameter, take-off and landing distance, had to be considered during this phase of the preliminary sizing. Maximum take-off and landing ground roll of 2000 ft. are specified in the design requirements. Standard relations contained in Reference 1 were used in the take-off sizing, which assumed a level runway with negligible wind effects.

These equations were used to calculate the thrust to weight ratio (T/W) to values required at each take-off condition. The results obtained are plotted in Figure 4.5.1.

The preliminary sizing to the landing ground roll distance was determined using the following equations, to calculate wing loading at landing (W/S)_L

FIGURE 4.4.1 SIZING TO TAKE-OFF AND LANDING CONFIGURATIONS

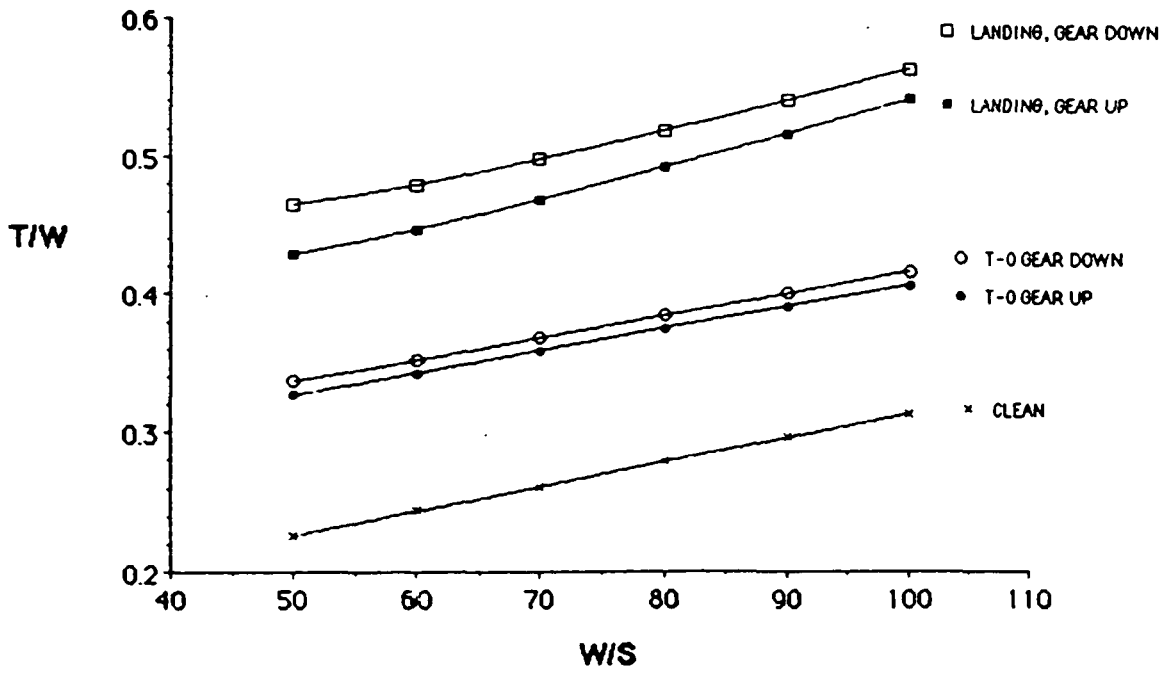
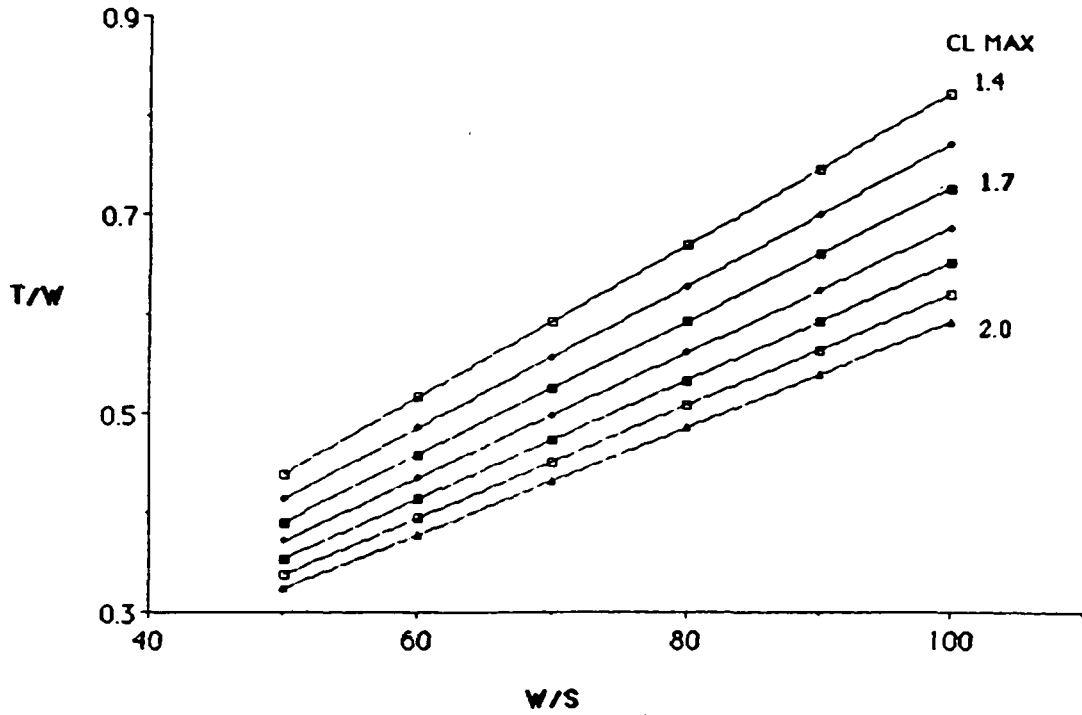


FIGURE 4.5.1 SIZING TO TAKE-OFF DISTANCE



$$V_{STALL} = (2 (W/S)_L / \text{DENSITY } C_{LMAX})^{1/2}$$

$$V_{STALL} = V_{APPROACH} / 1.3$$

$$V_{APPROACH} = (SFL / 0.3)^{1/2}$$

The total landing field length (SFL) was calculated by adding the landing ground roll to the distance required to clear a fifty foot obstacle in the landing approach flight path. See Figure 4.5.2 for a diagram of the landing approach used for this calculation. The wing loading at landing was then adjusted to values of wing loading at take-off (W/S)_{TO} using

$$(W/S)_{TO} = (W/S)_L (W_{TO} / W_{LMAX})$$

where,

$$W_{LMAX} = [W_{TO} - (W_{FUEL \text{ USED IN START/WARM-UP AND TAKE-OFF}})]$$

The final results for landing distance criteria are plotted in Figure 4.5.3.

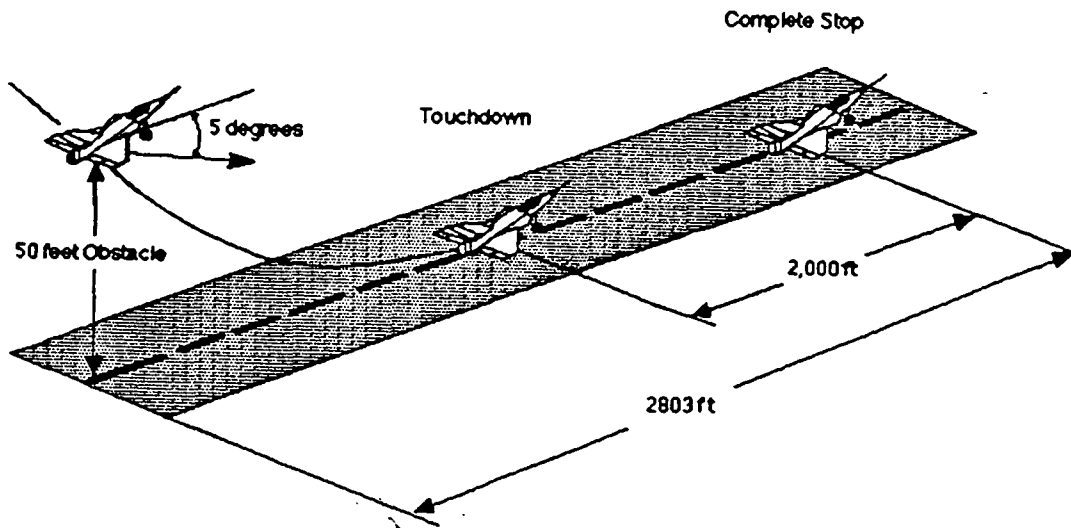
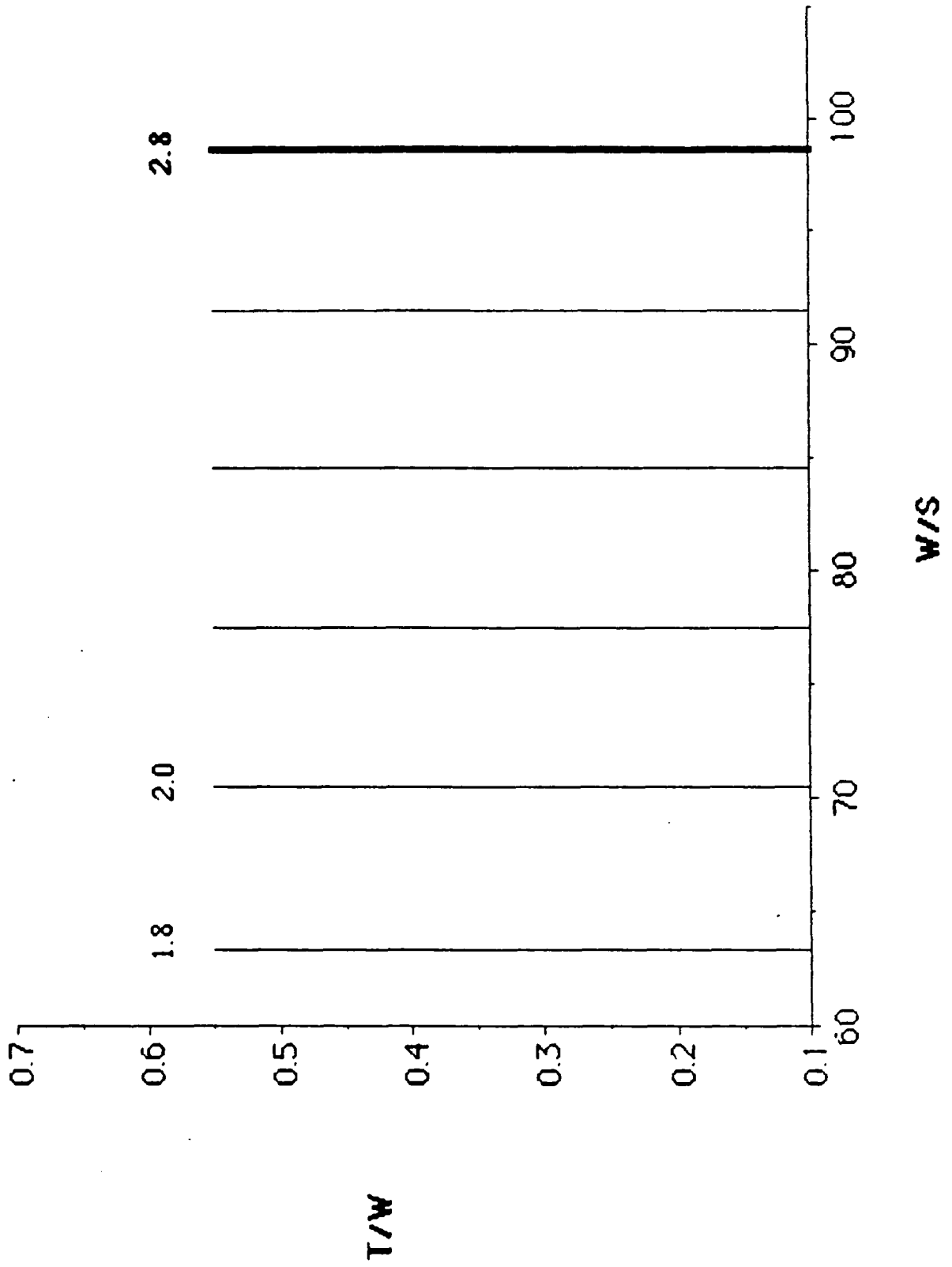


FIGURE 4.5.2 : LANDING DIAGRAM

FIGURE 4.5.3 SIZING TO LANDING DISTANCE



4.6 SIZING TO CRUISE AND MANEUVER REQUIREMENTS

The specific requirements for sustained maneuvering capability are contained in the mission profile specifications. The strictest maneuver given, a sustained 360 degree 4.5 g turn, was chosen as the design parameter for the maneuver sizing. The following equations and assumptions were made to calculate the thrust to weight ratios required at the specified wing loading values

$$T/W = (qC_{do})/(W/S) + (W/S)(n_{max})^2/(\pi Aeq)$$

where,

q = Maximum dynamic pressure (1000 psf)

C_{do} = Average profile drag coefficient (.015)

(incremented for compressibility)

n_{max} = Maximum g-load pulled (4.5)

A = Aspect Ratio (4.0)

e = Oswald efficiency factor (.825) [average value]

The results for thrust to weight from above were then adjusted to the required cruise speed values by multiplying by the correction factor

$$\text{correction factor} = W_{to}/(W_{to}-W_{0.5fuel}-W_{bombs}) = 1.60$$

these values were then adjusted again, using a thrust correction factor of 1.2 taken from data for typical engines used in existing close air support aircraft. This final calculation yielded the take-off thrust to weight values plotted in Figure 4.6.1. Also plotted in the same figure are the required

thrust to weight values at take-off for the cruise requirement. The following relation was used to determine these values for the required cruise Mach number of .744 at sea level.

$$T/W = C_{d0} (qS)/W + W/(qS\pi Ae)$$

where,

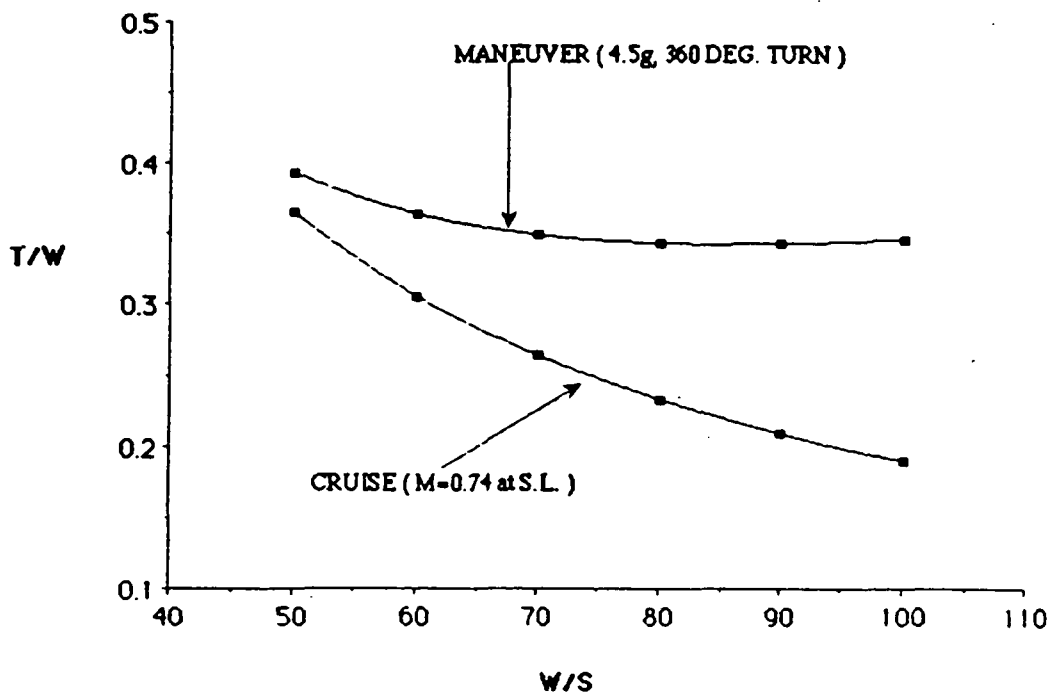
C_{d0} = average profile drag coefficient (.018)

$q = 1/2(\text{density})(V)^2 = 845.8 \text{ psf}$

A = Aspect ratio (4.0)

e = Oswald efficiency factor (.825)

FIGURE 4.6.1 SIZING TO CRUISE AND MANEUVER REQUIREMENTS

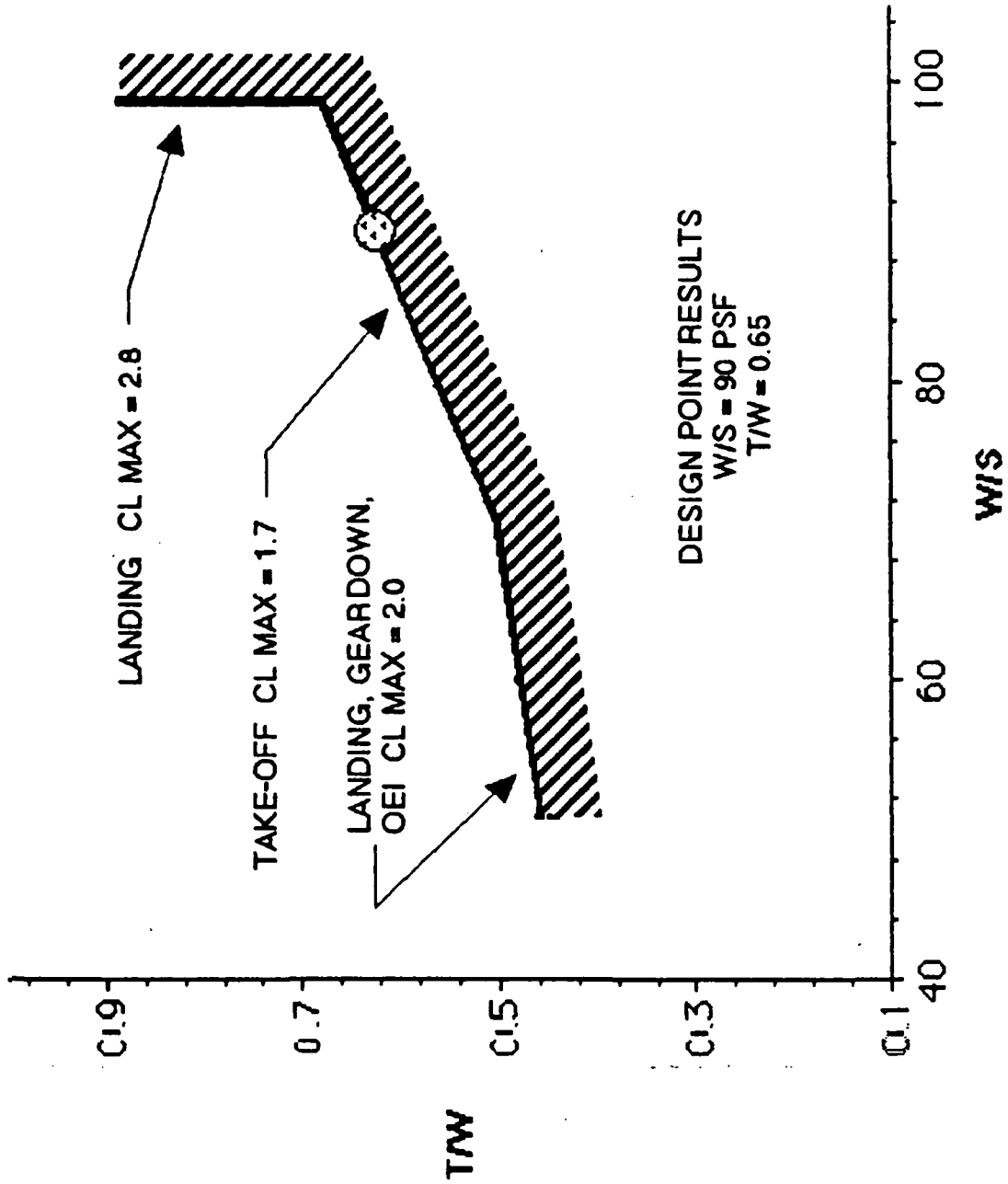


4.7 DESIGN POINT DETERMINATION

By combining all of the graphs generated in the previous sections, a range of thrust to weight ratios were determined for the assumed range of wing loadings. The sizing to landing with one engine out and landing gear-down was found to be the most restrictive of all the configurations considered. A CL_{max} of 2.8 was chosen from the sizing to landing requirement. By choosing this value, a higher wing loading could be considered for the Scorpion to lessen the effects of turbulence in low altitude, high speed flight. A CL_{max} value of 1.7 was chosen from the take-off sizing. This was a good average value that did not limit the envelope too severely and yet did not make the CL_{max} so high that an unreasonable amount of lift augmentation devices would have to be used thus increasing the take-off distance and aircraft cost. The final sizing results can be seen in Figure 4.7.1.

The design point chosen for the Scorpion was at the highest wing loading possible to reduce turbulence effects since the design mission will be flown at sea-level, and at the lowest thrust to weight ratio so that the size of the engine will not increase the estimated weight of the aircraft significantly. A thrust to weight ratio of 0.60 and a wing loading of 90 psf were chosen. This wing loading was also chosen in hopes of increasing the maneuverability of the aircraft since it is lower than most take-off wing loadings for similar aircraft, as evidenced in section 5.0 Configuration Comparison and Justification.

FIGURE 4.7.1 : PRELIMINARY SIZING RESULT



5.0 CONFIGURATION COMPARISON AND JUSTIFICATION

5.1 COMPARISON TO EXISTING CONFIGURATIONS

Figure 5.1.1 is a comparison of take-off thrust to weight vs. take-off wing loading for current configurations to that of the Scorpion. As one can see, all but two of the current CAS aircraft presently used are within the sizing envelope for the Scorpion. However, the Mirage 2000N and the Saab AJ-37 fall short of the range capabilities specified in the design mission profiles. Therefore, none of these configurations meet the design requirements. A summary of the characteristics for these aircraft, including their good and bad traits, can be found in Table 5.1.A.

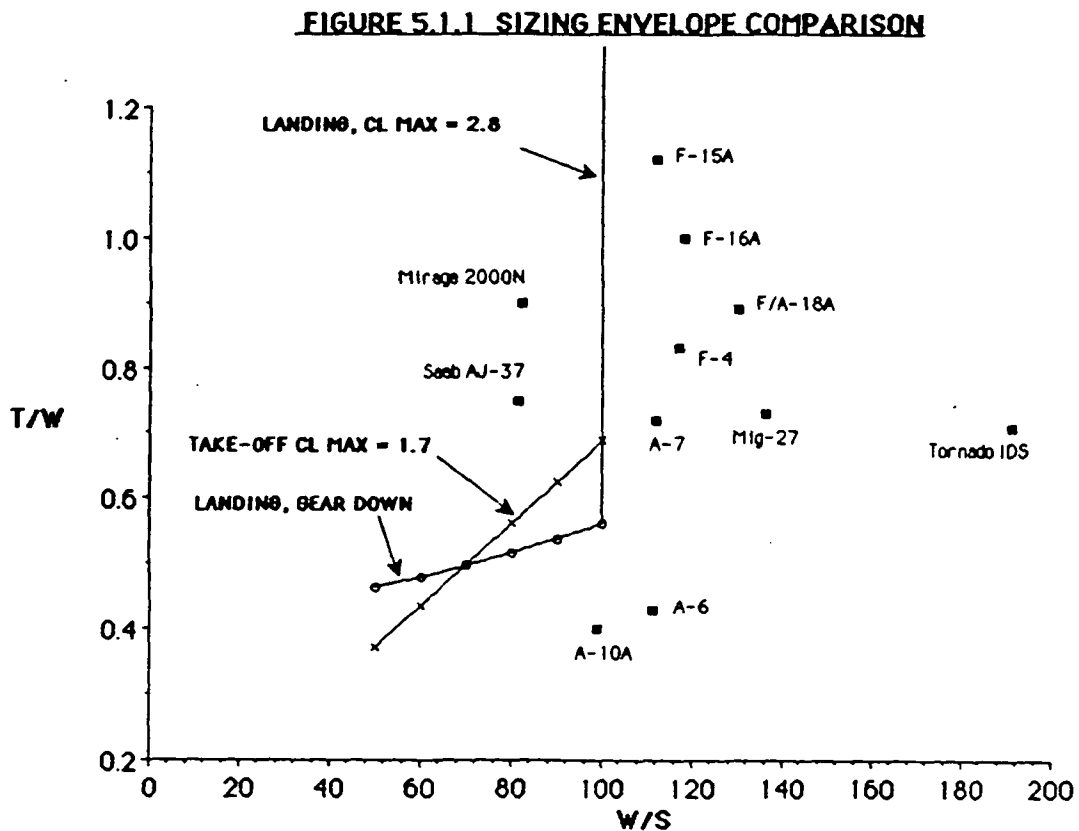


TABLE 5.1. A SIZING COMPARISON WITH EXISTING AIRCRAFT

Types of aircraft	W empty	W to max	T/W	W/S to max	V max high level	V max low level	Advantage	Disadvantage
Panavia Tornado IDS	31065	61700	0.51 to 0.71	191	2.2	1.2	<ul style="list-style-type: none"> * faster flight speed * similar payload capacity * similar fuel capacity * good short field performance * great lifting capacity and low level flight met by using a variable - sweep wing 	<ul style="list-style-type: none"> * cost
Mikoyan Mig-27 Flogger	24250	44313	0.57 to 0.73	136	1.6	0.95	<ul style="list-style-type: none"> * faster flight speed * variable-sweep wing * lighter empty weight * twin engines * heavy payload capacity * lighter empty weight * similar total T-O weight * similar landing distance * great slow speed maneuverability * Excellent survivability 	<ul style="list-style-type: none"> * less payload capacity * falls short of range capabilities * longer take-off distance * longer landing distance * slower flight speed * longer take-off distance * less fuel capacity
Fairchild A-10A Thunderbolt	21519	50000	0.4	99	0.59	0.68	<ul style="list-style-type: none"> * faster flight speed * lighter empty weight * similar payload capacity * short take-off distance * 5.5 g instantaneous * the high T/W ratio and moderate W/S in clean condition allowed an external payload to be carried that was nearly equivalent to the empty weight of the aircraft 	<ul style="list-style-type: none"> * falls short of range capabilities * longer landing distance * cost
General Dynamics F-16A Fighting Falcon	16234	35400	0.68 to 1	118	2	1.2	<ul style="list-style-type: none"> * faster flight speed * lighter empty weight * similar payload capacity * short take-off distance * 5.5 g instantaneous * the high T/W ratio and moderate W/S in clean condition allowed an external payload to be carried that was nearly equivalent to the empty weight of the aircraft 	<ul style="list-style-type: none"> * heavier empty weight * much longer take-off distance * much longer landing distance * carrier base aircraft * much higher approach speed
Grumman A-6 Intruder	26746	60400	0.32 to 0.43	111	0.94	0.85	<ul style="list-style-type: none"> * similar flight speed * greater payload capacity * similar take-off weight * greater fuel capacity * long range / loiter 	<ul style="list-style-type: none"> * heavier empty weight * much longer take-off distance * much longer landing distance * carrier base aircraft * much higher approach speed

AIRCRAFT COMPARISON (continued)

Types of aircraft	W empty	W to max	T/W	W/S to max	V max high level	V max low level	Advantage	Disadvantage
McDonnell Douglas F-4 Phantom	29536	61795	0.58 to 0.83	117	2.0+	1.19	<ul style="list-style-type: none"> * faster flight speed * similar empty weight * greater payload capacity * similar fuel capacity 	<ul style="list-style-type: none"> * longer take-off distance * longer landing distance * cost
LTV A-7 Corsair	09781	42000	0.72 max	112	N/A	0.92	<ul style="list-style-type: none"> * similar flight speed * similar payload capacity * lighter empty weight * lighter max take-off weight 	<ul style="list-style-type: none"> * much longer take-off distance * much longer landing distance * falls short of range capabilities
McDonnell Douglas F-15A Eagle	28600	56000	0.74 to 1.12	112	1.5	1.2	<ul style="list-style-type: none"> * faster flight speed * greater payload capacity * much greater max T-O weight * similar fuel capacity * surplus of specific excess power and relative low W/S promised a great deal of lifting capability * much shorter take-off distance 	<ul style="list-style-type: none"> * heavier empty weight * short in endurance * cost (landing distance N/A)
McDonnell Douglas F/A-18A Hornet	21830	51900	0.62 to 0.89	130	1.8	1.01	<ul style="list-style-type: none"> * faster flight speed * greater payload capacity * lighter empty weight * similar max take-off weight 	<ul style="list-style-type: none"> * falls short of range capabilities * carrier base aircraft * cost (take-off, landing distance N/A)
Dassault-Breguet Mirage 2000	17000	36375	0.59 to 0.9	82	2.35	1.2	<ul style="list-style-type: none"> * faster flight speed * greater payload capacity * lighter empty weight * short T-O, landing distance 	<ul style="list-style-type: none"> * falls short of range capabilities * delta wing decreases the maneuverability * cost
Saab AJ-37 Viggen	23150	40000	0.65 to 0.75	81	2.0+	1.19	<ul style="list-style-type: none"> * faster flight speed * similar empty weight * similar payload weight * very short T-O, landing distance * lighter take-off weight * canard foreplane give good STOL performance to a delta-wing layout adding lift and enhancing wing lift 	<ul style="list-style-type: none"> * falls short of range capabilities * cost

5.2 CONFIGURATION SELECTION AND JUSTIFICATION

5.2.1 HIGH SPEED ROTORCRAFT

NASA Ames Research Center is currently undergoing a preliminary design investigation to produce a high speed rotorcraft. This rotorcraft is to be capable of 450 knot cruise and a 650 nmi civilian or 350 nmi military mission.

There are several configurations that are being considered. These include high speed tilt-rotor, variable diameter rotor, stowed/folding rotor, X-wing and other stopped rotor arrangements. Some of these aircraft rely on rotor lift throughout the flight envelope, while others use rotor lift only in transition from take-off or landing to the high speed regime, where more conventional lift and propulsion would be used. These aircraft provide excellent maneuverability and require no airstrip to operate, hence they can be used very close to the battlefield. This advantage allows for high sortie rates and very short turnaround time, however, the disadvantages outweigh the advantages for this design mission.

Currently, the most favored concept is the advanced tilt/folding rotor. This aircraft would meet the range requirement of the CAS mission, and approach the desired cruise speed, but falls short with a payload capability of only 500 lbs. There are several other design shortfalls for this configuration. A high speed rotor would require a thin airfoil with swept tips. One of the most difficult design problems is in the aeroelastic tailoring that is needed for thin airfoils since they have a tendency to flutter and aeroelastically diverge. Also, better methods are needed for

vibration analysis; as vibrations are of key contention in the structural analysis of these airframes. Tilt rotor aircraft also have drawbacks in the field. They require an enormous amount of support and maintenance for the amount of flight time available. The workload for the pilot is also high, requiring more attention directed inside the cockpit, but in a close air support role, it is desirable to allow the pilot time to visually acquire the target and direct fire away from friendly forces. Also, due to the complexity of the aircraft, parts are expensive, increasing the life-cycle cost of the aircraft dramatically.

For the above listed reasons, it is felt that the tilt/folding rotor aircraft does not adequately meet the present requirements of the CAS role. It must be kept in mind that a large amount of expensive research and development work has yet to be completed for this aircraft configuration to become a reality. It is for these reasons that this configuration was not pursued.

5.2.2 POWERED LIFT

Present VERTOL and STOVL aircraft have the capability to meet the some CAS role requirements. However, for this design mission, the payload requirement is so high that huge engines would have to be used to enable the aircraft to take-off. Also, most of the disadvantages of this aircraft type are common to the tilt rotor as well: high maintenance/support requirements, high initial and parts costs, and high pilot workload. Since the Scorpion will have the use of a 2000 ft. airstrip, it is not deemed that jump jet capabilities present a plausible trade-off for the disadvantages offered.

5.2.3 FINAL RESULTS OF PRELIMINARY SIZING ANALYSIS

The design criteria given in section 2.0 was used to determine the sizing to landing and take-off configuration, take-off and landing distance, and cruise and maneuver flight conditions. In this way, the initial sizing of the aircraft was completed. A design point for the Scorpion was chosen within the sizing envelope that yielded a thrust to weight ratio of 0.60 and a wing loading of 90 psf. This plot also indicated the maximum take-off wing loading to be 100 psf. The comparison of this design to other configurations has shown that none of the aircrafts currently in use meet all of the requirements specified and no type of vertical take-off aircraft would meet the payload requirement. The next phase of the design procedure was to choose an aircraft configuration that maximized the desired qualities in a close air support aircraft mentioned earlier, while minimizing the costs of manufacturing and maintenance. The determinations made concerning configuration, as a result of this preliminary sizing and research, resulted in, the Scorpion, a twin-jet with a conventional configuration capable of high subsonic cruise speeds and high maneuverability to evade anti-aircraft fire and deliver ordnance accurately in close proximity to friendly forces. The cockpit will be designed to maximize visibility for the pilot in all CAS battle conditions. Also, twin canted vertical tails were chosen to maximize survivability and maneuverability at high angles of attack by preventing shielding of the vertical tail in this flight condition. The following sections provide detailed preliminary analyses of the Scorpion's design, performance characteristics and further refinement of the aircraft design.

6.0 COMPONENT DESIGN

6.1 FUSELAGE AND COCKPIT LAYOUT

6.1.1 FUSELAGE LAYOUT

The fuselage layout and design was driven primarily by the size of the GAU-8 cannon and its required location in the nose of the aircraft beneath the cockpit. The minimum length for the cannon-ammunition drum combination (21 feet) and the ammo drum diameter (3.9 feet), detailed in the specifications for the GAU-8 cannon taken from Reference 3, forced the design of a blunt nose cone and large increases in fuselage cross sectional area in the region forward of the cockpit. This resulted in large increases in profile drag and made area ruling of the fuselage very difficult. Since, the Scorpion carries such a large complement of internal fuel, avionics and the two engines are buried in the fuselage, this determined the layout of all the major components from the very beginning of preliminary design. The mean diameter of the fuselage, determined from a scaled drawing of the aircraft, is 8.4 feet which yielded a overall fuselage fineness ratio of 6.2, which is relatively low for this type of aircraft. The Fairchild Republic A-10, which currently fills the close air support role and carries the same cannon, had a configuration which reduced the fineness ratio by mounting the engines to the fuselage exterior and carries a larger portion of its fuel in the wing rather than in the fuselage. However, this was not possible for the Scorpion because it would result in a large amount of profile drag and wave drag in the transonic region at which the aircraft must be able to cruise. Figure 6.1.1.1. shows the inboard layout of the Scorpion. The structural layout of the fuselage is detailed in section 7.0 Structures and

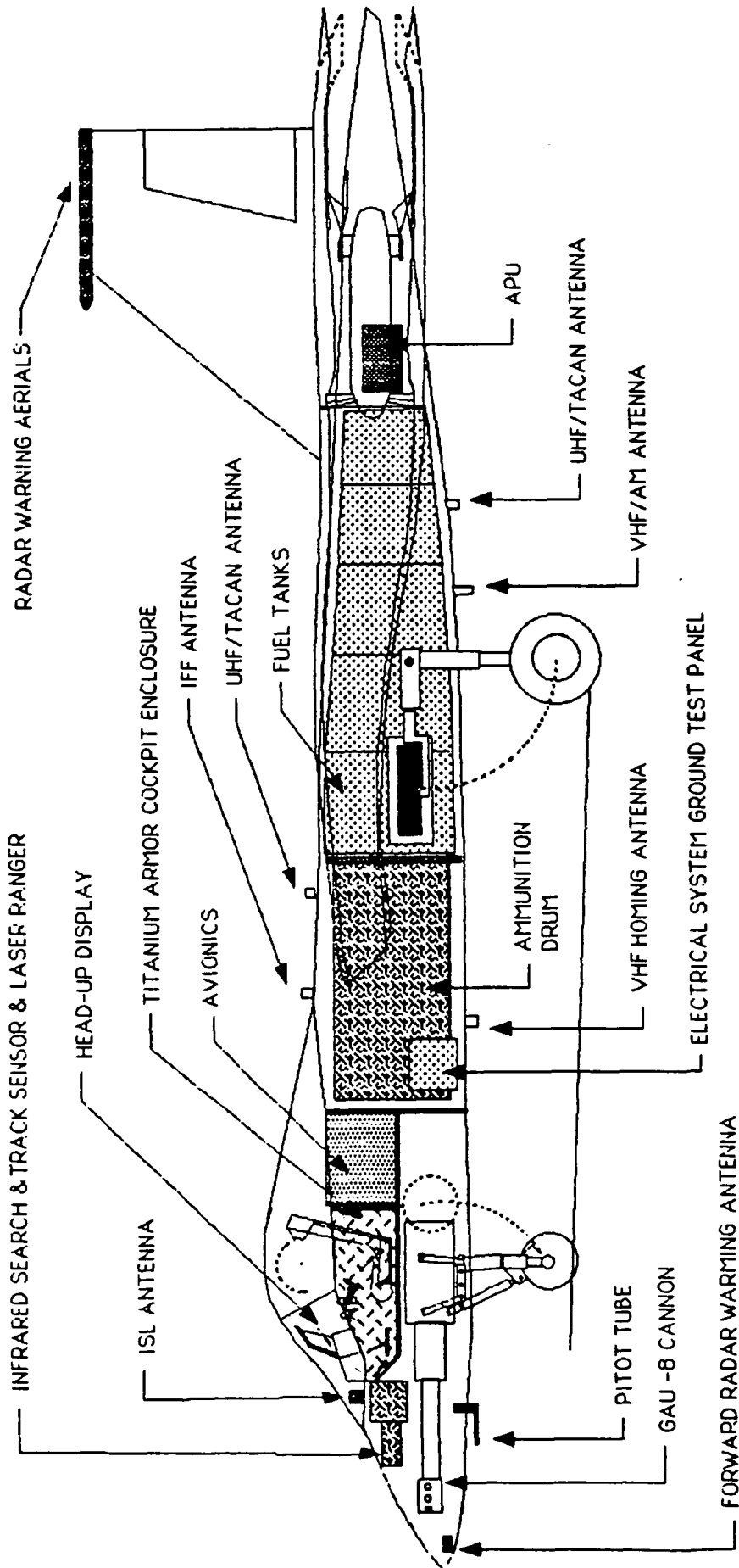


FIGURE 6.1.1.1 FUSELAGE LAYOUT

Materials and the major system layouts are shown in section 12.0 Systems Layout.

6.1.2 COCKPIT DESIGN

The main purpose of the Scorpion is to provide support to friendly forces that are in close proximity to enemy forces. Consequently, the pilot must be concerned with the proceedings on the ground, not in the cockpit. This was the driving force behind the design of the cockpit. The canopy is a bubble canopy that allows for maximum vision of the surrounding skies. The pilot seat is raised so that the pilot has a line of sight twenty degrees down the nose of the aircraft (see Figure 6.1.2.1) This far exceeds the minimum requirement of twelve degrees as specified by military specifications. A line of sight of forty-five degrees down the side of the aircraft is also provided. This provides for a good field of vision for the pilot allowing him to see both the surrounding airspace and the ground.

The instrument panel is designed to ease flight instrument reading. The pilot is provided with a head-up display as well as multifunction display screens to reduce the amount of instrumentation the pilot must monitor. This also helps to reduce the pilot workload and aid in keeping his attention on the outside environment. Figure 6.1.2.2 presents a detailed layout of the instrument panel.

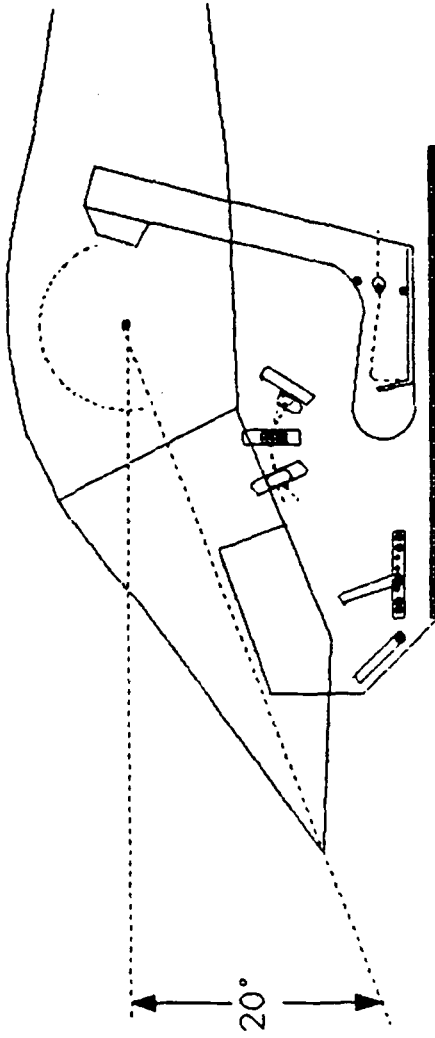
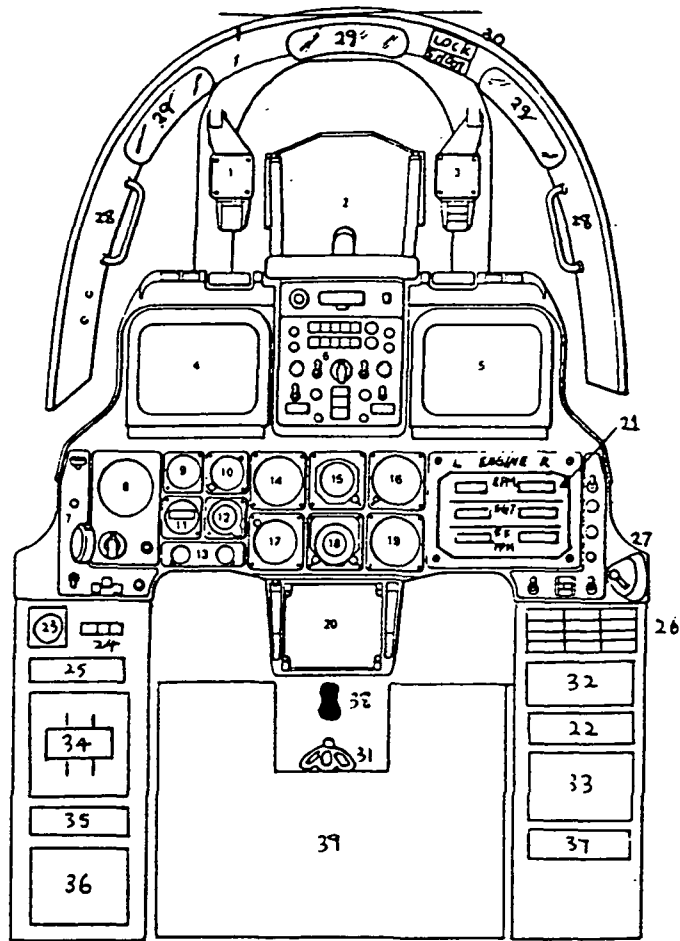
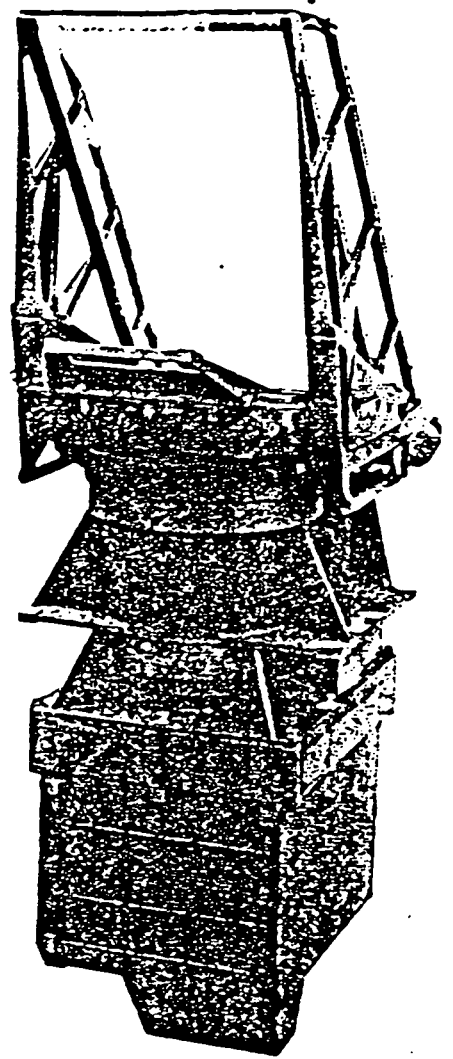
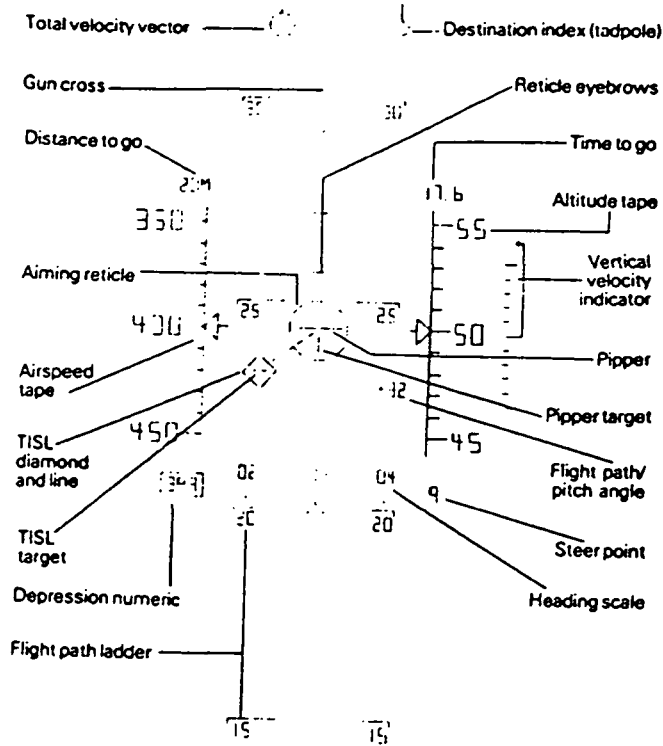


FIGURE 6.1.2.1 : COCKPIT LINE OF SIGHT



- | | |
|--|-------------------------------------|
| 1. Acceleration indicator | 19. Vertical velocity indicator |
| 2. Head-up display | 20. Armament control panel |
| 3. Standby compass | 21. Digital engine monitor display |
| 4. Left multifunction display | 22. ECM control panel |
| 5. Maverick TV display | 23. Back pressure indicator |
| 6. Display controls | 24. Emergency/ parking brake |
| 7. Landing controls | 25. Stores jettison indicator |
| 8. Fuel quantity indicator | 26. Caution light indicator |
| 9. Angle of attack indicator | 27. Static-pressure source selector |
| 10. Clock | 28. Canopy frame handle |
| 11. Channel frequency indicator | 29. mirrors |
| 12. Standby attitude indicator | 30. Lock/shoot indicator |
| 13. Hydraulics systems indicators | 31. Canopy jettison level |
| 14. Airspeed indicator | 32. Environmental control system |
| 15. Attitued director | 33. Navigation control |
| 16. barometric altitude indicator | 34. Throttle quadrant |
| 17. Radar warning receiver azimuth indicator | 35. Exterior lights |
| 18. Horizontal situation indicator | 36. Communications |
| 37. Interior lights | 37. Interior lights |
| | 38. Control stick |
| | 39. Seat |

FIGURE 6.1.2.2A : INSTRUMENT PANEL



INS HUD control unit

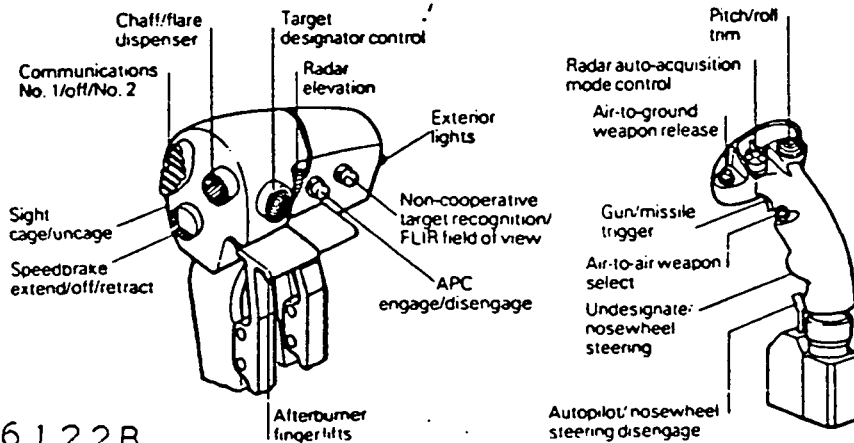
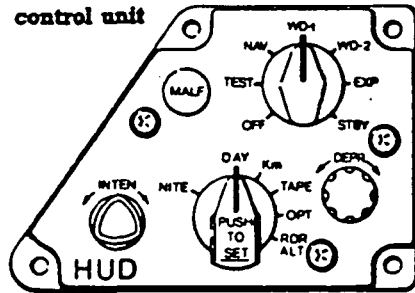


FIGURE 6 1.2.2.B

6.2 WING AND LIFT AUGMENTATION SYSTEM

6.2.1 WING PLANFORM PARAMETERS

From preliminary sizing analyses, using the maximum take-off weight and the chosen wing loading of 90 psf, a equivalent projected area of 590 sq. ft. was obtained. A high aspect ratio was chosen because it allowed for better maneuverability at low speeds, it incurred less induced drag and it allotted for more hard points under the wing as opposed to a delta wing or a cranked arrow. A root-tip ratio of 0.36 was chosen to be as close to 0.38 in hopes of achieving an elliptical wing lift distribution.

The airfoil chosen for the wing is a NACA 64A410. This airfoil was chosen for the transonic cruise requirement. In particular, it has a maximum thickness of 10%, a thinner airfoil increases the critical mach number and delays drag rise. Moreover, the lift distribution is such that the forces are distributed evenly along the chord instead of at the leading edge (refer to Figure 6.2.1.1). This allows for the wing spars to carry the loads more evenly than the typical distribution would and reduces torque at the root.

From analysis using Reference 12, it was found that the wing had to be swept back twenty degrees to further increase the critical mach number so that it is above the cruise mach number of 0.744. However, sweeping the wing back causes a build-up of the boundary layer at the tip and results in tip stall. Using Reference 13, a two degree washout was estimated to prevent the problem. This series of NACA airfoils also has one of the higher

values of maximum lift coefficients. The 64A410 has a $C_{l\max}$ of 1.5 and stalls at sixteen degrees.

6.2.2 LIFT AUGMENTATION SYSTEMS:

An nonaugmented $C_{l\max}$ of 1.66 was determined for landing conditions. According to the preliminary sizing, a $C_{l\max}$ of 2.5 is necessary to meet the 2000 ft strip landing requirement. This was the limiting factor in choosing the lift augmentation system. From preliminary sizing, Fowler flaps and leading edge slats (which can be seen on Figure 6.2.2.1) were found to be sufficient to obtain this $C_{l\max}$. Simpler flaps were also feasible. This would reduce the weight and the cost of the wing. However, using a simpler flap system would require the flaps to cover the entire span. This would not leave enough room for ailerons and would require the use of spoilers. Since spoilers inherently incur a large amount of parasite drag and cause a large yawing moment, the advantage of using a more costly lift augmentation system and ailerons for increased low speed maneuverability outweighed the savings gained using the simpler flaps and spoilers.

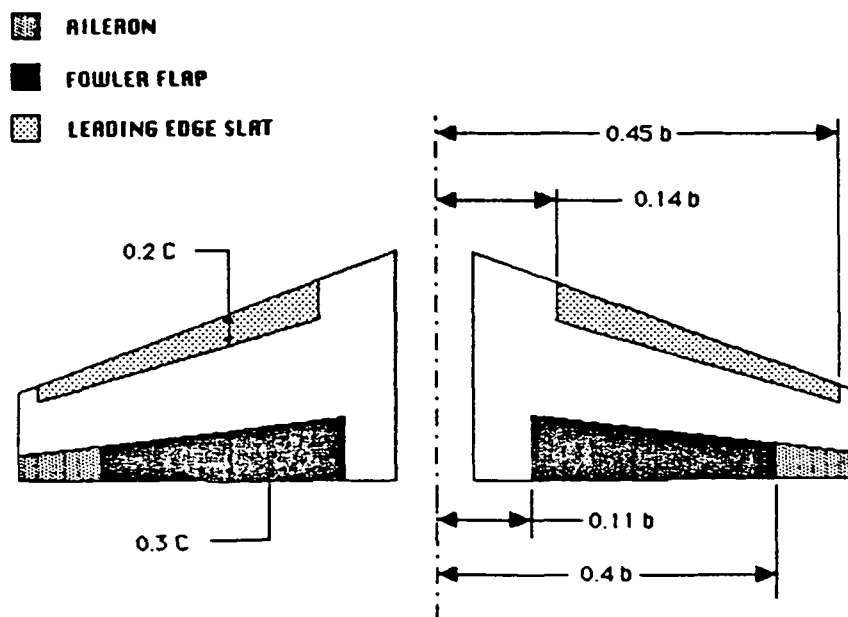


FIGURE 6.2.2.1 : FLAP SYSTEM

6.3 EMPENNAGE:

The empennage consists of two horizontal stabilators and two twin vertical tails canted out 20 degrees from the vertical axis. Two of each type of control surface was selected for redundancy, hence increasing the survivability of the aircraft. The vertical tails were canted out to keep them in the freestream flow at high angles of attack. Horizontal stabilators were preferred over conventional horizontal tails because they provided the necessary amount of control with less surface area; consequently decreasing the parasite drag of the tail. In addition, they are lighter and less expensive than conventional tails.

For both the horizontal and vertical tails, a NACA 0009 airfoil was selected. A thinner airfoil was chosen as compared to that of the wing to guarantee the critical mach number is equivalent or greater than that of the wing. Also this airfoil is symmetric so as much lift can be generated in a downward direction as in an upward direction for trim and maneuvering considerations. Both control surfaces are swept back again to increase the critical mach to fulfill the transonic cruise requirement.

The empennage was sized using longitudinal and directional x-plots. A static margin of two percent stability was chosen which resulted in a total horizontal tail area of 60 square feet and a total projected vertical tail area of 148 square feet. Both surfaces were placed far back to provide adequate pitch and yaw control. The vertical tails are positioned slightly in front of the horizontal stabilators to provide enough clearance so that both control surfaces can be deflected simultaneously. Also, the vertical tails are larger than vertical tails of existing aircraft of similar weights to

provide enough control for large yawing moments that are produced in one engine inoperative flight. The rudder is thirty percent of the chord and covers sixty percent of the span.

6.4 PROPULSION INTEGRATION

Scorpion's propulsion system was designed and evaluated using the methods developed in References 2 and 6. These methods require manufacturers data for uninstalled engines for a range of altitudes, Mach numbers and throttle settings. Engine data satisfying these requirements were found from General Dynamics manufacturers data included in appendix A. This static test data was based on ideal conditions and would have to be adjusted to account for inlet inefficiencies, and power extraction unique to Scorpion. It was found that this turbofan engine fulfilled Scorpion's specifications for weight, thrust, and size while performing all mission phases. The following paragraphs document how these effects were calculated and sample calculations can be found in the appendix.

6.4.1 INLET EFFICIENCIES

The highest possible inlet efficiency was sought while minimizing foreign object ingestion and cannon exhaust inhalation. A "clean" air supply, free of turbulence and foreign objects, would help maximize inlet efficiency. During ground operation, the above wing inlet decreases the likelihood of foreign object ingestion while contoured inlet lips minimize flow separation to help decrease turbulence and provide a symmetric pressure distribution across the compressor face. At the design cruise condition, 500 kts at sea level standard, an engine air mass flow rate of 175 lbs/sec and a 4.4 square foot inlet area were determined based on theory outlined in Reference 6. To minimize inlet pressure loss, and increase engine performance, the inlets are placed slightly ahead of the leading edge to prevent boundary layer ingestion. To determine the inlet efficiency, the inlet pressure loss was calculated for an incompressible flow.

This resulted in an inlet efficiency of 0.97.

6.4.2 POWER EXTRACTION

The Scorpion's electrical, pneumatic and mechanical systems will be powered from bleed air taken from the engines. Electrical power will run such systems as flight controls through a fly by wire system. Engine start-up and fuel tank pressurization will be powered by a bleed air supplied pneumatics system. Lacking a detailed evaluation of bleed air, electrical, and mechanical requirements, Table 6.1 in Reference 6 was used to estimate a 300 HP value for power extraction.

The determination of power extracted and Inlet efficiency was then used to plot the engine performance. Equation 2 shows how available thrust (T_{av}) was calculated.

$$T_{av} = (T_{tst}/a_v) * (1 - 0.35 * K_t * M_1 * (1 - \eta_{inl}/\eta_{inc}) - 550(P_{extr}/U_1))$$

Figure 6.4.2.1 plots the available thrust versus flight speed for maximum nonaugmented thrust and figure 6.4.2.2 plots available thrust versus flight speed for maximum augmented thrust, for a range of altitudes. Figure 6.4.2.3 presents the variation of specific fuel consumption versus altitude, used to find the Scorpion's best cruise altitude for maximum range. The thrust data was then used to evaluate Scorpion's performance for rate of climb and maneuverability.

Afterburners were deemed necessary to propel Scorpion to take-off speed within the 2,000 foot limit specified, and also served to maximize combat maneuverability. The engine weight of 2,200 pounds, and length of

FIGURE 6.4.2.1 THRUST VS VELOCITY AT ALTITUDE

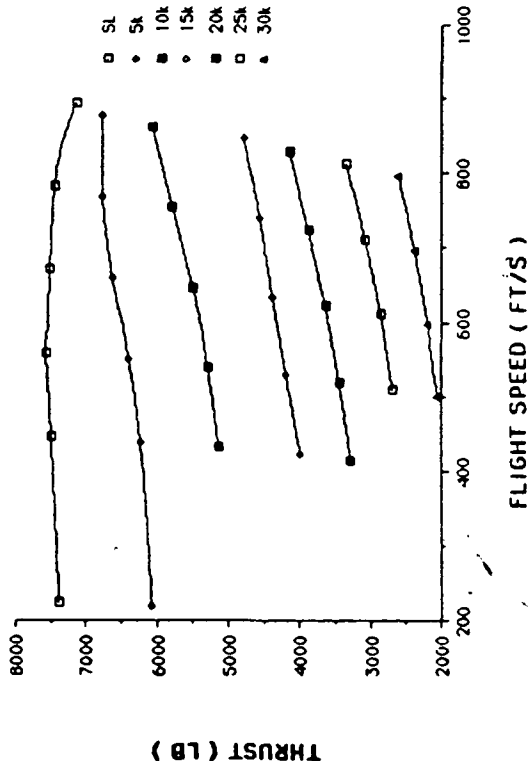


FIGURE 6.4.2.2 AUGMENTED THRUST VS. VELOCITY

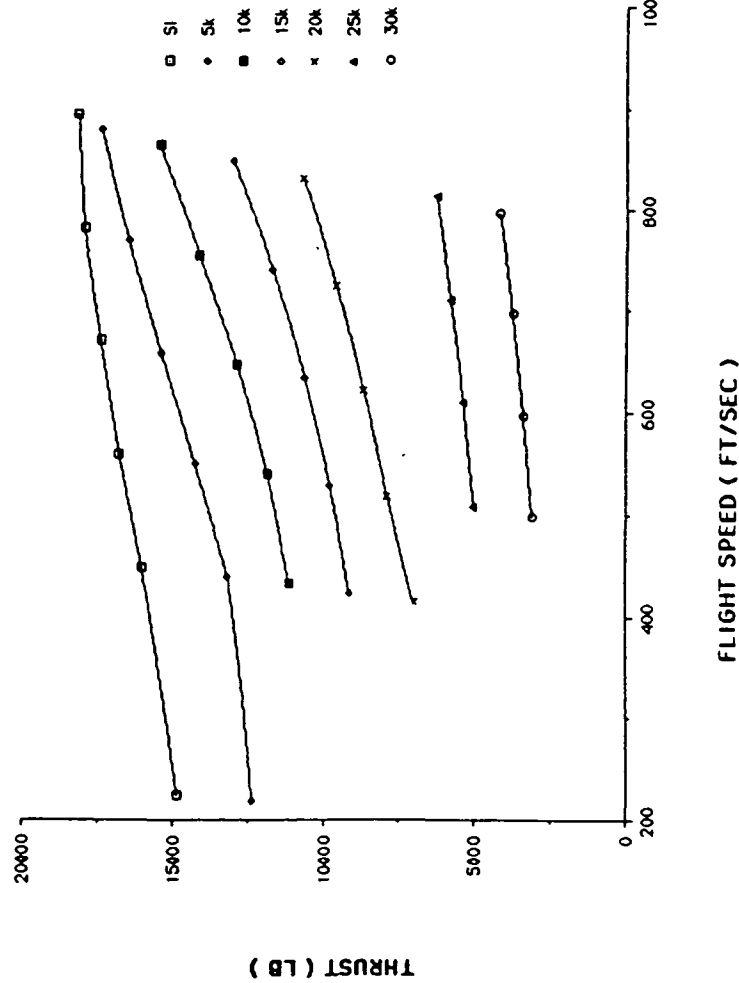
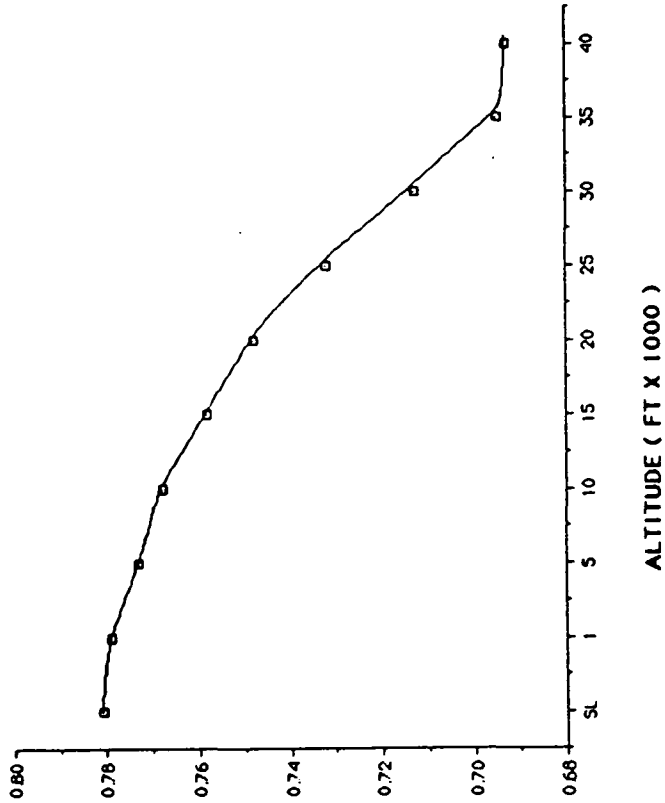


FIGURE 6.4.2.3: Thrust Specific Fuel Consumption vs. Altitude (at M=0.7)



13 feet also satisfies overall aircraft weight and length considerations quite well. The propulsion data, previously calculated, indicate two General Dynamics turbofan engines will fulfill Scorpion's role as a close air support aircraft.

These engines were placed in the rear of the aircraft to help balance the weight of the Gau 8 cannon located in the front of the fuselage. They were also placed partly submerged within the fuselage to reduce the profile drag of the aircraft. However, they were kept three feet apart with armor between them in the possibility that one engine incurs damage it will not affect the other one as severely. This increases the survivability of the Scorpion. Placing the propulsion in the rear of the aircraft also facilitates in the maintenance of them. They can easily be removed by sliding them out of the aircraft.

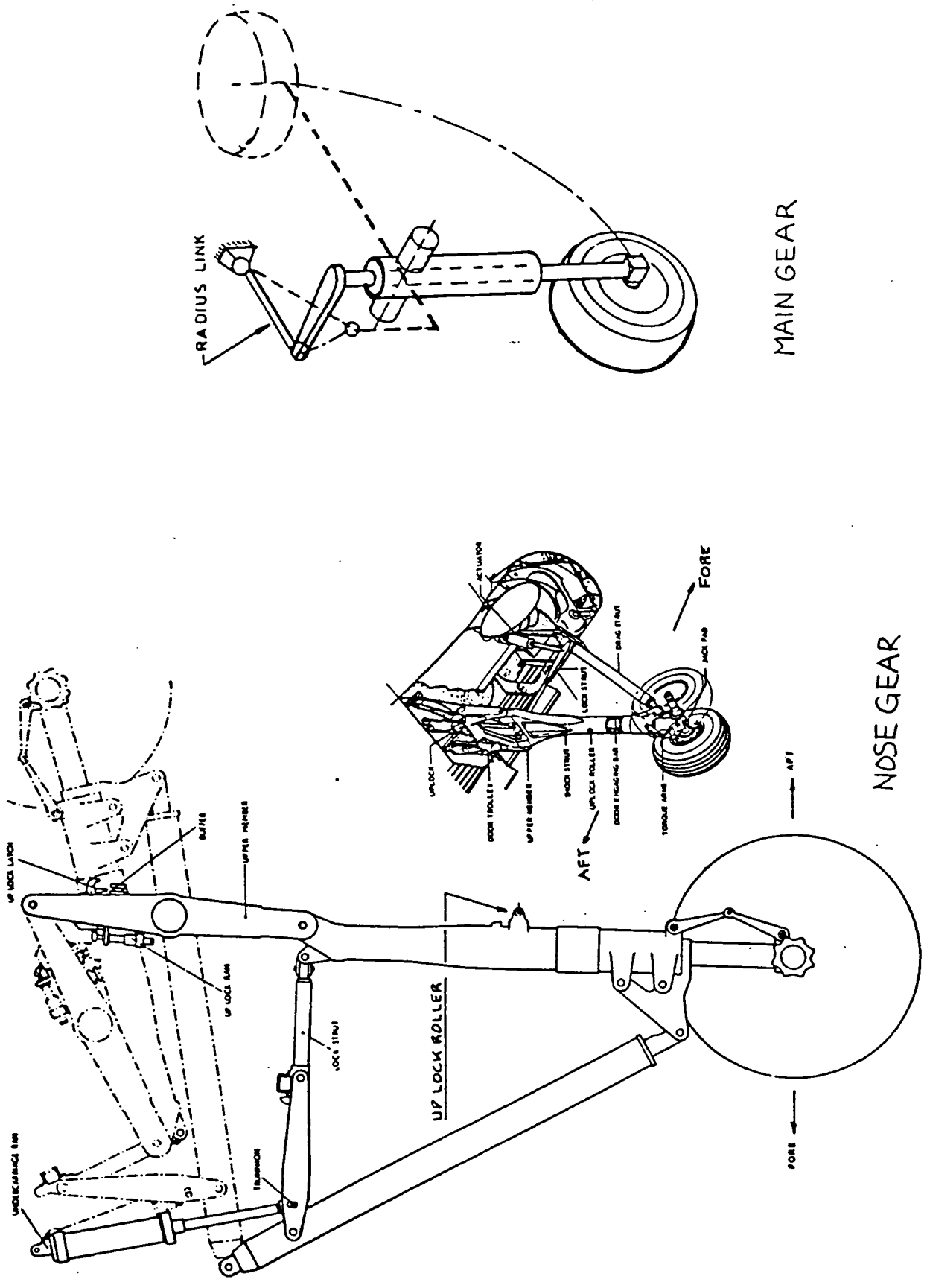
6.5 LANDING GEAR

The Scorpion's landing gear was optimized for ruggedness and performance on rough unimproved airstrips. A design sink speed of twelve feet per second, the maximum for United States Air Force and ground based United States Navy aircrafts was assumed. The final results are tabulated in Table 6.5.A and retraction schemes are shown in Figure 6.5.1. The maximum static loads were calculated from free body diagrams, then multiplied by a safety factor of 1.07 to yield the static loads shown in the table. The maximum dynamic loads were estimated using the factor $f(\text{dyn}) = 1.50$ suggested by Reference 4, to estimate these values. The take-off roll and landing touchdown velocities were determined then multiplied by a safety factor of 1.10. All values and dimensions are tabulated in Table 6.5.A and the retraction scheme is presented in Figure 6.5.1. Larger tires than required were selected to keep the tire pressures below 80 psi for rough field operation.

The landing gear lengths and placement were optimized to obtain the clearance angles for take-off rotation and lateral tip over criteria. These angles are also shown in Table 6.5.A. Foreign object damage (FOD) clearance angles for the debris from the nose gear into the inlets is also shown, and was exceeded in the vertical direction, but laterally, deflection guards are necessary and prudent for this aircraft's design mission profile.

TABLE 6.5.A : RESULTS OF LANDING GEAR SIZING

Take-off Speed	159 MPH	
Landing speed	135 MPH	
	<u>NOSE GEAR</u>	<u>MAIN GEAR</u>
Max. Static Load (lb)	6158	23446
Max. Dynamic Load (lb)	9237	35169
<u>TIRES</u>	2	2
B.F. Goodrich	22 X 7.75 - 11.5	37 X 14 - 14
8 ply tire		
Inflation Pressure	80 psi	160 psi
Max. speed	160 MPH	225 MPH
<u>STRUTS</u>		
Length (in.)	11	19.5
diameter (in)	3	4
<u>CLEARANCE ANGLES (deg)</u>		
Take-off Rotation	15.5	
Lateral Tip-over	42	
<u>FOD ANGLES (deg)</u>		
Vertical	34	
Lateral	9	*** Deflection Guards Required***



MAIN GEAR

NOSE GEAR

FIGURE 6.5.1. LANDING GEAR

7.0 STRUCTURES AND MATERIALS

7.1 STRUCTURES

The structural layout of the Scorpion is presented in Figure 7.1.1. to 7.1.6. Figure 7.1.1 shows the top view presenting the locations of pressure bulkheads, spars and hard point locations. The pressure bulkheads shown allows for cockpit pressurization to 10,000 feet altitude. Four main spars are used in the wing to transfer loads to the torque box. Four hard points on each wing and three hard points on the fuselage, for a total of eleven hard points, allow for various weapons loading scenarios as shown in section 13.0 Weapons and Integration. Titanium casing surrounding each engine, when coupled with the large engine separation achieved, allow for excellent survivability of the propulsion system. Figure 7.1.2 features the wing structure layout and its relationship to the wing control surfaces. Figure 7.1.3 presents wing-fuselage integration design, detailing the methods used to transfer the wing loads to the torque box. Figure 7.1.4 shows the structure associated with the horizontal stabilators. The stabilator's loads are distributed over the two aft engine frames, where the actuator is located as shown. Figure 7.1.5 presents the side view of the Scorpion's structural layout featuring the landing gear locations. The nose gear loads are distributed between a bulkhead and a frame located in the nose, while the main gear loads are supported by the two aft wing spars in the torque box of the fuselage. Figure 7.1.6 shows the supporting structures for the vertical tails. These loads are also distributed through three engine structure frames and the remaining structure supplies rigidity to the tails.

Overall, an average amount of structural synergism was achieved in the design of the landing gear, wing spars and torque box.

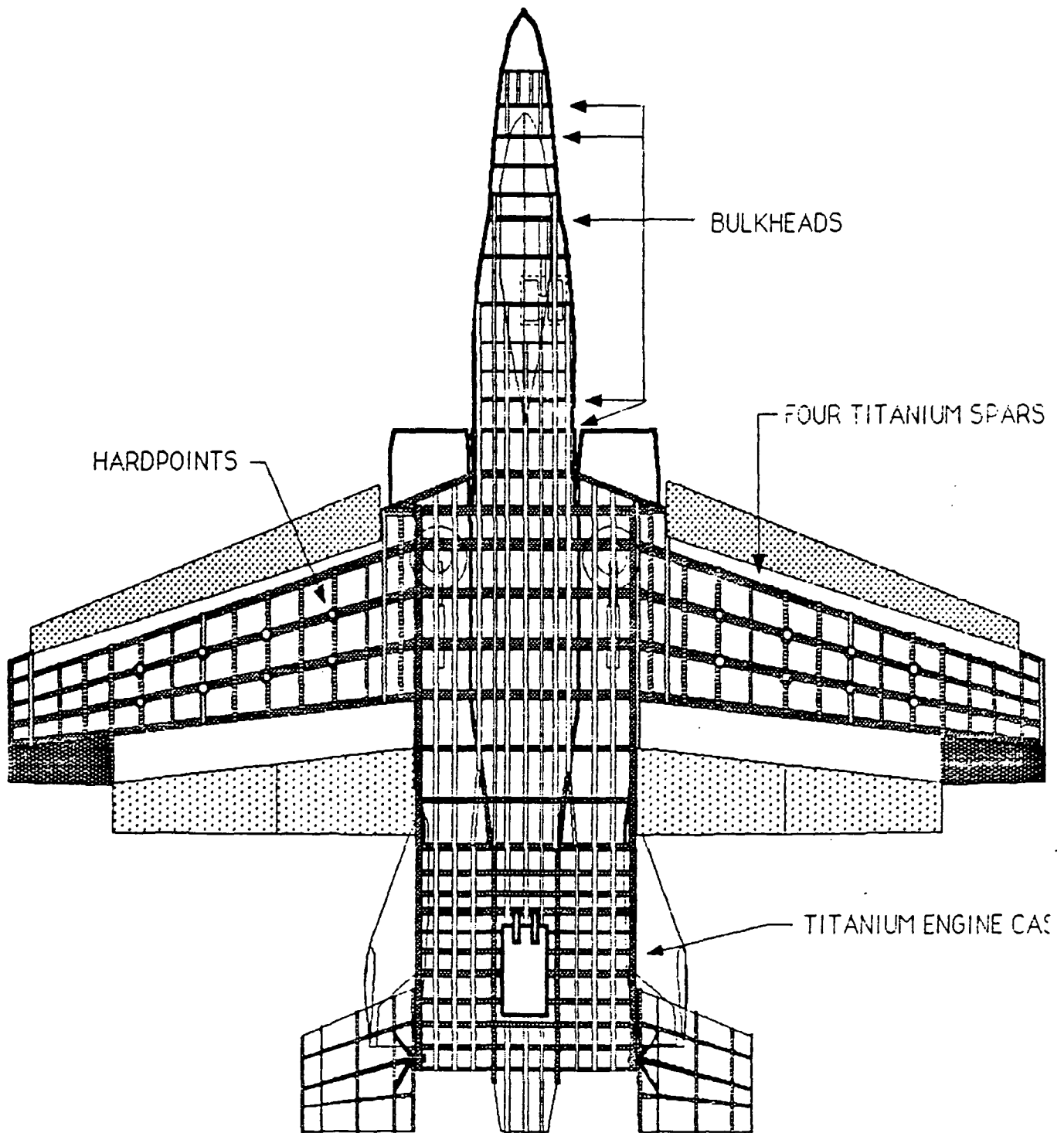


FIGURE 7.1.1 : STRUCTURE LAYOUT

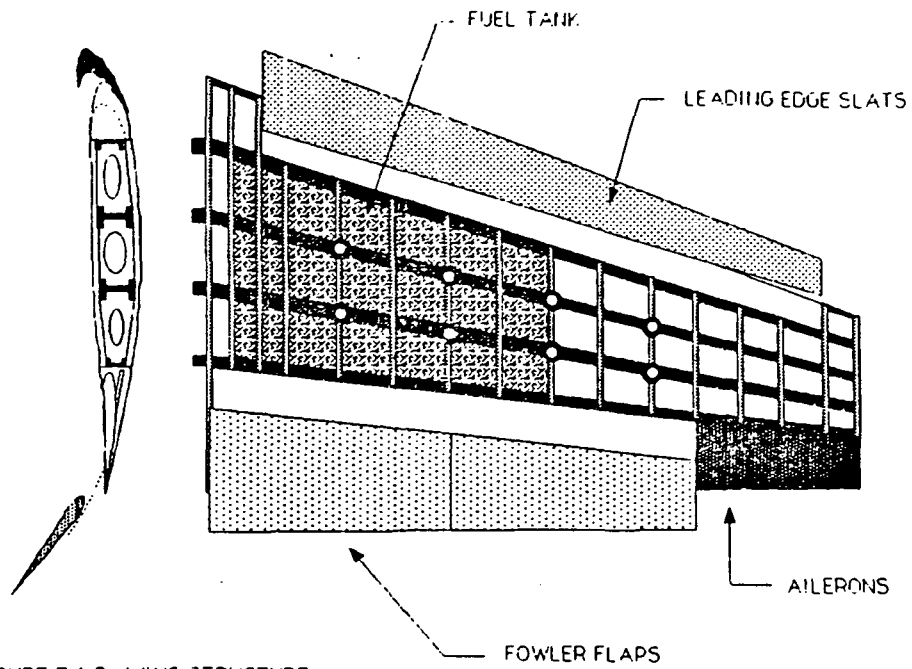


FIGURE 7.1.2 : WING STRUCTURE

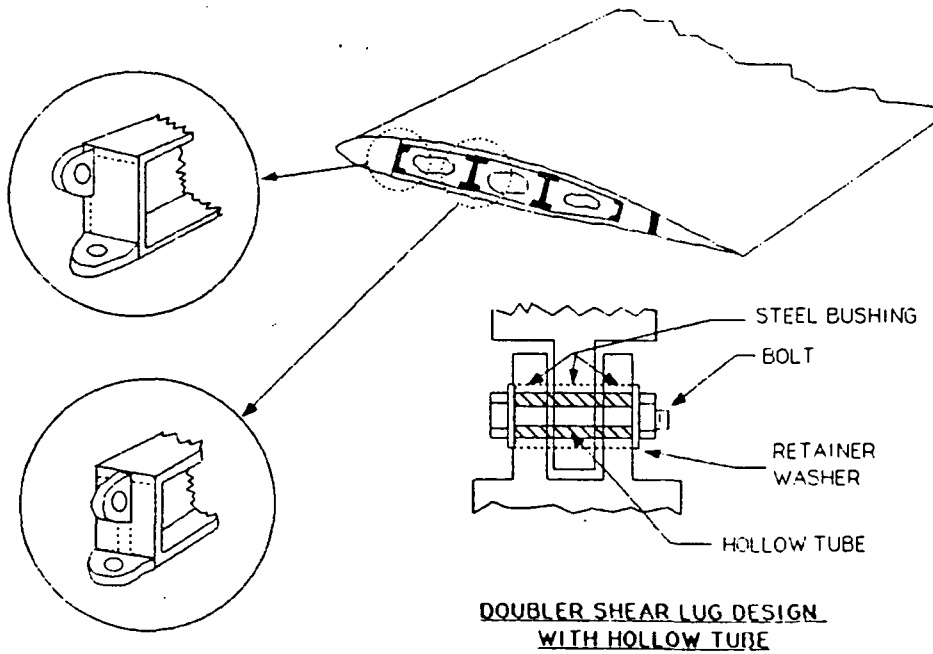


FIGURE 7.1.3 : WING-FUSELAGE STRUCTURE INTEGERATION

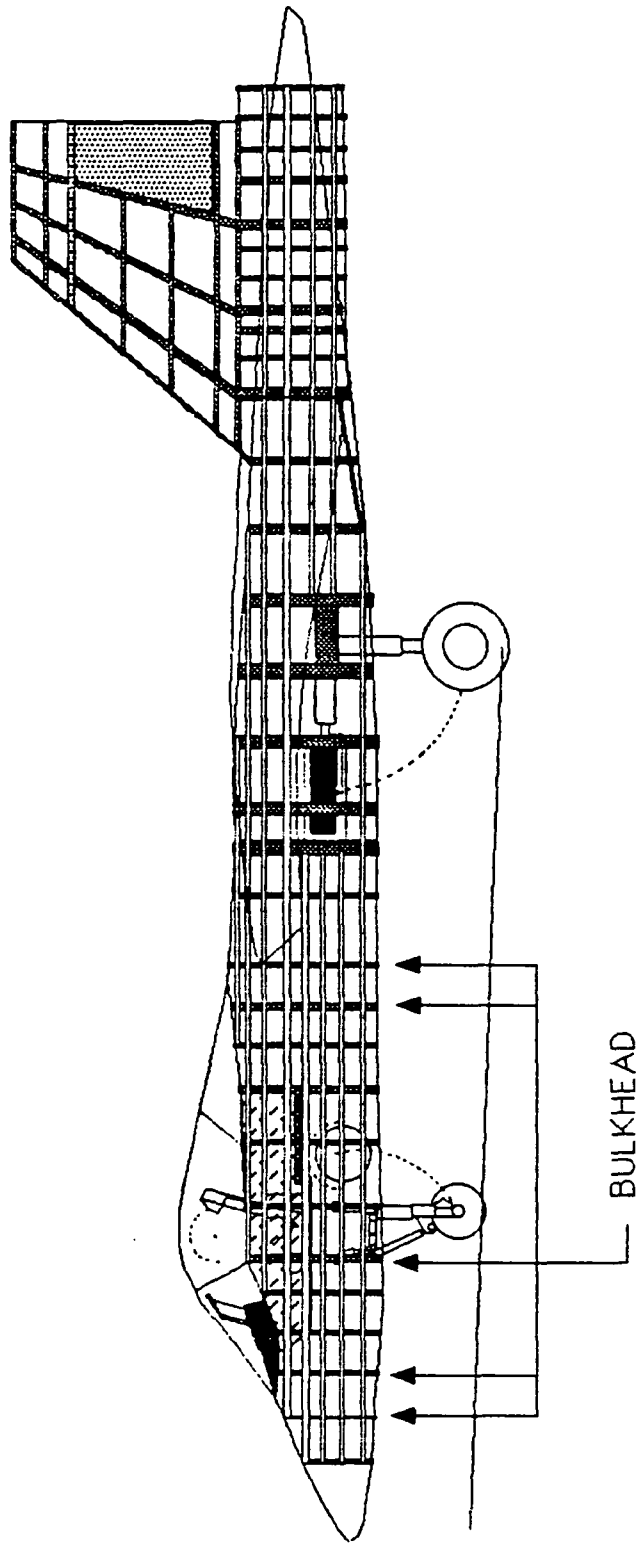


FIGURE 7.1.5 STRUCTURE LAYOUT

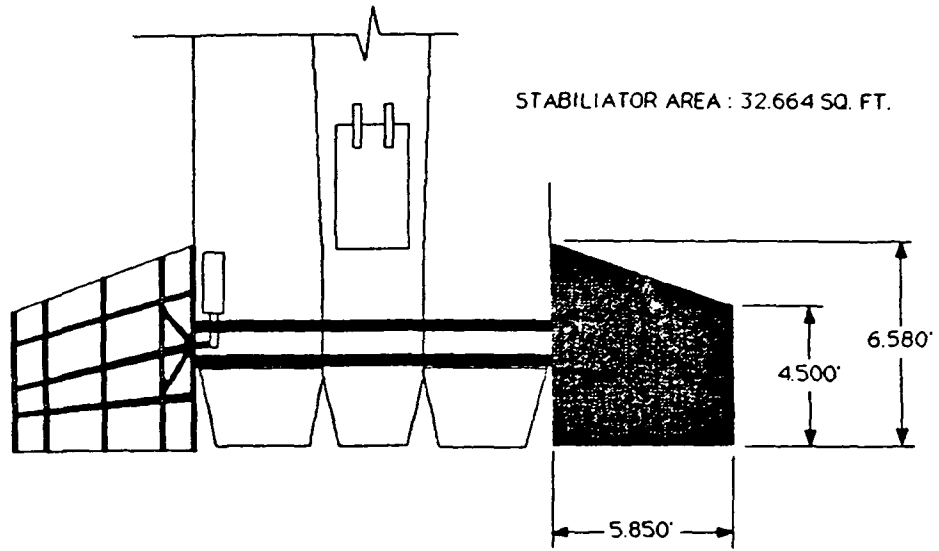


FIGURE 7.1.4 HORIZONTAL STABILATOR AND SUPPORTING STRUCTURE

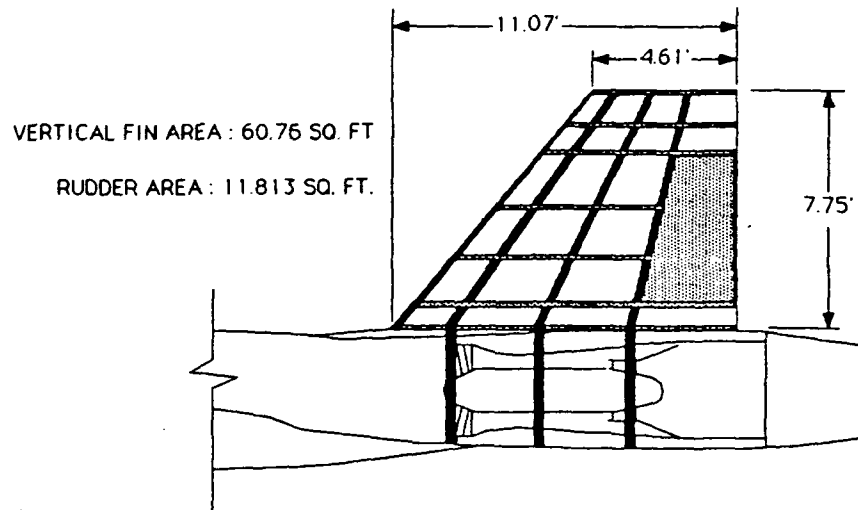


FIGURE 7.1.6 VERTICAL TAIL AND SUPPORTING STRUCTURE

7.2 MATERIALS

Figure 7.2.1 shows the materials used for the major structural components of the Scorpion. The Scorpion uses primarily aluminum in its structure due to its high strength, light weight, low cost and machinability. Steel is used for the nozzles and some highly loaded structural components, such as the landing gear struts and the bulkheads and frames supporting their loads. Titanium will be used in the wing spars and torque box due to its high strengths and on a portion of the stabilizers' skin, as shown, because of its high melting temperature. The use of titanium was avoided primarily due to its high cost. The canopy will be composed of Plexiglas with aluminum framing and the nose cone will consist of fiberglass, primarily due to weight considerations, since radar was not used in the Scorpion. A fiberglass nose cone will also ease manufacturing, since a simple mold can be used to construct the openings needed for the IR system, cannon fire and exhaust ports. The majority of the underside of the Scorpion is covered with Titanium armour. This will help to protect the aircraft from ground fire. Figure 7.2.2 presents the armor layout.

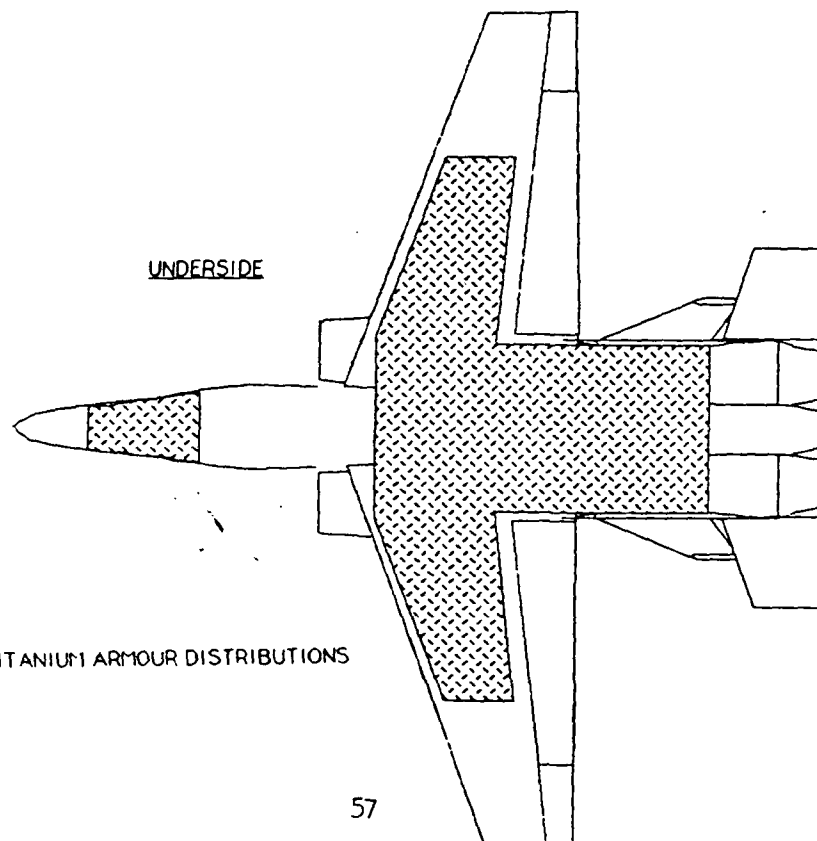
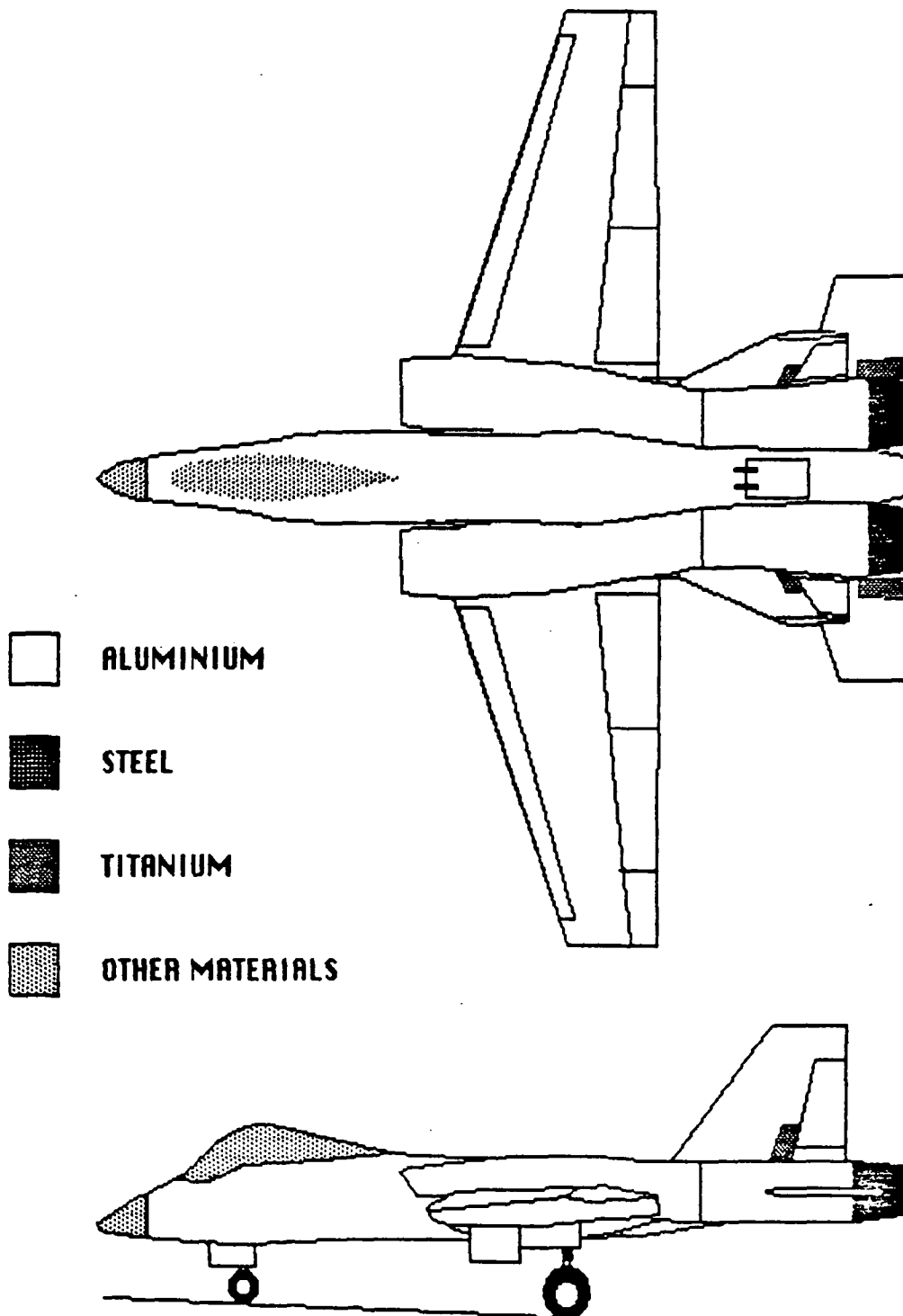


FIGURE 7.2.2 TITANIUM ARMOUR DISTRIBUTIONS

FIGURE 7.2.1 : SCORPION MATERIALS DISTRIBUTION



8.0 CENTER OF GRAVITY AND MOMENT OF INERTIA ANALYSES

8.1 WEIGHT AND BALANCE ANALYSIS AND CENTER OF GRAVITY EXCURSION

Table 8.1.A shows the data acquired using the following methods to determine the center of gravity (c.g.) locations for the Scorpion under different loading scenarios. The X-reference point is located three feet in front of the nose and the Z-axis reference is at ground level. The c.g. locations on the Y-axis are zero due to symmetry. From the loading conditions, a c.g. excursion diagram was constructed as shown in Figure 8.1.1. Using Reference 5, the Scorpion's empty weight was determined by breaking the aircraft into three component groups: structures, powerplant and fixed equipment. For each group shown in Table 8.1.A, the items comprising that group are listed.

For each item in the fuselage group, empirical relations obtained from Reference 5 were used to calculate the weights and horizontal and vertical locations of the centers of gravity. For the powerplant group, manufacturer's data on the General Electric low bypass turbofan engine was used for the weight and c.g. locations. The inlet weight was calculated using empirical relations, and the c.g. location of the aircraft utilizing a scaled drawing of the aircraft showing inlet geometry as it varies along its length. For the fixed equipment group, empirical relations were used for some items, while others were estimated using data for similar existing aircraft from several sources such as References 8 and 9. The c.g. locations were estimated from a scaled drawing of the Scorpion by ascertaining their locations using existing aircraft schematics. The empty weight c.g. location

was determined by analyzing the data at this point. The operating empty weight was determined by adding trapped fuel and oil and the pilot to the empty loading scenario.

In order to obtain the total take-off weight c.g. location, fuel and payload were added to the operating empty loading scenario. As the data indicates, 40% of the total fuel is stored in the wing sections -- near the root. Twelve bombs are located in the fuselage and eight are located on the wings, four on each side as close to the center line as possible. The bombs were carried on the fuselage for two reasons. First, to leave room for other lighter weapons on the wing hardpoints. Second, to reduce the inertia of the aircraft when rolling about the longitudinal axis, thus increasing the Scorpion's roll rate and maneuverability.

The maximum c.g. excursion is shown graphically in Figure 8.1.1., along with the static margins (1.6% - 2.1% stable) and the aerodynamic center locations for the wing, tail and entire aircraft.

FIGURE 8.1.1 : CENTER OF GRAVITY EXCURSION

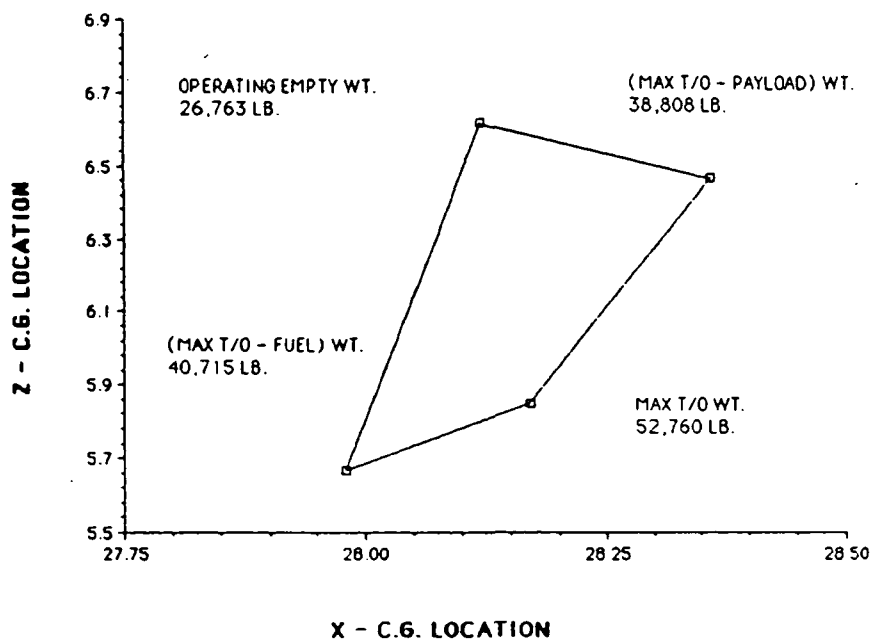


TABLE B.1.A.: WEIGHT AND BALANCE CALCULATION

STRUCTURES	Weight lb	CG x location ft from rslpt	Mmt. lbf-ft	CG y location ft from rslpt	Mmt. lbf-ft	CG z location ft from rslpt	Mmt. lbf-ft
1. Fuselage group	3613	26.40	95383	0.00	0	6.30	22762
2. Wing group	5651	31.00	175181	0.00	0	6.10	34471
3. Empennage group	1032	49.00	50568	0.00	0	9.90	10217
4. Main Gear	1760	30.00	52800	0.00	0	5.30	9329
5. Nose Gear	500	15.80	7900	0.00	0	5.00	2500
TOTAL STRUCTURE WT.	12556	30.41	381832	0.00	0	6.31	79278
POWERPLANT							
1. Engines	4340	46.80	203112	0.00	0	7.60	32984
2. Inlets	556	32.60	18126	0.00	0	8.00	4448
3. Fuel system	926	33.00	30558	0.00	0	6.50	6019
4. Prop. system	833	46.80	38984	0.00	0	7.60	6331
TOTAL POWERPLANT WT.	6655	43.69	290780	0.00	0	7.48	49782
FIXED EQUIPMENT							
1. Filtril & Hydrlic sys.	1387	31.00	42997	0.00	0	7.00	9709
2. Electric sys.	550	23.00	12650	0.00	0	7.20	3960
3. Instruments	100	11.00	1100	0.00	0	7.60	760
4. Avionics	1500	17.00	25500	0.00	0	7.40	11100
5. Anti-De-icing & Pressurization Eq.	311	36.00	11196	0.00	0	7.60	2364
6. Oxygen sys.	17	13.00	221	0.00	0	7.20	122
7. Furnishings	127	14.00	1778	0.00	0	7.10	902
Ejection seat	73	14.00	1022	0.00	0	6.40	467
Emergency eq	100	14.00	1400	0.00	0	6.60	660
Misc. eq	500	27.40	13700	0.00	0	4.40	2200
8. Armament	1620	10.40	16848	0.00	0	5.00	8100
9. Weapons sys	220	22.70	4994	0.00	0	6.50	1430
Cannon	150	8.20	1230	0.00	0	6.20	930
Ammo Drum	200	26.00	5200	0.00	0	5.40	1080
IR	212	32.70	6932	0.00	0	6.40	1357
10. Fit test instruments	7067	20.77	146768	0.00	0	6.39	45141
11. Paint	26278	31.18	819381	0.00	0	6.63	174200
TOTAL FIXED EQ. WT.	26278	31.18	819381	0.00	0	6.63	174200
TOTAL EMPTY WT.	26278	31.18	819381	0.00	0	6.63	174200
Trapped fuel	250	39.90	10374	0.00	0	5.30	1378
Crew	235	14.00	3150	0.00	0	7.60	1710
OPERATING EMPTY WT.	26763	31.12	832905	0.00	0	6.62	177288

FUEL

1. (4) Fuselage tanks	7252	33.00	239316	0.00	0	6.80	49314
2. (4) Wing Tanks	4793	30.00	143790	0.00	0	6.00	28758
TOTAL FUEL WT.	12045	31.81	383106	0.00	0	6.46	76072
PAYLOAD							
1. GAU-8 rounds	2106	22.70	47906	0.00	0	6.50	13689
2. Fuselage bombs (12)	6060	32.00	193920	0.00	0	3.20	19392
Fuse. Bomb racks (2)	638	32.00	20416	0.00	0	3.20	2042
3. Wing bombs (8)	4040	32.00	129280	0.00	0	3.20	12928
Wing Bomb racks (2)	638	32.00	20416	0.00	0	3.20	2042
4. Sidewinders/Rails	470	35.60	16732	0.00	0	7.30	3431
TOTAL PAYLOAD WT.	13952	30.72	428570	0.00	0	3.84	53523
TOTALS							
TOTAL TAKE-OFF WT.	52760	31.17	1644581	0.00	0	5.85	308883

C.G. TRAVEL

fl. % max
0.05 0.42

STATIC MARGIN (% max)

EMPTY 1.6
OP EMPTY 2.1
TAKE-OFF 1.7

AERODYNAMIC CENTERS (LEI FROM NOSE)

EMPTY 28.37
OPERATING EMPTY 27.30
TAKE-OFF 46.80

8.2 MOMENTS AND PRODUCTS OF INERTIAS

The moments of Inertia were also calculated using the weight and balance data for the Scorpion. Table 8.2.A shows the empty moments and product of inertias. Table 8.2.B shows the moments and products of inertias for the fully loaded aircraft. These values were calculated using the following relations for each component and then summing the inertia values for each loading condition. These values strongly effect the maneuverability, roll rates and pitch rates for the aircraft.

TABLE 8.2.A : EMPTY WEIGHT MOMENTS AND PRODUCTS OF INERTIA

	Ixx Slug-ft ²	Iyy Slug-ft ²	Izz Slug-ft ²	Ixy Slug-ft ²	Iyz Slug-ft ²	Ixz Slug-ft ²
STRUCTURES						
1. Fuselage group	12	2580	2568	0	0	177
2. Wing group	49	55	6	0	0	17
3. Empennage group	343	10532	10129	0	0	1070
4. Main Gear	97	173	76	0	0	86
5. Nose Gear	41	3719	3678	0	0	390
TOTAL STRUCTURE INERTIA	543	17060	16517	0	0	2539
POWERPLANT						
1. Engines	127	33048	32921	0	0	2046
2. Inlets	32	67	35	0	0	34
3. Fuel system	0	96	95	0	0	-7
4. Prop. system	24	6343	6319	0	0	393
TOTAL POWERPLANT INERTIA	185	39554	39369	0	0	2466
FIXED EQUIPMENT						
1. Flt ctrl & Hydrlic sys.	6	7	1	0	0	-3
2. Electric sys.	6	1150	1145	0	0	-80
3. Instruments	3	1269	1266	0	0	-61
4. Avionics	28	9408	9380	0	0	-510
5. Anti- , De-icing & Pressurization Eq.	9	234	225	0	0	-45
6. Oxygen sys	0	175	175	0	0	-5
7. Furnishings						
Ejection seat	1	1167	1166	0	0	-32
Emergency eq.	0	670	670	0	0	9
Misc. eq	0	918	918	0	0	2
8. Armament	77	300	222	0	0	131
9. Weapons sys.						
Cannon	134	21888	21754	0	0	1705
Ammo Drum	0	492	492	0	0	7
IR	1	2464	2463	0	0	46
10. Flt test instruments	9	176	167	0	0	40
11. Paint	0	16	15	0	0	-2
TOTAL FIXED EQ. INERTIA	274	40334	40059	0	0	1292
TOTAL EMPTY INERTIAS	1001	96947	95946	0	0	6297
Trapped fuel	14	629	615	0	0	-94
Crew	7	2972	2065	0	0	-117
OPERATING EMPTY INERTIA	1022	99648	98626	0	0	6087

ORIGINAL PAGE IS
OF POOR QUALITY

TABLE 8.2.B : TAKE-OFF MOMENTS AND PRODUCTS OF INERTIA

	Ixx Slug-ft ²	Iyy Slug-ft ²	Izz Slug-ft ²	Ixy Slug-ft ²	Iyz Slug-ft ²	Ixz Slug-ft ²
STRUCTURES						
1. Fuselage group	22	2580	2557	0	0	-139
2. Wing group	11	16	5	0	0	-7
3. Empennage group	525	10726	10200	0	0	2315
4. Main Gear	17	92	75	0	0	36
5. Nose Gear	11	3685	3673	0	0	204
TOTAL STRUCTURE INERTIA	586	17097	16511	0	0	2306
POWERPLANT						
1. Engines	411	33375	32964	0	0	3682
2. inlets	30	115	35	0	0	53
3. Fuel system	12	108	96	0	0	34
4. Prop. system	79	6406	6327	0	0	707
TOTAL POWERPLANT INERTIA	582	40004	39422	0	0	4475
FIXED EQUIPMENT						
1. Flt ctrl & Hydrlic sys.	57	58	1	0	0	-8
2. Electric sys.	31	1173	1142	0	0	-188
3. instruments	9	1275	1265	0	0	-109
4. Avionics	111	9478	9366	0	0	-1022
5. Anti-De-icing & Pressurization Eq.	29	255	226	0	0	22
6. Oxygen sys	1	175	175	0	0	-13
7. Furnishings						
Ejection seat	6	1170	1164	0	0	-84
Emergency eq.	1	670	669	0	0	-21
Misc. eq.	2	919	917	0	0	-40
8. Armament	33	254	221	0	0	85
9. Weapons sys.						
Cannon	37	21769	21733	0	0	894
Ammo Drum	3	494	491	0	0	-37
IR	1	2462	2461	0	0	-37
10. Flt test instruments	1	168	166	0	0	15
11. Paint	2	17	15	0	0	5
TOTAL FIXED EQ. INERTIA	324	40336	40013	0	0	-479
TOTAL EMPTY INERTIAS	1492	97438	95946	0	0	6304
Frooded fuel	2	618	616	0	0	-39
Crew	21	2094	2063	0	0	-210
OPERATING EMPTY INERTIA	1515	100140	98625	0	0	6055
FUEL						
1. (4) Fuselage tanks	202	956	754	0	0	390
2. (4) Wing Tanks	3	208	204	0	0	-25
TOTAL FUEL INERTIA	205	1163	959	0	0	365
PAYLOAD						
1. GAU-8 rounds	27	4726	4699	0	0	-358
2. Fuselage bombs (12)	1328	1457	130	0	0	-415
Fuse. Bomb racks (2)	140	153	14	0	0	-44
3. Wing bombs (8)	335	972	86	0	0	-276
Wing Bomb racks (2)	140	153	14	0	0	-44
4. Stopwinders/Falls	31	317	287	0	0	34
TOTAL PAYLOAD INERTIA	2550	7779	5229	0	0	-1043
TOTALS						
TOTAL INERTIAS AT TAKE-OFF WEIGHT	4271	109083	104812	0	0	5377

**ORIGINAL PAGE IS
OF POOR QUALITY**

9.0 AERODYNAMICS

In order to analyze the performance of the design, the aerodynamic characteristics had to be obtained. From these traits, drag polars were established and consequently, the aircraft capabilities were evaluated.

9.1 LIFT:

The airplane lift characteristics were determined by finding the following: 1) zero-lift angle of attack, 2) lift curve slopes, 3) airplane zero-angle of attack lift coefficient and 4) $C_{L \max}$. These properties were calculated for a range of mach numbers, including the transonic cruise speed.

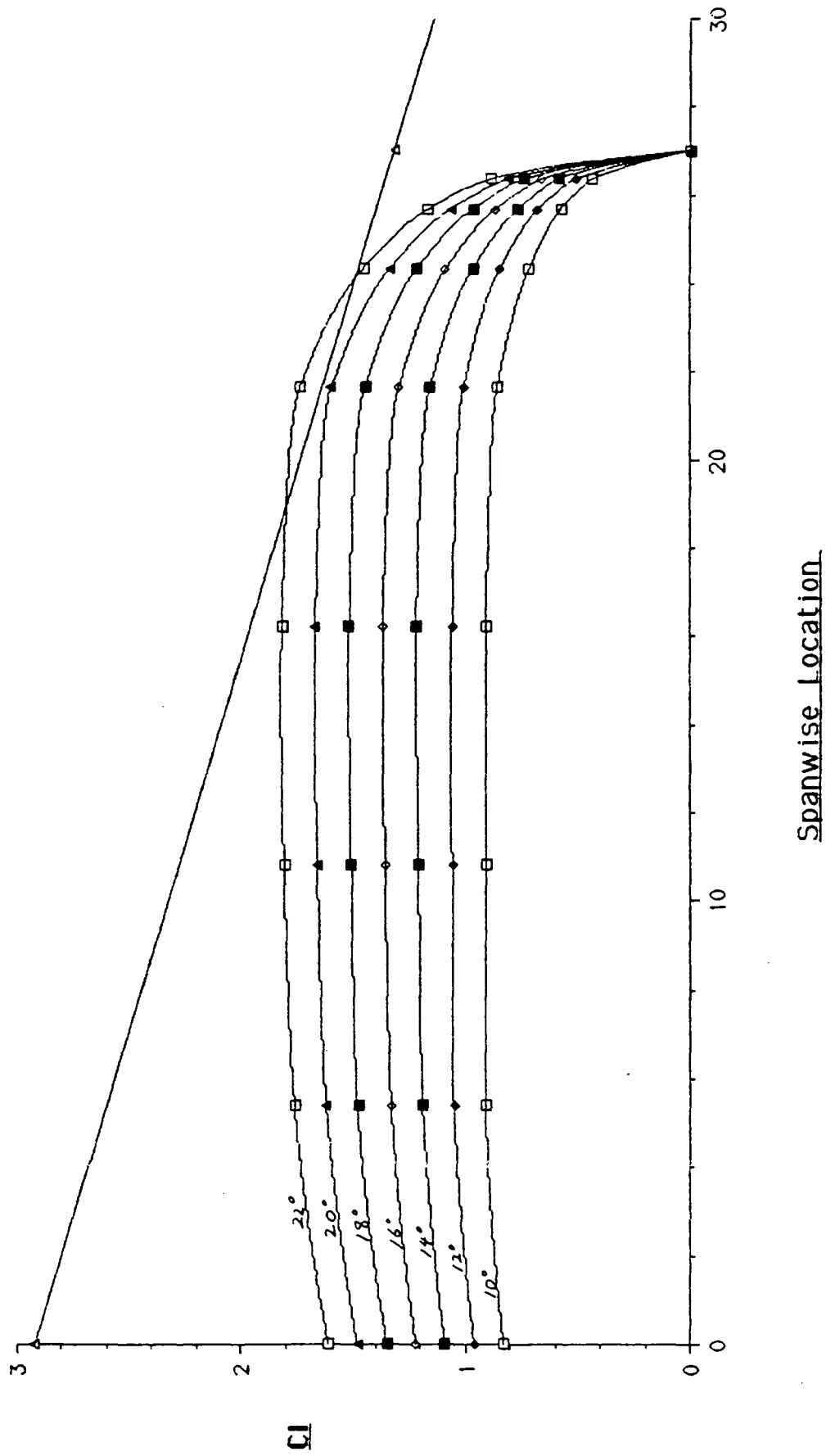
The lift curve slope of the entire aircraft was obtained using the lift curve slopes of the wing and the effect of the horizontal stabilator. The method outlined was obtained from Reference 6. Although the vertical tails are canted, they are canted a small amount -- twenty degrees -- making their horizontal projected areas very small. Also the the airfoil used for the twin tails was symmetric and at zero-angle of attack produces no lift. Thus, the lift due to these projected areas was considered negligible in the analysis. From a rough estimate of trim requirements using moments of the wing about the aircraft center of gravity location, a trim angle of negative one degree was estimated. This would produce a down-force of about 400 pounds. Taking into account the least amount of lift necessary, which occurs during cruise at the operating empty weight, this is only one percent of the total lift generated. Consequently, only the

lift produced by the wing-body was considered to contribute to the overall lift of the aircraft.

The maximum lift coefficients of the aircraft were based on the maximum lift of the wing, and adjusted for the effects of the wing-body combination. The maximum lift of the wing was determined using a combination of several methods. Using Reference 11, the lift distribution of the wing was determined, refer to figure 9.1.1. This method took into account the type of airfoil used and the wash-out angle. From the figure one can see that the wash-out is sufficient to prevent tip stall at the lower angles of attack. The lift distribution is also similar to an elliptical lift distribution. This resulted in a fairly efficient wing design; the efficiencies varied from 94% TO 97%. Using Reference 6, the incremental maximum lift coefficients were adjusted for the varying Reynolds numbers along the span. This was assumed to be a linear decrease and can be seen in Figure 9.1.1. The first curve the line intersected with was assumed to be the stall angle of the wing at that flight speed. The corresponding curve was then integrated for the maximum lift coefficient of the wing. The previously obtained lift curve slopes and these CL max were plotted against the angle of attack. Unfortunately, the line did not increase linearly up to CL max, but exhibited a marked increase at the stall angle. Therefore, it was assumed that this method predicted too high a value for CL max.

A different method was then utilized which is outlined in Reference 10. This method only accounted for the sweep of the wing and the aspect ratio. It did not regard the wash-out angle. Consequently, this procedure estimated stall angles and CL max that were very low. Knowing that washout helps to delay stall and increases CL max, the first method was

FIGURE 9.1.1 : Spanwise Lift Distribution for $M=2$



assumed more accurate in estimating the stall angle. To obtain the CL max, the angle which the lift distribution method predicted was used in conjunction with the lift curve slope. A graph of CL as it varies with angle of attack and mach number can be seen on Figure 9.1.2. A variation of CL was also calculated due to flap deflection for a flight speed of Mach 2. This is presented in Figure 9.1.3.

9.2 WETTED AREAS

A summary of the wetted areas is presented in Table 9.2.A. The wing and empennage areas were estimated by measuring the projected areas off of a scaled drawing and doubling those values. The fuselage wetted area was approximated by dividing the fuselage into eight smaller sections and obtaining the surface areas of these smaller sections. However, the contours of each section was unique. So each section was modeled as a cylinder by finding the equivalent diameter using :

$$d = \sqrt{[(4S_{fus})/\pi]}$$

where S_{fus} is the frontal area of each section.

TABLE 9.2.A: SUMMARY OF WETTED AREAS

Plane Part	Area (sq ft)
fuselage	1362.71
wing	829.44
horizontal stabilator (total)	121.68
vertical tail (total)	257.32
total	2571.14

FIGURE 9.1.2: CL VS. ANGLE OF ATTACK FOR DIFFERENT FLIGHT SPEEDS

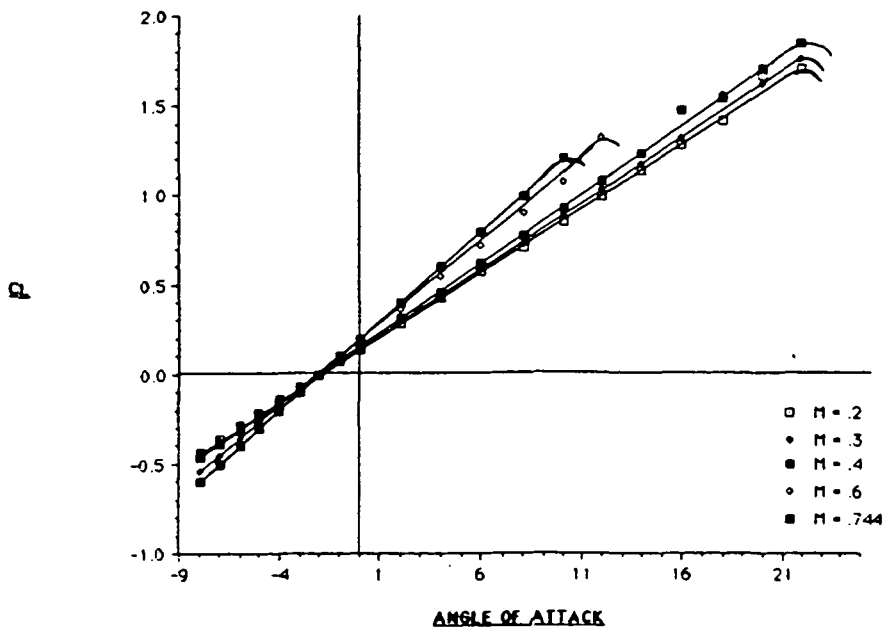
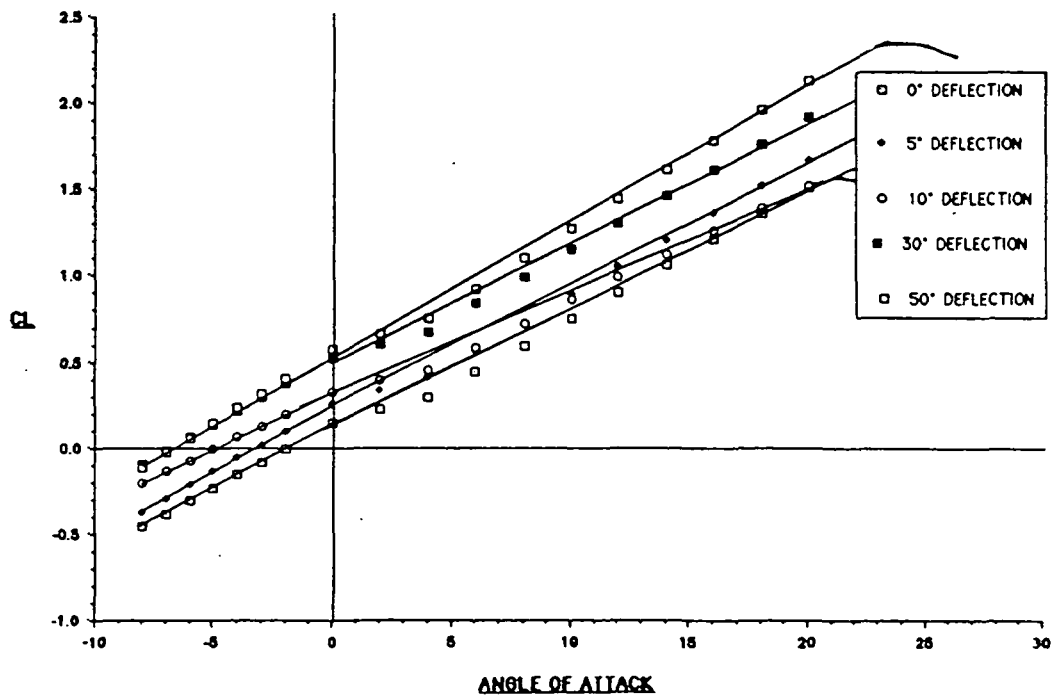


FIGURE 9.1.3: CL vs. ANGLE OF ATTACK FOR DIFFERENT FLAP DEFLECTIONS



9.3 DRAG POLARS

Drag polars were estimated using the CL and the wetted surface areas. Both the subsonic and the transonic region were evaluated. Since both the wings and the empennage's critical mach numbers were above the cruise mach number, subsonic methods were used to find their drag at cruise. A graph of drag as it varies with mach number can be found on Figure 9.3.1 and a graph of CD as it varies with CL can be seen on Figures 9.3.2 and 9.3.3. Note that 9.3.3 is the drag polar for the clean airplane. Drag polars were also calculated for landing configuration. This can be seen in Figure 9.3.4.

Since the Scorpion is required to cruise at transonic speeds, it was deemed necessary to employ area ruling to reduce drag, especially wave drag. Using the Sears-Haack curve as the ideal model, the fuselage was then recontoured to obtain an area change as close as possible to the ideal without having to rearrange the internal layout. The final result can be seen in Figure 9.3.5.

FIGURE 9.3.1: VARIATION OF DRAG WITH MACH NUMBER

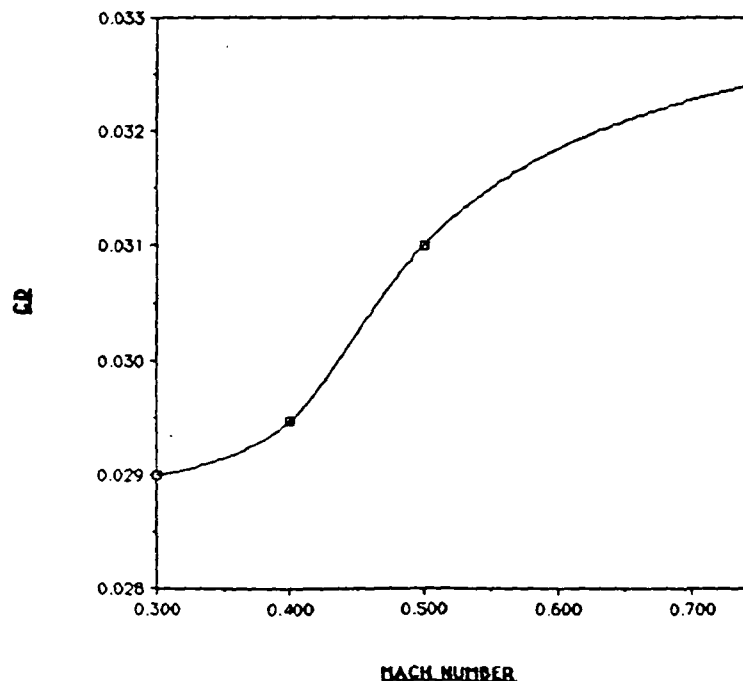


FIGURE 9.3.2 : DRAG POLARS FOR PLANE W/O STORES AT SEA-LEVEL

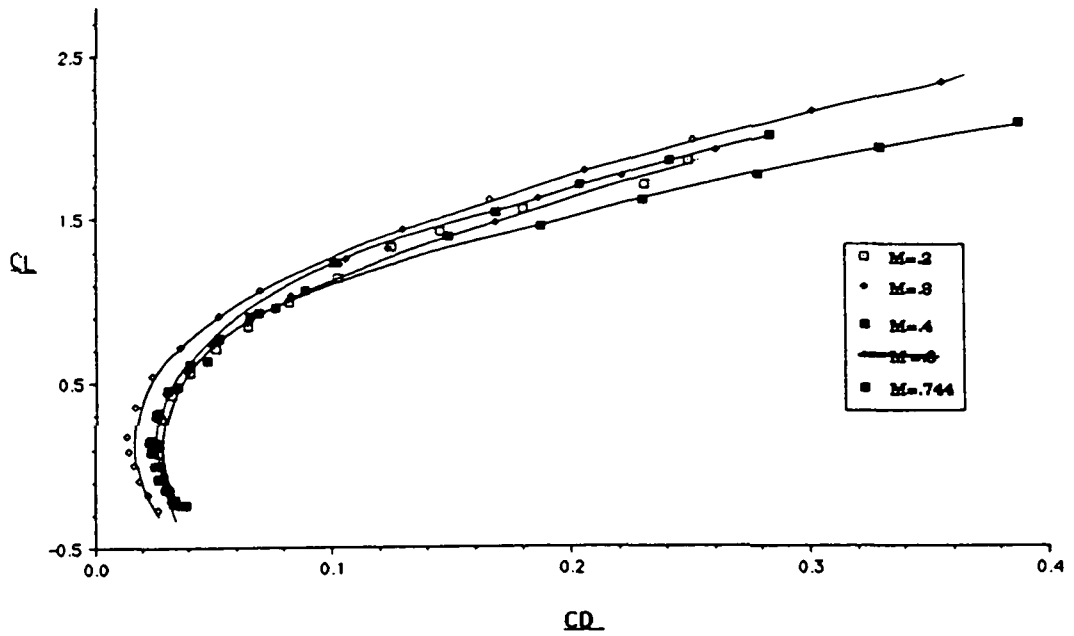


FIGURE 9.3.3 : DRAG POLARS FOR PLANE W. STORES AT SEA-LEVEL

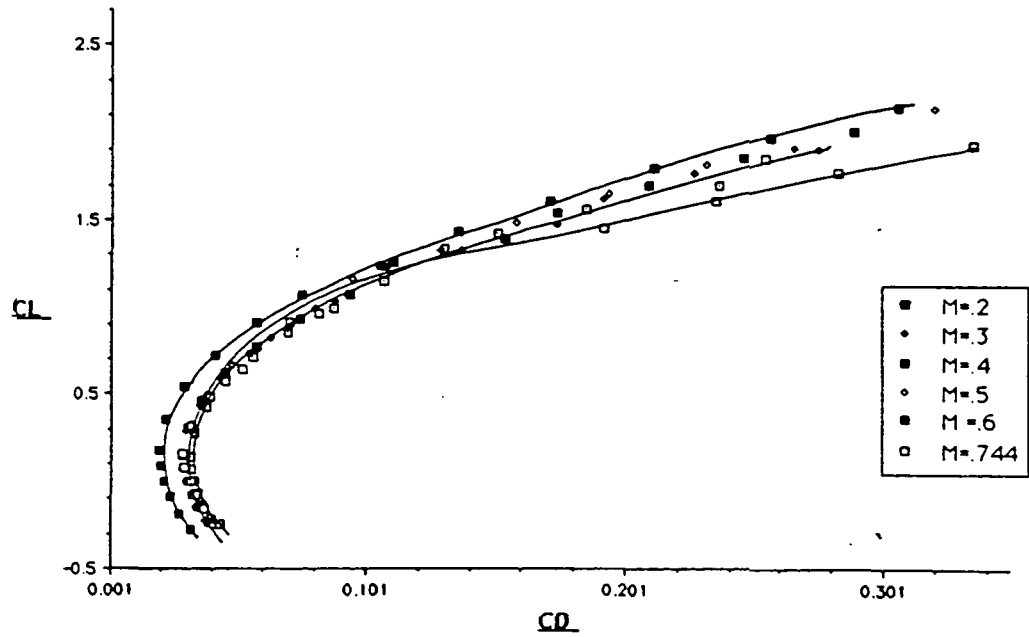


FIGURE 9.3.4: DRAG POLAR FOR LANDING CONFIGURATION

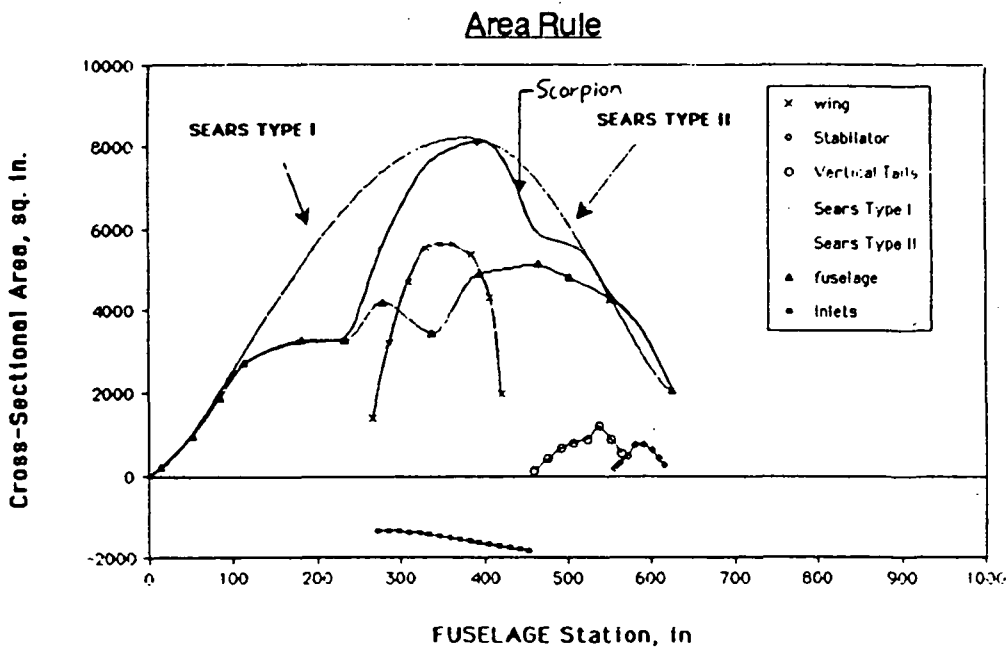
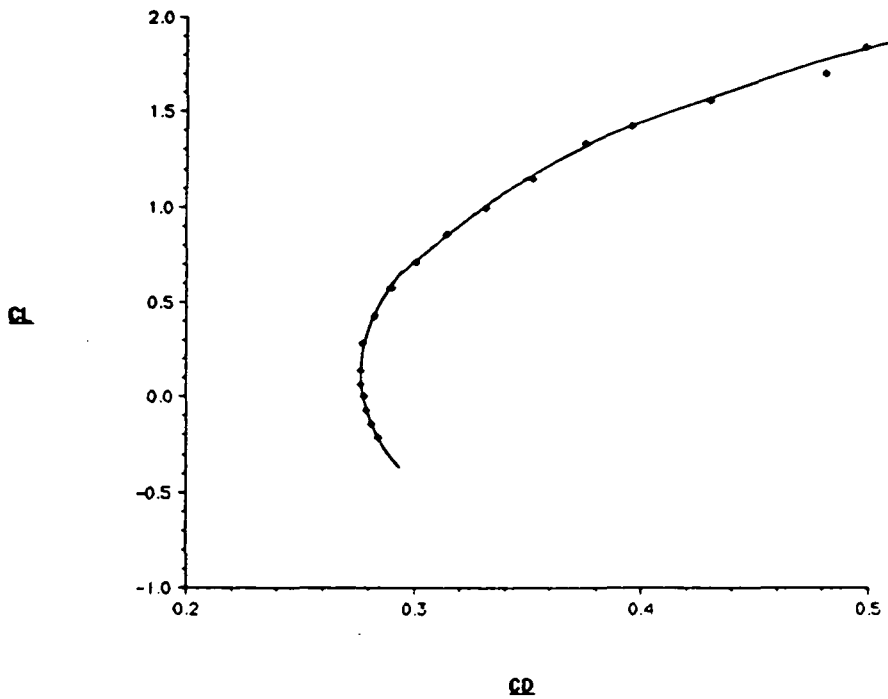


FIGURE 9.3.5 : AREA RULING

10.0 Stability and Control

The Scorpion is a conventionally configured aircraft with twin vertical stabilizers. This allows for the use of a method of stability and control analysis based on empirical trends since there are large amounts of design and test data available for aircraft of this type.

In this analysis, the aircraft is assumed to be a rigid body, therefore aeroelastic effects are not considered. Also, the method used is for subsonic speeds, thus uncertainties increase at higher speeds with shock formation and compressibility effects.

The object of the Scorpion design concept was to produce a neutral or marginally stable close air support aircraft. The static margin of the Scorpion is approximately two percent which allows maneuverability with survivability. The aircraft is maneuverable, but controllable in the event of a system failure. Neutrally stable aircraft also offer the advantage of having minimal trim drag.

Unstable aircraft configurations were considered from the vantage point of maneuverability, but these were deemed inappropriate for the large GAU 8 30mm cannon. Unstable aircraft require extensive avionics and electronic control systems, which we had hoped to reduce with a marginally stable airplane and keep costs down.

The center of gravity excursion was calculated upon completion of the equipment and planform layout found in section 8.0. The static margin varies from 1.5% at maximum takeoff weight without payload (38,808 lbs) to 2.0% at maximum takeoff weight without fuel (40,715 lbs).

Stability derivatives were used to determine longitudinal flying qualities. Specification MIL-F-8758B defines level 1 phugoid damping coefficients to be greater than 0.04. The Scorpion meets level one flying qualities for both approach to landing and cruise configurations with damping coefficients of 0.05 and 0.26 respectively. Short period specifications dictate damping coefficients to be between 0.35 and 1.30 for level one flying qualities in the cruise configuration, with a damping coefficient of 0.28. This results in a marginal increase in pilot and a possible reduction in mission effectiveness during the slow flight and landing regimes. An increase in horizontal tail area could easily improve this situation, but this would be at the expense of center of gravity and aerodynamic center considerations since the Scorpion is a compact aircraft. For these reasons, and since the Scorpion is marginally stable, a pitch damper utilizing rate gyros will be investigated as a possible solution to regaining level one flying qualities.

Lateral stability approximations for dutch roll were calculated indicating that there may be insufficient lateral damping. Specifications allow for minimal damping coefficients of 0.19 and 0.02 for levels one and two flying qualities respectively. Minimum dutch roll frequencies are 1.0 and 0.4 for level one and two. The Scorpion meets level one flying qualities for approach to landing and cruise with dutch roll frequencies of 1.63 and 5.35 per second. The Scorpion meets only level two flying qualities in approach and cruise damping coefficients of 0.14 and 0.11 respectively. For more inherent stability, dihedral could be reduced, or the vertical tail area increased. This would sacrifice spiral stability, but for this type of aircraft and mission it would not cause any problems since the pilot is

likely to be actively flying and maneuvering the aircraft. Use of yaw dampers could regain level one flying qualities without these penalties.

Flight Condition	1	2
	Power Approach	Normal Cruise
Altitude (ft)	Sealevel	Sealevel
Air Density (slugs/ft ³)	.0023	.0023
Speed (fps)	220 (M=.2)	810 (M=.74)
Angle of Attack (deg.)	10	0
Flap Configuration	Extended 40 deg.	No Flap Extended
Weight (lbs)	29,000	52760

Speed Coefficients

C_{L_1}	.835	.110
C_{D_1}	-.213	-.017
$C_{T_{X_1}}$.213	.017
C_{D_u}	.0004	.0512
C_{L_u}	.167	.113
C_{m_u}	-2.92	-1.07
$C_{T_{X_u}}$	-.488	-.035

$C_{\dot{u}}$	-0.006	-0.009	$C_{\dot{H}} \dot{u}$	-0.025	-0.14	Z_a (1/s ²)	-169	-1312
Roll Rate Derivatives								
$C_{\dot{r}}$	-0.081	-1.45	Angle of Attack Derivatives			M_0 (s ⁻²)	-34	-5.27
$C_{\dot{l}}$	-0.396	-3.76	C_D	0.34	1.867	M_1 (s ⁻¹)	-0.0004	-0.0075
$C_{\dot{p}}$	-0.105	-0.009	C_m	-0.084	-1.106	M_0 (s ⁻¹)	-292	-967
Pitch Rate Derivatives								
$C_{\dot{q}}$	0	0	$C_{m_{\dot{a}}}$	0	0	Lateral Dimensional Derivatives		
$C_{\dot{e}}$	6.09	5.20	Rate of Angle of Attack Derivatives			Y_b (1/s ²)	-29.1	-213.8
$C_{\dot{e}}$	-2.69	-2.70	$C_{\dot{a}}$	0	0	Y_r (1/s)	-1.77	-3.34
Yaw Rate Derivatives								
$C_{\dot{r}}$	-3.74	-3.54	$C_{m_{\dot{r}}}$	-0.001	-0.00015	N_b (s ⁻²)	2.6	28.2
$C_{\dot{l}}$	1.21	2.07	Angle of Sideslip Derivatives			N_r (s ⁻¹)	-32	-88
$C_{\dot{p}}$	-1.35	-1.11	$C_{\dot{r}}$	-0.754	-0.754	Short Period		
Longitudinal Dimensional Derivatives								
$X_{\dot{u}}$ (s ⁻¹)	-0.23	-0.36	$C_{\dot{l}}$	-1.38	-0.49	W_N (s ⁻¹)	1.9	2.6
$Z_{\dot{u}}$ (s ⁻¹)	-3.22	-1.16	$C_{\dot{b}}$.136	.118	Z	.28	.49
Dutch Roll								
			Rate of Angle of Sideslip Derivatives			W_N (s ⁻¹)	1.63	5.35
			$C_{\dot{r}}$	-0.2	-0.3	Z	14	11
			$C_{\dot{l}}$	-0.02	-0.04			

11.0 AVIONICS

In order to maximize the capabilities of the Scorpion, an avionics package has been chosen that will reduce the pilot's workload and aid him in the tracking and acquisition of targets. The package also includes devices that will facilitate the operating of the Scorpion during all types of weather conditions as well as during day and night conditions.

The avionics package includes software to aid in flight control. Since the Scorpion is stable, a less sophisticated system will be used to lower the overall cost of the aircraft. The flight computer is encased in titanium and placed high, behind the pilot. This reduces the possibility of the system being hit and damaged by ground fire. However, in the event that the system is damaged, the Scorpion's stability will enable enough controllability to be maintained for the pilot to eject. The main target tracking and acquisition device the Scorpion has is an infrared search and track sensor. This passive system was chosen to reduce the electronic signature and decrease the effectiveness of radar-seeking anti-aircraft weapons which in turn increases the combat survivability of the Scorpion. The Scorpion also carries a LANTIRN navigation pod to abet in flying during adverse weather conditions and at night. The avionics layout is featured in Figure 11.0.1.

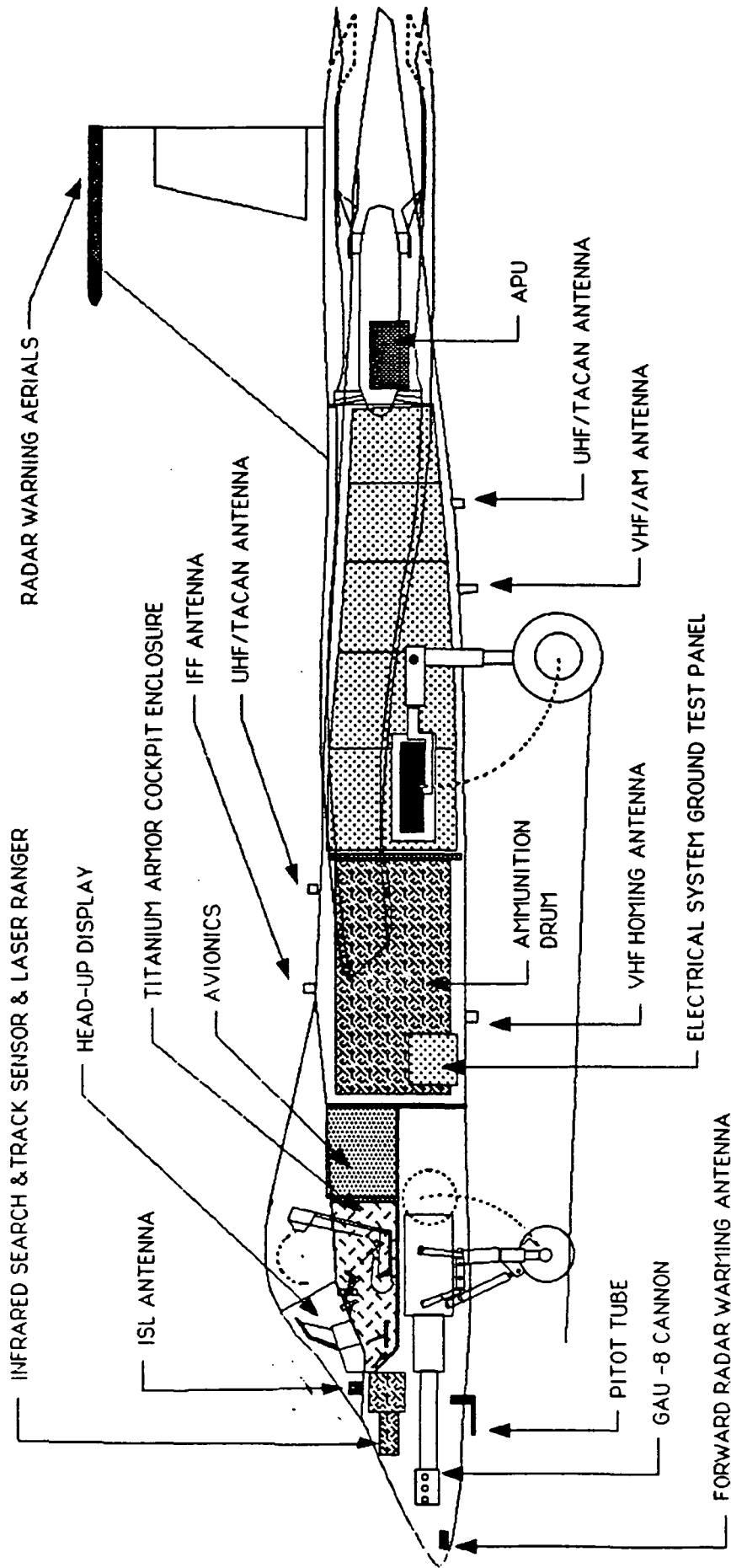


FIGURE 11.0.1 AVIONICS LAYOUT

12.0 SYSTEMS LAYOUT

The Scorpion has a fly-by-wire system as shown in Figure 12.0.1. This was chosen over a hydraulic system to decrease the overall weight of the aircraft. The network also includes a back-up system with each scheme being independent and completely self-contained. A redundant system was included to increase the survivability of the Scorpion. Along with the fly-by-wire, electrohydrostatic servo-actuators are used for all control surfaces. These type of actuators are self-contained and lighter than mechanically signalled hydrostatic actuators and less expensive than electromechanical actuators. The main flap is divided into two smaller flaps each controlled by one self-contained actuator. This reduces the per unit cost of each actuator and increases the survivability of the aircraft by reducing the chance of a system-wide failure. No redundant actuators will be required for the wing, further decreasing the cost of the wing.

The fuel system consists of two wing tanks and five fuselage tanks. The system is designed so that the wing tanks are emptied first, therefore the wing will be dry before the aircraft reaches the battlefield enabling the rest of the fuel to be better protected in the fuselage. This also enhances the maneuverability of the Scorpion by reducing the moment of inertia of the wing and thereby increasing the Scorpion's roll rates. The remainder of the fuel is used by alternating fuselage tanks located in the rear with fuel tanks located in the front so as to reduce c.g. travel. Furthermore, five smaller tanks are used as opposed to one large tank so as to decrease shifting of the fuel during maneuvering and to decrease the possibility of losing all the fuel with one direct hit. A jettison system is also provided

to help alleviate the problem of vapor lock due to sudden pressure changes often experienced during take-off and maneuvering or to eject extra fuel before landing. Figure 12.0.2 features the fuel system layout.

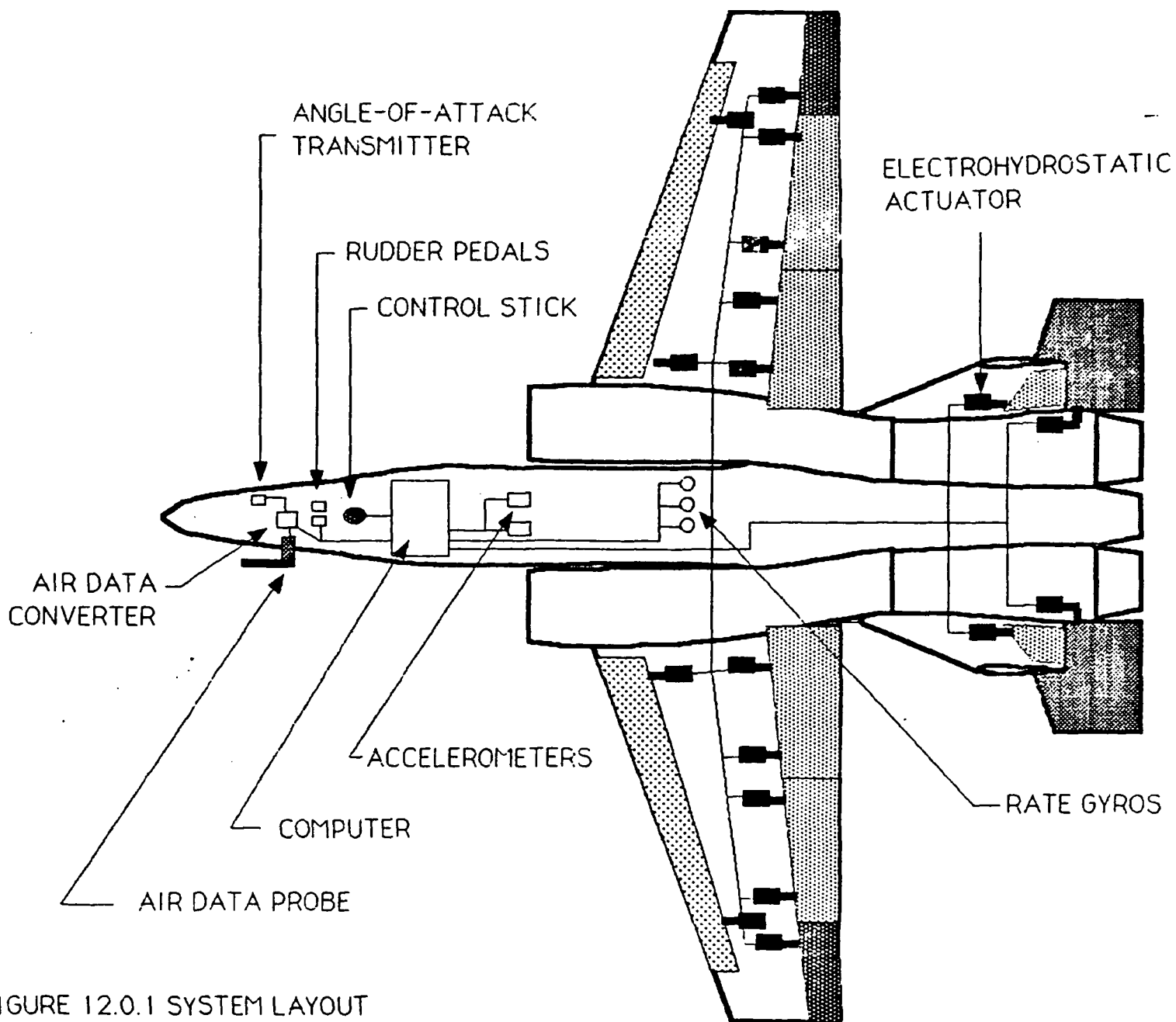


FIGURE 12.0.1 SYSTEM LAYOUT

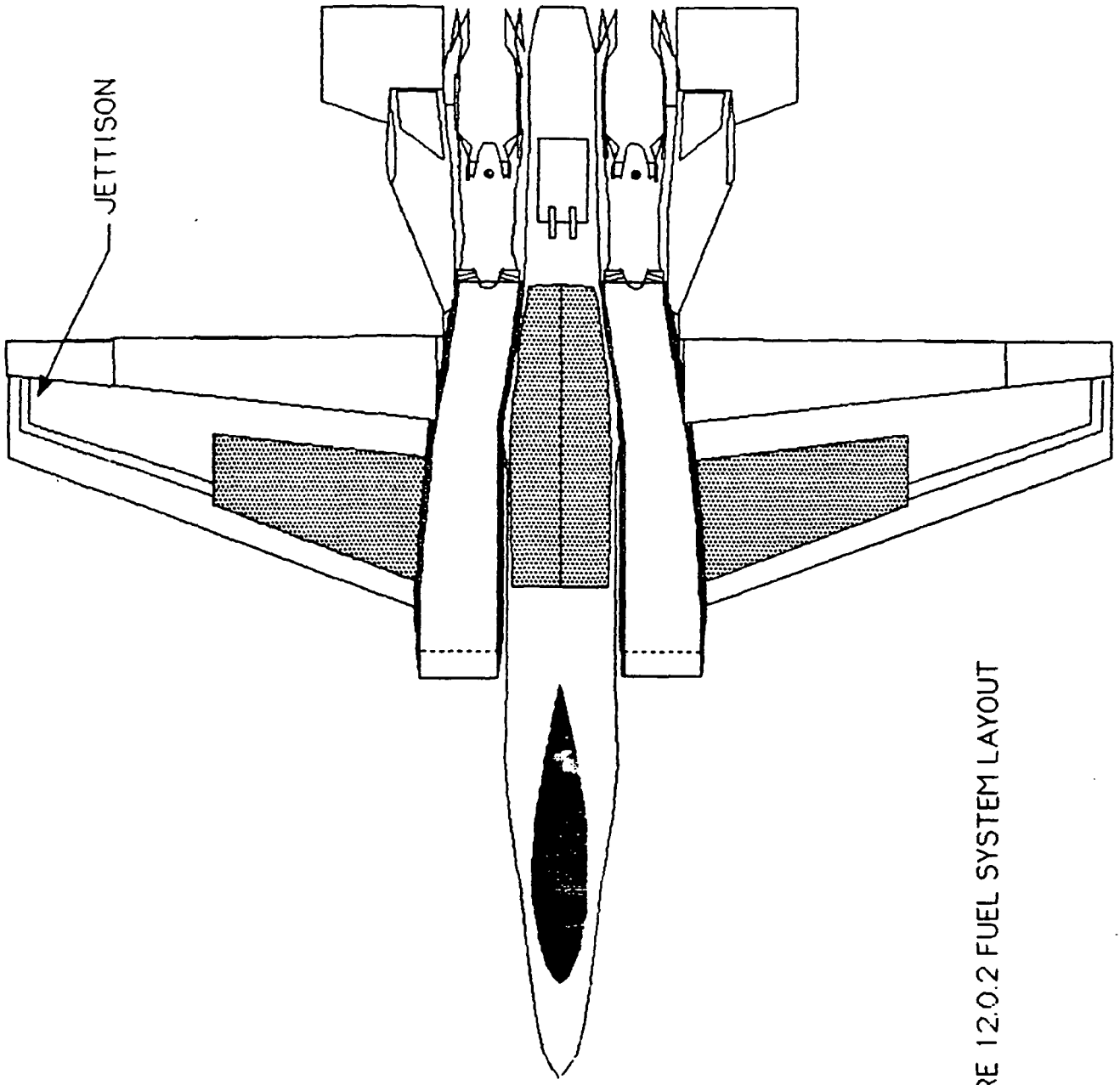


FIGURE 12.0.2 FUEL SYSTEM LAYOUT

13.0 WEAPONS INTEGRATION

In today's economic climate, it is essential to design an aircraft that can meet and fulfill many different roles. The Scorpion is capable of performing several types of combat missions as well as a close-air support mission. Through weight and balance analyses, it was found that the scorpion is capable of carrying various mission loads detailed below. The Gau-8 cannon is carried at all times. For a detailed presentation of how the Scorpion will carry each of these loads and their specifications refer to Figure 13.0.1A-B and Figure 13.0.2.A-B.

DESIGN REQUIREMENT:

20 MK-82 GP BOMBS
2 AIM-9L SIDEWINDERS

CLOSE AIR SUPPORT ANTI-ARMOUR:

20 MK-20 ROCKEYE CLUSTER BOMBS
1 AAS-35 PAVE PENNY
1 ALQ-119 ECM POD

COUNTER-INSURGENCY:

22 AGM-65 ABCD MAVERICK

FORWARD AIR CONTROL:

16 LAU-3 ROCKET PODS
2 AIM-9L SIDEWINDERS
1 FUEL TANK

PREPARATORY ATTACK:

20 GBU-12 LASER GUIDED BOMBS
2 AIM-9L SIDEWINDERS

DAY ARMED RECONNAISSANCE:

12 MK-20 ROCKEYE CLUSTER BOMBS
8 AGM-65 ABCD MAVERICKS
1 ALQ-119 ECM PODS

NIGHT ARMED RECONNAISSANCE:

10 AGM-65 ABCD MAVERICKS
4 LUNDY CHAFF/FLARE SYSTEM
2 AIM-9L SIDEWINDERS
1 ALQ-119 ECM POD

COMBAT RESCUE ESCORT:

8 LAU-3 ROCKET PODS
2 AIM-9L SIDEWINDERS
6 AGM-65 ABCD MAVERICKS
1 FUEL TANK
1 ALQ-119 ECM POD

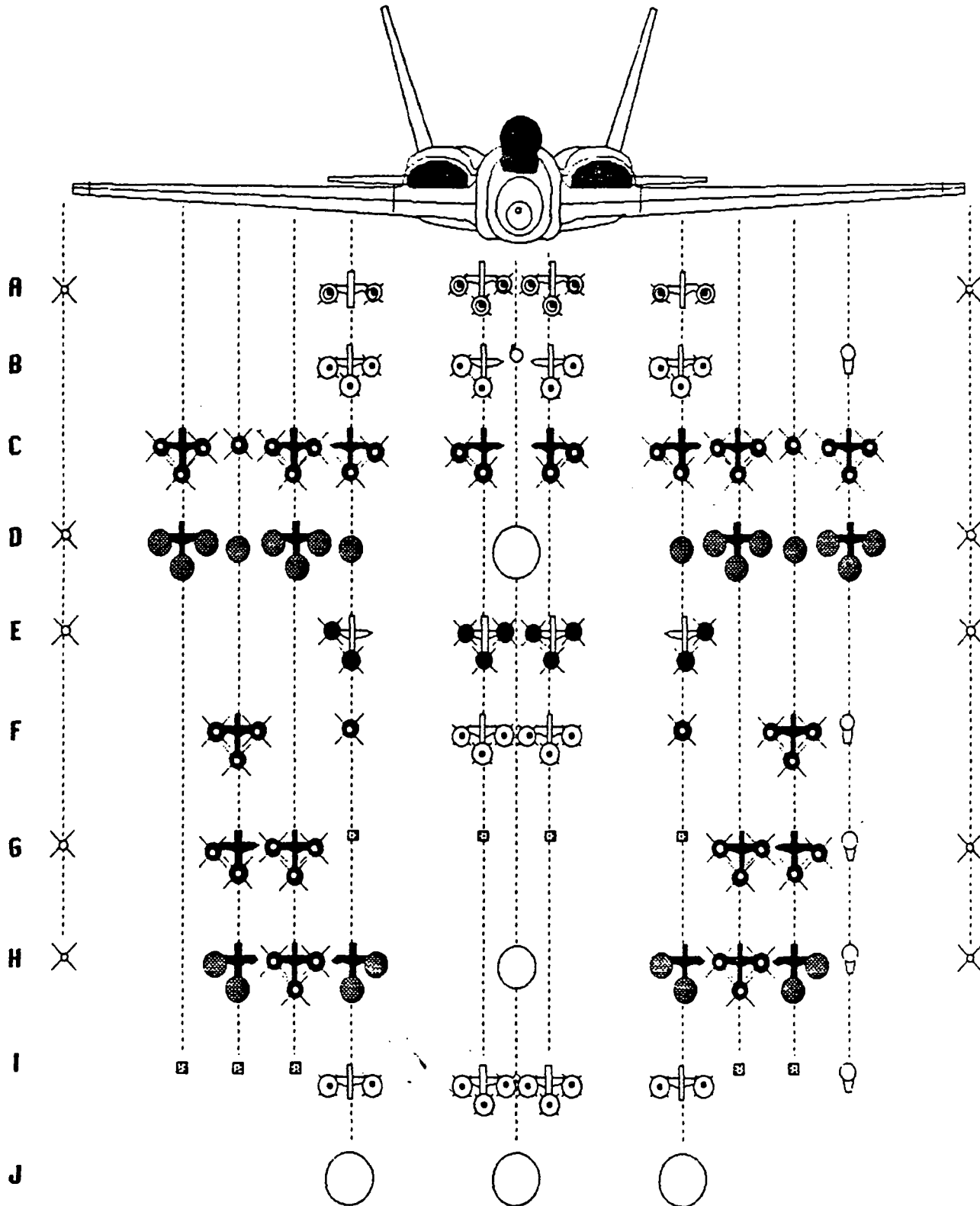
MARITIME STRIKE:

20 MK-20 ROCKEYE CLUSTER BOMBS
5 LUNDY CHAFF/FLARE SYSTEM
1 ALQ-119 ECM POD

FERRY MISSION:

3 FUEL TANKS

FIGURE 13.0.1A : ALTERNATIVE MISSION LOADS















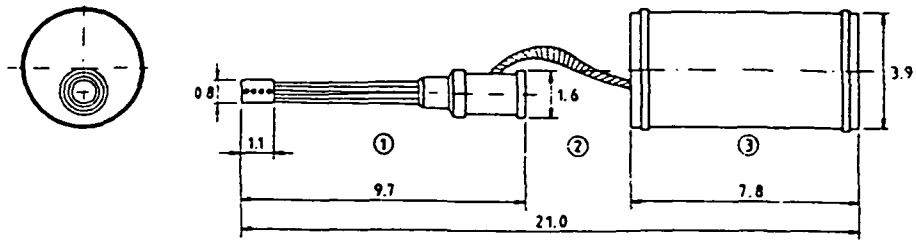
SEE FOLLOWING PAGE FOR KEY

FIGURE 13.0.18 : ALTERNATIVE MISSION LOADS

- A. DESIGN REQUIREMENT
- B. CLOSE AIR SUPPORT ANTI-ARMOUR
- C. COUNTER-INSURGENCY
- D. FORWARD AIR CONTROL
- E. PREPARATORY ATTACK
- F. DAY ARMED RECONNAISSANCE
- G. NIGHT ARMED RECONNAISSANCE
- H. COMBAT RESCUE ESCORT

SYMBOLS

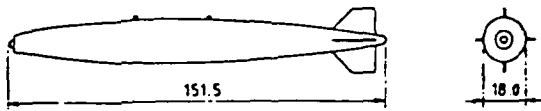
	TER		AGM-65 ABCD MAVERICK
	MER		LAU-3 ROCKET POD
	AIM-9L		LUNDY CHAFF/ FLARE SYSTEM
	MK-82 GP BOMB		AAS-35 PAVE PENNY
	MK-20 ROCKEYE CLUSTER BOMB		ALQ-119 ECM POD
	GBU-12 LGB		FUEL TANK



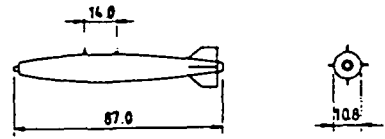
KEY

- 1. GAU-6A 7-BARREL 30 MM GUN
- 2. AMMO FEED CHUTING
- 3. AMMO STORAGE DRUM

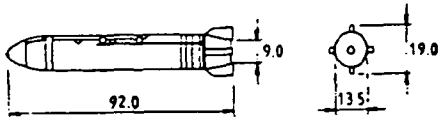
MK 84 GP BOMB



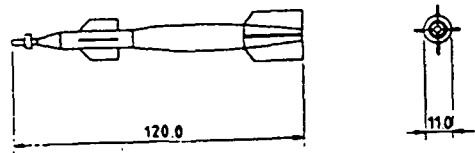
MK 82 GP BOMB



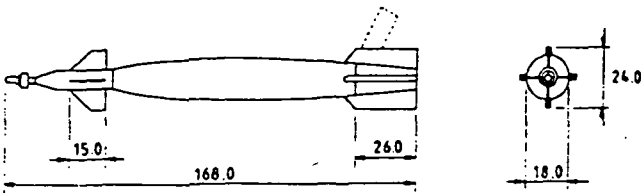
MK 20 "ROCKEYE"



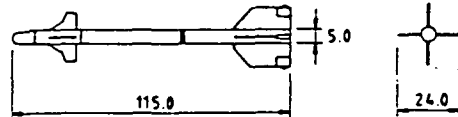
GBU-12/B PAVEWAY II



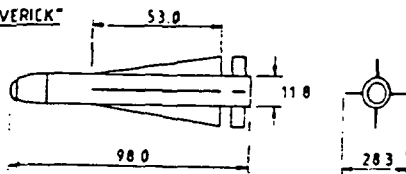
GBU-10/B PAVEWAY II LGB



AIM-9L "SIDEWINDER"



AGM-65 A/B/C/D "HAVERICK"



ALQ-119(V)-15 STANDARD USAF ECM POD

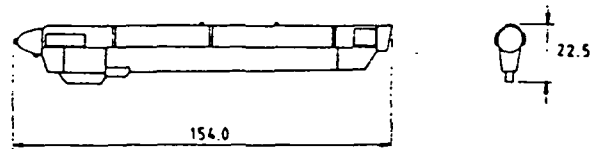
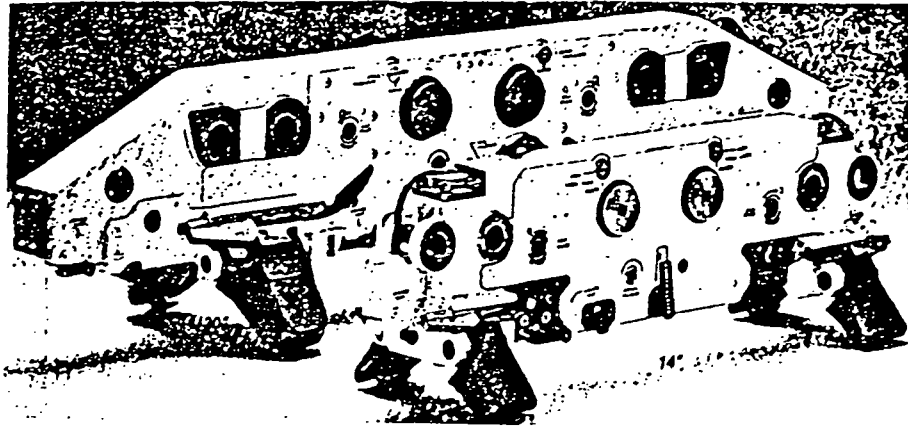
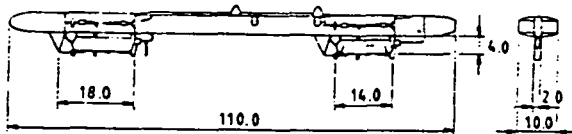


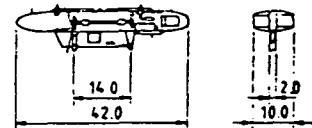
FIGURE 13.0.2.A. WEAPON DISMENSIONS



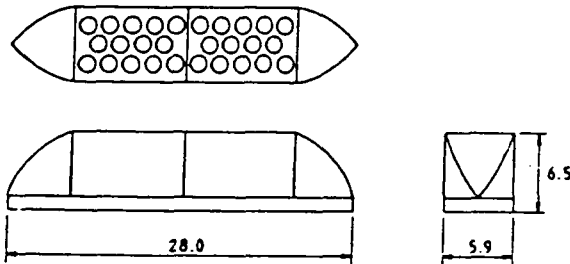
USAF MULTIPLE EJECTOR RACK (MER)



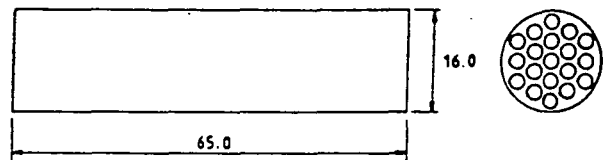
USAF TRIPLE EJECTOR RACK (TER)



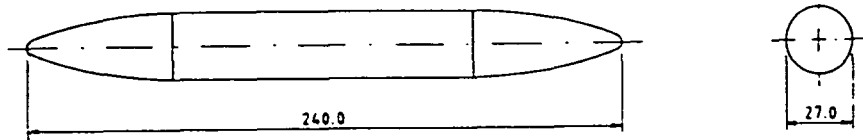
LUNDY CHAFF/FLARE SYSTEM



LAU-3 2.75" ROCKET LAUNCHER



370 US GAL (MDD F-4) $W_E = 289$ LBS



600 US GAL (MDD F-4) $W_E = 306$ LBS

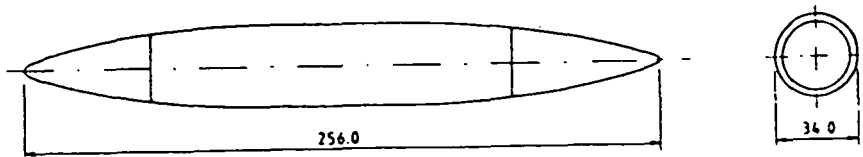


FIGURE 13.0.2B

14.0 GROUND SUPPORT REQUIREMENTS

The Scorpion was designed to keep ground support to a minimum, hence, decreasing its turn-around time and increasing its sortie rates. The fuselage is located five feet above the ground, which increases the accessibility of the panels and ports to the ground crew. Most access panels and ports are located on the side or bottom of the aircraft, thus reducing the need for ladders or access to the top surface of the aircraft.

Primary ground support required for the Scorpion include refueling, weapons reloading, inspection of major structural components and maintenance of engines and systems. The engines are removed by loosening the bolts which mount the engines to the engine mounts and sliding them through the back of the Scorpion.

Refueling of the fuselage tanks will take place through a port positioned on the underside of the fuselage and the wing tanks will be refueled through openings on the underside of the wing. Access panels on the underside of the wing will allow inspection of the wing structure and flight control systems. They are placed to facilitate access to the hydrostatic actuators in the event of their replacements. Weapons reloading will require munitions carts equipped with hydraulic lifts. The wing of the Scorpion facilitates this since the hardpoints are located only six feet from the ground. Panels for the stabilators and the vertical tails are located at the base of each surface. Again the stabilators' hydrostatic actuators are easily accessed for inspection and replacement.

The avionics and control systems are examined through panels on the side and bottom of the fuselage. The avionics are approached by opening the door on the side of the fuselage and inspected or repaired by sliding the trays out that contain the electronic components. Both the infrared search and track finder and the GAU 8 cannon can be scrutinized through doors located on the left side of the fuselage. The door for the infrared camera is adequately large for easy removal of the system. The GAU 8 cannon system can be easily removed through several panels on the underside of the fuselage. This will allow the entire system to be lowered for easy repair and replacement. The ammo drum can also be reloaded using this panel. Figure 14.1 shows the layout of the Scorpion's access panels.

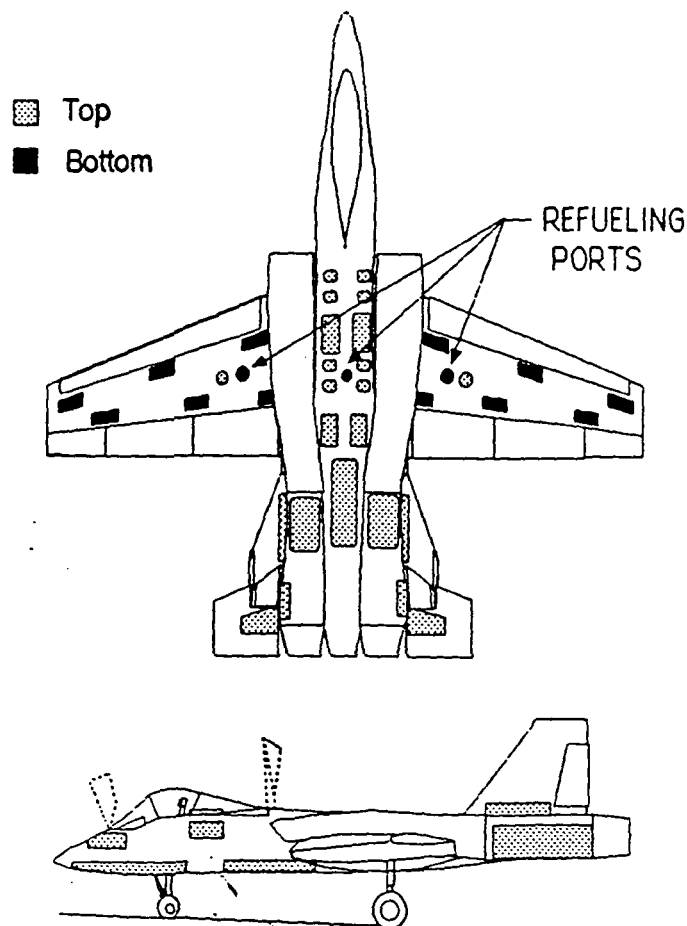


FIGURE 14.1: ACCESS PANELS

15.0 COST ANALYSIS

The latest version of the Development and Procurement Costs of Aircraft (DAPCA IV) model, developed by the RAND Corporation, taken from Reference 15, were used in estimating the Scorpion's cost. Four life cycle cost elements comprise the DAPCA IV model and are broken down as follows:

- Research, Development, Testing, and Evaluation (RDT&E)
- Production
- Operations and Maintenance
- Disposal.

Each of these life cycle cost elements used a cost estimation relationship (CERs) which was dependent on one or more of the following; aircraft weight, maximum velocity, life cycle, and/or production quantity. The CER then yields either cost or labor hours, which is then multiplied by the appropriate hourly rate to reveal total cost. Sample calculations supporting this cost analysis can be found in the appendix. A 500 aircraft production run and a 20 year life cycle established the total life cycle cost which is comprised of the four elements listed above, each of which is documented in the following text.

15.1 RESEARCH, DEVELOPMENT, TESTING AND EVALUATION

The RDT&E phase includes development support and flight test costs. Development-support costs (CD), modeled in equation 1, are the non-recurring costs of manufacturing support of RDT&E, including fabrication of mockups, subsystem simulators, structural test articles, and various other test items used during RDT&E. Flight test costs (CF), modeled in equation 2, cover all costs incurred to demonstrate airworthiness for Mil-Spec compliance except for the costs of the flight test aircraft themselves. Flight test costs include planning, instrumentation, flight test operations, data reduction, and engineering and manufacturing support of flight testing. The total RDT&E cost was found to be 200 million dollars which occupies 0.3% of the total life cycle cost.

$$CD = 45.42 (WE 0.63) (V 1.3) \quad 1)$$

$$CF = 1243.03 (WE 0.325) (V 0.822) (FTA 1.21) \quad 2)$$

15.2 PRODUCTION

Production or "Flyaway" cost consists of hours involved in engineering (HE), manufacturing (HM), tooling (HT), quality control (HQ), and the costs associated with manufacturing materials (CM), engines (CEng), and avionics (CAvionics).

Engineering hours (HE), modeled in equation 3, include airframe design and analysis, test engineering, configuration control, and system engineering. Manufacturing hours (HM), modeled in equation 4, comprise the costs to fabricate the aircraft, including forming, machining, fastening, subassembly fabrication, and final assembly. Tooling hours (HT), modeled in equation 5, embrace preparation for and during production. Quality control hours (HQ), modeled in equation 6, encompass receiving inspection, production inspection, and final inspection. Each of the preceding elements (HE, HM, HT, HQ) were appropriately multiplied by the current 1986 hourly "Wrap" rates to determine associated labor costs. Direct salaries, employee benefits, overhead, and administrative costs comprise the hourly Wrap rates and are as follows,

- RE = \$ 59.10

- RM = \$ 50.10

- RT = \$ 60.70

- RQ = \$ 55.40

Manufacturing materials cost (CM), modeled in equation 7, include the structural raw materials, such as aluminum and steel, plus the electrical, hydraulic, and pneumatic systems, the environmental control system, fasteners, clamps, and similar standard parts. In DAPCA IV, engine costs (CM) are assumed to be known. Two engines are required in the Scorpion and using reference (Roskam,J.,Airplane Cost Estimation: Design, Development, Manufacturing and Operating, Pt VIII, pg. 328, fig.B4) a 1.6 million dollar per engine cost was found based on the take-off thrust. Avionics costs (CAvionics) are assumed to be 5-25% of flyaway costs depending on sophistication. Avionics costs were assumed at 15% giving a CAvionics of 2.5 million dollars.

The Production costs were then adjusted to reflect 1991 dollars and profitability. Labor and material costs detailed above were calculated in constant 1986 dollars and found to be 7.32 billion dollars. By using a January 1991 Consumer Price Index of 135, provided by Standards and Poors, and a profitability of 10%, the 1991 "future" value yielded a 17.3 million dollar per aircraft cost.

$$HE = 4.86 (WE 0.777) (V 0.894) (Q 0.163) \quad 3)$$

$$HM = 7.37 (WE 0.82) (V 0.484) (Q 0.641) \quad 4)$$

$$HT = 5.99 (WE 0.777) (V 0.696) (Q 0.263) \quad 5)$$

$$HQ = 0.133 \quad RQ \quad 6)$$

$$CM = 11.0 (WE 0.921) (V 0.621) (Q 0.799) \quad 7)$$

15.3 OPERATIONS AND MAINTENANCE

Operation and Maintenance (O&M) costs were determined from assumptions as to how the aircraft will be operated. The major operating costs are fuel, crew salaries, and maintenance. Methods used in determining these costs are outlined in the following statements.

The fuel costs per aircraft per year were determined from a typical design mission profile. Using the Scorpion's profile warm-up, take-off, dash out, attack, dash in, and landing, a 1.5 hour mission time requiring an average of 12,045 lbs of fuel was calculated. This gave an approximate 8,040 pounds of fuel burned per hour. Next, Reference 15 was used to find an average of 400 yearly flight hours per aircraft, and using the price for jp-4 fuel, a 2.79 billion dollar operating cost was calculated for a 20 year operating period.

Crew expenses were determined by how many flight-crew members are kept on active-duty roster to operate the aircraft. Fighter aircraft require 1.1 persons per aircraft on average. Each person or crew member serves 2,080 hours per year, which when multiplied by the engineering wrap rate, and number of aircraft, yield a 6.76 million dollar per year crew cost.

Maintenance activities are lumped together under Maintenance Man Hours per Flight Hour (MMH/FH). Reference 15 indicates a MMH/FH of 16. From the MMH/FH and flight hours per year, found earlier, the

maintenance man hours per year were multiplied by the manufacturing wrap rate to give a 160 million dollar per year maintenance cost.

The total life cycle operations and maintenance costs reflect expenses associated with the Scorpion's 20 year life. These combined costs are much larger than the RDT&E and Production costs. The total life cycle operations and maintenance costs were found to be 59.1 billion dollars.

15.4 DISPOSAL

The final element making up life cycle cost concerns disposal. After a 20 year life, the Scorpion would be flown out to Arizona, "pickled" and stored. This would require approximately 1% of total life cycle cost or 120 million dollars for the entire fleet.

15.5 TOTAL LIFE CYCLE COST

Combing the four life cycle elements, Research, Development, Testing and Evaluation (RDT&E), Production, Operation and Maintenance (O&M), and Disposal, the 500 aircraft Scorpion program proposes a 91.6 billion dollar total life cycle cost for the entire fleet.

16.0 MANUFACTURING BREAKDOWN

A design-to-cost philosophy was used to develop the manufacturing approach for the Scorpion. Manufacturing processes will be kept simple as possible and straight forward manufacturing techniques such as riveting will be used. Modular construction of the fuselage and torque box of the wing enable final assembly to be carried out quickly.

Fuselage will consist of three modular sections, one containing the wing torque box and the main landing gear while the forward fuselage section will contain the nose gear. Early stage fitting of the landing gear will facilitate the movement of the structure through the remaining production. Each fuselage section will be built independently, then assembled to the remaining wing structure and empennage with their corresponding control surfaces. Engines, avionics and armament will complete the assembly cycle. FIGURE 16.0.1. presents the manufacturing breakdown of the Scorpion.

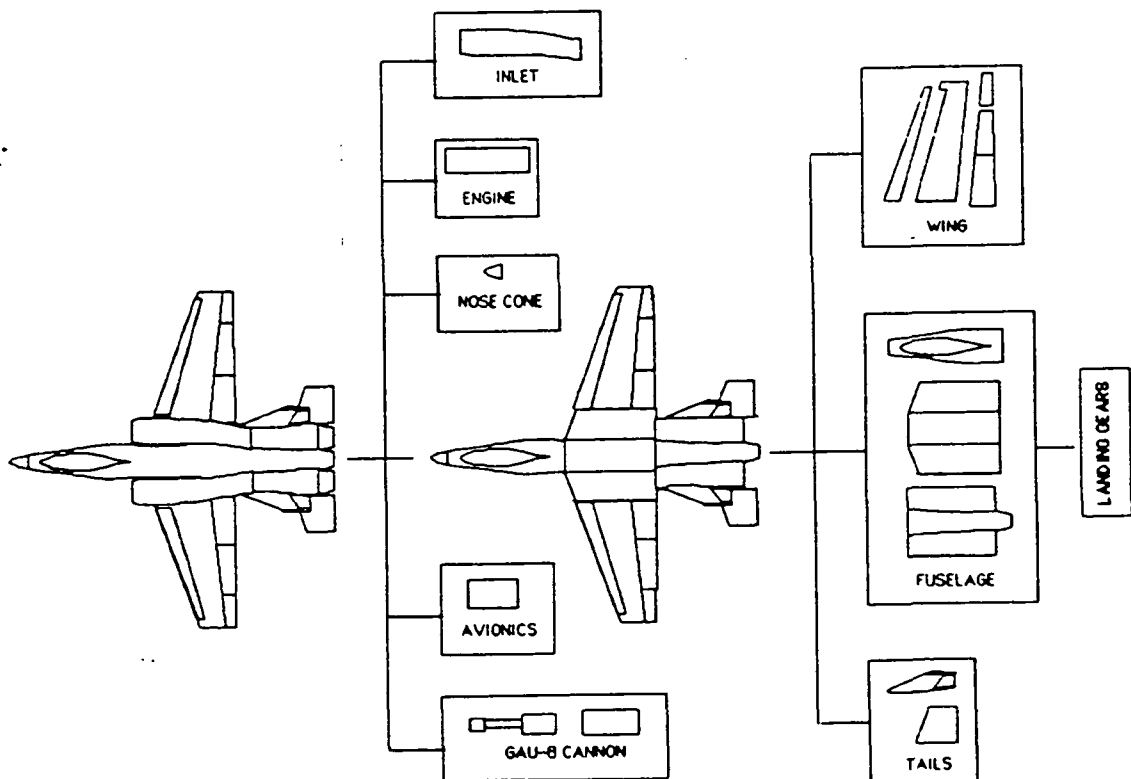


FIGURE 16.0.1. MANUFACTURING BREAKDOWN

17.0 CONCLUSION

This preliminary design sequence resulted in an aircraft that is rugged, reliable and capable of flying in adverse operating conditions. The Scorpion meets or exceeds all of the mission requirements and constraints specified, but is also capable of fulfilling other roles. The Scorpion excels in range, payload capabilities and rate of climb. However, the Scorpion needs improvement in the following areas: low-speed maneuverability, nonaugmented maximum velocity at sea-level and acceleration.

In order to widen the maneuvering envelope a supercritical airfoil is being investigated. This type of airfoil would increase the aerodynamic limits of the Scorpion, thus decreasing the minimum maneuvering speed. This would result in better low-speed maneuverability by increasing turn rates and decreasing turn radii. This in turn improves reattack time. Furthermore, increasing the aerodynamic limits could possibly decrease the cost of the Scorpion by simplifying the lift augmentation system.

A more powerful propulsion system would serve to increase maximum velocity and acceleration capabilities; resulting in a wider flight envelope. A thorough investigation of this modification will be made to determine if the advantages outweigh the additional fuel, weight and cost penalties incurred.

REFERENCES:

1. Roskam, J. , Airplane Design: Part I, Preliminary Sizing of Airplanes, Roskam Aviation and Engineering Corporation, Rt 4, Box 274, Ottawa, Kansas, 66067, 1990
2. Roskam, J. , Airplane Design: Part II, Preliminary Configuration Design and Integration of the Propulsion System, Roskam Aviation and Engineering Corporation, Rt 4, Box 274, Ottawa, Kansas, 66067, 1990
3. Roskam, J. , Airplane Design: Part III, Layout Design of Cockpit, Fuselage, Wing and Empennage, Roskam Aviation and Engineering Corporation, Rt 4, Box 274, Ottawa, Kansas, 66067, 1990
4. Roskam, J. , Airplane Design: Part IV, Layout Design of Landing Gear and Systems, Roskam Aviation and Engineering Corporation, Rt 4, Box 274, Ottawa, Kansas, 66067, 1990
5. Roskam, J. , Airplane Design: Part V, Component Weight Estimation, Roskam Aviation and Engineering Corporation, Rt 4, Box 274, Ottawa, Kansas, 66067, 1990
6. Roskam, J. , Airplane Design: Part VI, Preliminary Calculation of Aerodynamic, Thrust and Power Characteristics, Roskam Aviation and Engineering Corporation, Rt 4, Box 274, Ottawa, Kansas, 66067, 1990
7. Roskam, J. , Airplane Design: Part VII, Determination of Stability, Control and Performance, Roskam Aviation and Engineering Corporation, Rt 4, Box 274, Ottawa, Kansas, 66067, 1990
8. Lambert, M., et. al., Jane's All the World's Aircraft: 1990-1991, Jane's Information Group Inc, 1340 Braddock Place, Suite 300, Alexandria, Virginia 22314-1651, 1990

9. Taylor, J. W. R., Jane's All The World's Aircraft: 1986-1987. Jane's Publishing Inc., 4th Floor, 115 5th Avenue, New York, New York, 10003, 1986
10. Hoak, D.E., et al, USAF Stability And Control Datcom. Flight Control Division, Air Force Flight Dynamics Laboratory, WPAFB, Ohio, 45433-0000, 1975 revised
11. Abbott, I. H. and Von Doenhoff, E., Theory of Wing Sections, Dover Publications, New York, 1959
12. Panda - Program for Analysis And Design of Airfoils. Desktop Aeronautics, P.O. Box 9937, Stanford, Ca 94305, 1987
13. Kroo, L., Wing Design: A Discrete Vortex Method For Wing Aerodynamics. Desktop Aeronautics, P.O. Box 9937, Stanford, CA, 1987
14. Fink, D., et al, Aviation Week and Space Technology
15. Raymer, D.P., Aircraft Design: A Conceptual Approach. American Institute of Aeronautics and Astronautics, Inc., 370 L'Enfant Promenade, S.W., Washington, D.C., 20024, 1989
16. Bonds, R., et al, The Great Book of Modern Warplanes. Crown Publishers, 225 Park Avenue South, New York, New York, 10003, 1987
17. Spick, M., Modern Attack Aircraft. Prentice Hall Press, Gulf + Western Building, Gulf + Western Plaza, New York, New York, 10023, 1987
18. Spick, M., Modern Fighter Combat. Prentice Hall Press, Gulf + Western Building, Gulf + Western Plaza, New York, New York, 10023, 1987